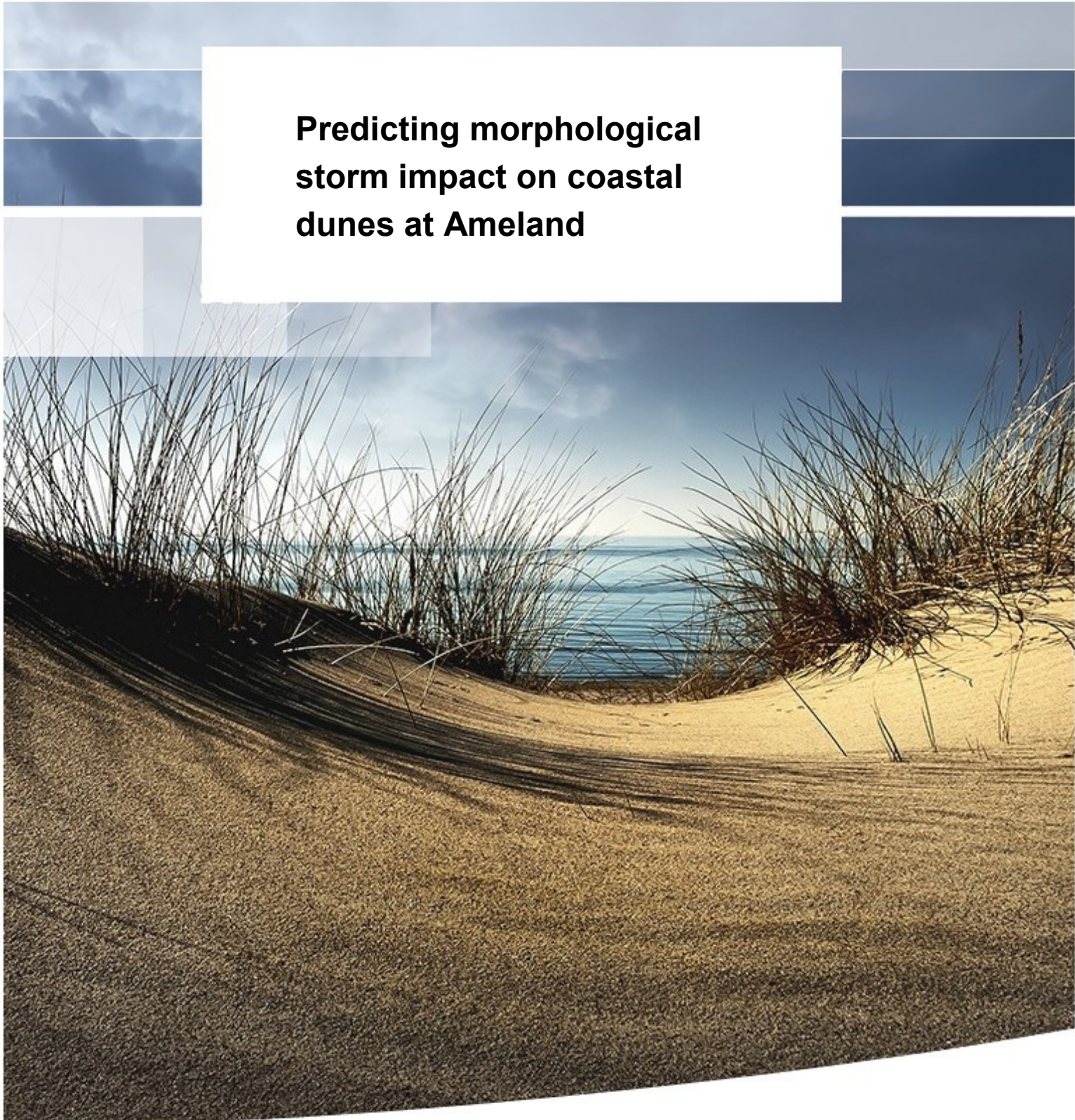


**Predicting morphological
storm impact on coastal
dunes at Ameland**



Thesis for the degree Master of Science

Predicting morphological storm impact on coastal dunes at Ameland

Simulating storm response on coastal dunes at barrier islands, in the presence of gentle slope beaches, with the numerical model XBeach in a 2DH (depth average) setting

A. Terlouw BSc
Student Civil Engineering and Management,
Department Water Engineering & Management,
University of Twente, Enschede, 2013

Supervisors:
dr.ir. J.S. Ribberink
dr. K. M. Wijnberg
ir. P.F.C. van Geer
ir. A.R. van Dongeren PhD
dr.ir. M. Boers

Voor mijn zus en haar man, voor hun verlies, een groot verdriet voor ons allen:

*Het losse zand stuift, zwiept en schuurt,
om tot rust te komen tussen helm en doorn
voor de dicht begroeide duinenrij
een nieuw stuk duin wordt geboren,
waar de eerste duinenrij,
verzwolgen door de woeste zee,
is verloren.*

Acknowledgement

First and foremost I offer my sincerest gratitude to my daily supervisors ir. P.F.C. van Geer and dr. K. M. Wijnberg for their patience, help and all the feedback they gave. I would also like to say thanks to my supervisors, dr.ir. J.S. Ribberink, ir. A.R. van Dongeren, PhD dr.ir. M. Boers for their assistance during my research.

Apart from my supervisors, I would to thank to Guido van der Salm, for listening to all my stories about nothing and my complains about everything, for showing his interest for my research and giving me valuable hints.

Finally, I would like to express my gratitude to all those who gave me the possibility to complete this thesis. I owe much gratitude to many people I did not mention. Nevertheless, I would like to thank them all for their extensive help and support.

Summary

The coastal zone is a focal point in the Dutch economy where a large number of social and economic activities are concentrated. Coastal dunes are the first (and last) line of defense against flooding of the coastal zone from sea. Therefore, the safety of these coastal dunes needs to be assessed whether or not they provide sufficient protection for the region at any given storm event.

Current used methods are not sufficient to assess safety of the coastal region in case of complex situations. Complex situations require two-dimensional process-based prediction tools, such as XBeach. However, if XBeach is used for the assessment of safety, it has to be extensively tested and validated. Therefore, XBeach was applied on a complex case. The presented case is one of beaches with a gentle slope, where infragravity waves are expected to be of significant importance.

The presented case includes the extraordinary storm, the 'Allerheiligenstorm' November 1st, 2006. This storm resulted in overwash at the barrier island Ameland. Due to the fact that pre and post storm LIDAR data of Rijkswaterstaat were available, morphological impact could be identified.

The results revealed that the available LIDAR data was of insufficient quality for the required modeling scale. This might be due to different calibration methods, incorrect use of correction factors, visual correction and the collection of the data by different companies. One cannot expect accurate result from when using these data with the model XBeach. This resulted into a qualitative research approach for assessing storm impact. So, criteria were defined based on the storm impact scale of Sallenger (2000) to identify the extent of the locations affected by different impact regimes. Four subsequent levels of storm impact regimes were used: swash, collision, overwash and inundation.

Data analyses revealed that the maximum storm impact resulted in overwash for two locations at Ameland. Between these locations, there was a notable difference in extent of the storm impact regime. At the first overwash location (Paal22) only little impact of the overwash was observed. At the second location (DeHon) abundant overwash could be recognized.

XBeach simulation showed accurately predicted the occurrence of overwash during the Allerheiligenstorm. The extent of the overwash occurrence showed to be at Paal22 underestimated. At DeHon the extent of overwash occurrence was overestimated. The order of the magnitude showed to be same. Results might be affected by the use the transport limiter and the inaccuracies in the bed level height. Sensitivity analyses showed that impact during collision and swash sensitive to the use of the overwash transport limiter. Overwash occurrence showed to be sensitive to an increase of 20 cm of the bed level height. Infragravity at the dune front reached in the simulations by XBeach a high of about 0.5 m.

Recommendations are to add missing physical processes to improve model performance. Short wave run-up and vegetation are not accurately represented in the XBeach model. As a consequence, if the threshold to overwash in XBeach is slightly exceeded, overwash is underestimated due to the lack of short wave run-up. Overestimation of overwash by XBeach might occur due to model inaccurately represents vegetation.

Content

1	Introduction	1
1.1	Background	1
1.2	Problem statement	1
1.3	Research goal and statement	2
1.4	Research approach	3
1.5	Report outline	4
2	Literature review	5
2.1	Definitions in the coastal zone	5
2.2	Sediment transport processes	6
2.2.1	Short waves	6
2.2.2	Long waves	7
2.3	Storm impact	9
2.3.1	Impact scale regimes	9
2.3.2	Modeling storm impact	11
3	Research conditions and data	13
3.1	Research area	13
3.2	Storm conditions	14
3.3	Available data	15
4	Data analyses	17
4.1	Methodology	17
4.2	Data quality investigation	19
4.2.1	Results quality assessment	19
4.2.2	Results quality improvement	24
4.2.3	Discussion	25
4.2.4	Conclusion	26
4.3	Results observations	26
4.3.1	Location Paal22	27
4.3.2	Location DeHon	30
4.4	Conclusions	33
5	Modeling in XBeach	34
5.1	Methodology	34
5.1.1	Model background	34
5.1.2	Model setup	37
5.1.3	Simulating results	39
5.2	Results simulation location Paal22	40
5.2.1	Morphological impact predictions	40
5.2.2	Morphological impact regimes	42
5.2.3	Hydrodynamic conditions	45
5.3	Results simulation location DeHon	45
5.3.1	Morphological impact predictions	45
5.3.2	Morphological impact regimes	47
5.3.3	Hydrodynamic conditions	51
5.4	Conclusions	52

6 Sensitivity analyses	53
6.1 Methodology	53
6.2 Results sensitivity to bed level changes	54
6.3 Results sensitivity to Smax	57
6.4 Conclusions	57
7 Analyses results and discussion	58
7.1 Observed versus simulated results	58
7.1.1 Location Paal22	58
7.1.2 Location DeHon	60
7.2 Discussion	62
7.2.1 Predicting storm impact with XBeach	62
7.2.2 Communicating predicted storm impact	62
8 Conclusions and recommendations	64
8.1 Conclusions	64
8.2 Recommendations	65
9 Bibliography	66
10 Appendix A: Results data analyses	69
11 Appendix B: XBeach model setup	71
11.1 Bathymetry setup	71
11.1.1 Processing LIDAR of location Paal22	71
11.1.2 Processing LIDAR of location DeHon	72
11.2 Wave boundary condition	73
12 Appendix C: Used parameters	74
13 Appendix D: Wave conditions	75
14 Appendix E: Wave force error in XBeach	80

1 Introduction

1.1 Background

People have always favored the coastal zone because of its unique resources. They are attracted by the fertile lands in the coastal plains and abundant marine resources, and by the easy access to international markets. The coastal zone is a focal point in many national economies where a large number of social and economic activities and their impacts are concentrated.

Because of the attractiveness of these coastal zones, they are often densely populated. It is expected that the importance of most coastal areas will further increase, due to the ever-increasing number of people, who want to find a place here. At the same time, many of these important coastal zones are below or around storm surge level. For this reason it is essential to protect all the people and resources in these coastal zones against flooding by the sea.

How are these coastal zones protected? Sea walls, dikes and breakwater are some examples of protection. However, along many coastal zones, coastal dunes are the first (and last) line of defense. These coastal dunes need to be assessed whether or not they provide sufficient protection for the coastal zone against flooding from the sea. One important cause of flooding from the sea is if overwash at coastal dunes occurs.

To assess the safety of the coastal zone to overwash, prediction models should contain the essential physics of dune erosion (Roelvink et al., 2010). Recent research shows that especially the infragravity waves are essential in assessing resiliency to overwash of coastal dunes, they are recognized as one of the main causes of (overwash) storm impact on coastal dunes (van Thiel de Vries et al., 2008; Williams et al., 2012). Although these infragravity wave heights are small in deep water, infragravity wave run-up on beaches can be as much as several decimeters to one meter (Ruessink, Houwman, et al., 1998). Hence, dune erosion prediction tools should incorporate knowledge about infragravity waves.

Furthermore, recent research on infragravity waves revealed that the effect of these waves are related to the steepness of the beach (Battjes et al., 2004). The beach along most of the Dutch coast can be characterized as a beach with a mild slope. To investigate the effect of different beach slope, flume experiments tests were performed (van Thiel de Vries et al., 2008). The major limitation of these flume experiments is their two-dimensional nature, excluding the longshore dimension. This dimension can be included and investigated by numerical (2DH) models.

Current methods to assess the resilience of the coastal dunes in the Netherlands are based on a deterministic semi-probabilistic approach. They (currently) don't contain all the essential (infragravity wave) physics and cannot predict overwash occurrence. Also, they can only at the moment only be successfully applied along a uniform coast (Roelvink et al., 2010). If more variability (as is the case for most of the Dutch coast) is present, or infragravity waves are of importance, nowadays used semi-probabilistic approaches aren't valid anymore (Roelvink et al., 2009; Van Dongeren et al., 2003).

1.2 Problem statement

In complex situations, advanced process-based prediction tools are required to accurately assess the resilience of the coastal dunes. State of the art research showed that for testing the resilience of the coastal dunes to overwash, it is important to incorporate the erosion

processes that are caused by infragravity waves (Roelvink et al., 2009; van Thiel de Vries et al., 2008). These processes can be included in (2DH) process-based models such as XBeach.

For the use of such an advanced process-based prediction tool in the formal assessment of the safety of dunes as flood protection, it is required (by law) that the model is extensively tested and validated. XBeach is such a model that can be used in these more complex situations for the assessment of safety, provided that the model is validated.

The hydrodynamics and morphodynamics of XBeach have been extensively validated against (1D) flume experiments (Daly et al., 2012; Dong et al., 2009; Williams et al., 2012) and some (2DH) field cases (Lindemer et al., 2010; McCall et al., 2010; Roelvink et al., 2009). In addition, we want to validate XBeach for beaches with a gentle slope¹. Since gentle slope beaches are present along the Dutch coast, this validation is essential if we want to use this prediction tool for these conditions. If successful, XBeach could reliably predict overwash storm impact on the Dutch coastal dunes and improve the quality of the assessment of safety.

A storm event in 2006 provides conditions for validation of XBeach regarding the prediction of sediment transport related to dune erosion. At the 1st of November 2006, at neap tide, a severe storm resulted in overwash and breaching of the dune system of Ameland, whereby large volumes of sand were eroded and the dune foot position was significantly displaced. Duros+, the model used nowadays to assess the safety, cannot predict overwash of the dune system of Ameland. XBeach, including the effect of infragravity waves during the storm, should.

For this event a hindcast² of the hydrodynamics are available, as these were calculated for another study (Alkyon Hydraulic Consultancy & Research, 2007). In addition, LIDAR³ data and aerial pictures were collected shortly after the storm. It allows an investigation of the morphologic overwash impact of the storm. As a consequence, this storm provides the research conditions for the validation of overwash occurrence by XBeach for mild beach slope conditions.

1.3 Research goal and statement

The overall motivation of this research is to improve the prediction of storm impact on coastal dunes with the numerical modeling program of XBeach. The objective of this research is to validate overwash predictions by XBeach for coastal dune at beaches with a gentle slope. Therefore, we will analyze data and simulate the morphological impact on the coastal dunes of the barrier island Ameland of the Allerheiligenstorm of November 1th, 2006.

¹ The mild-slope regime is defined by (Battjes et al., 2004) if the value less than about 0.3 for the normalized bed slope parameter defined by $\beta = (h_x/\omega)\sqrt{g/h}$, in which h_x is the bed slope, ω the sub harmonic frequency, h a characteristic depth in the shoaling zone and g the gravitational acceleration.

² A hindcast is also known as back testing; closely estimated boundary conditions of a past event are entered into a validated model to obtain more detailed results of the event.

³ LIDAR (Light Detection And Ranging) is an optical remote sensing technology that can measure the altitude by using pulses from a laser.

To fulfill this objective, two (main) research questions are presented:

(i) How can observed and measured data of dune erosion, at the barrier island Ameland during the Allerheiligenstorm, be used for validation of XBeach?

- What is the quality of the collected data?
- What morphological impact can be identified from the measured and observed data?
- Which locations of Ameland can be used to model and validate overwash simulations by XBeach?
- Which schematizations in XBeach to simulate the Allerheiligenstorm are possible with the data?

(ii) How well can XBeach predict overwash storm impact on coastal dunes for the case of barrier island with a gentle beach slope?

- How does the predicted storm impact compare to the observations?
- Which conditions govern the occurrence and magnitude of the simulation of overwash?
- What is the effect of the wave height of infragravity waves on overwash occurrence?

1.4 Research approach

Below a description of each phase of the research approach can be found.

Literature study: An overview is given of the different storm impact regimes, and the relevant sediment transport processes in these regimes. In additions, possible modeling approaches of morphological storm impact regimes are explained.

Data analyses: To have confidence in the observed and simulated results, a prerequisite is to have accurate data. Therefore, first the quality of the data will be assessed. Secondly, (if necessary) the accuracy of the data will be improved. The following step is the data analyses approach, will be to identify morphological Allerheiligenstorm impact that was observed and measures. Overwash locations will be identified, and at these locations morphological impact will be quantified. The results are obtained to compare it with model simulations later on.

XBeach modeling: simulations of the identified overwash locations at Allerheiligenstorm. in XBeach will be analyzed to identify the predicted morphological impact. The results of the analyzed can be use to compare it with observed and measured data. To this end, it will be used to validate XBeach.

Analyzing results: The measured, observed and simulated data will be compared with regard to each other.

The above is followed by a discussion and completed by a chapter containing conclusion and recommendations.

1.5 Report outline

This thesis starts in the second chapter with a literature review. The literature begins with explaining the definitions that used in this thesis. The chapter will continue with a paragraph over sediment processes and a paragraph investigating the different modeling approaches of storm impact in the coastal zone.

The third chapter consists of a description of the research area, storm surge conditions and measured data. The next chapter will present the data analyses. In this chapter, first the data methodology is laid out and the quality of the data investigated. This is followed by a data analyses of the observed and measured morphological storm impact. The fifth chapter is used to present the modeling methodology of XBeach, the set up of the grids used in XBeach and it presents the simulated morphological storm impact predictions by XBeach

These chapters are followed by a chapter presenting sensitivity analyses of parameters used in XBeach and a chapter where the results will be compared and analyzed. Finally, this thesis is completed by a discussion, conclusion and recommendations.

2 Literature review

This chapter gives an overview of the relevant physical processes that take place during a storm. The first paragraph will explain used definitions. Next, literature that explains morphological storm impact is reviewed. Finally, different approaches in modeling storm impact are investigated.

2.1 Definitions in the coastal zone

Many natural processes are active in de coastal zone, making it a dynamic unique environment. Due to the dynamic nature of the coastal zone, it is sometimes difficult to define clear definitions and boundaries for the different (sub)areas in the coastal zone. In this paragraph, the definitions and of the coastal zone are explained.

The coastal zone is the transition zone between sea and land that is regularly affected by marine processes. This zone extends from the continental shelf landwards until the first topographic features that are not affected by storm surge and waves. The coastal zones, and the relevant terms in the coastal zone, are depicted in Figure 1 .

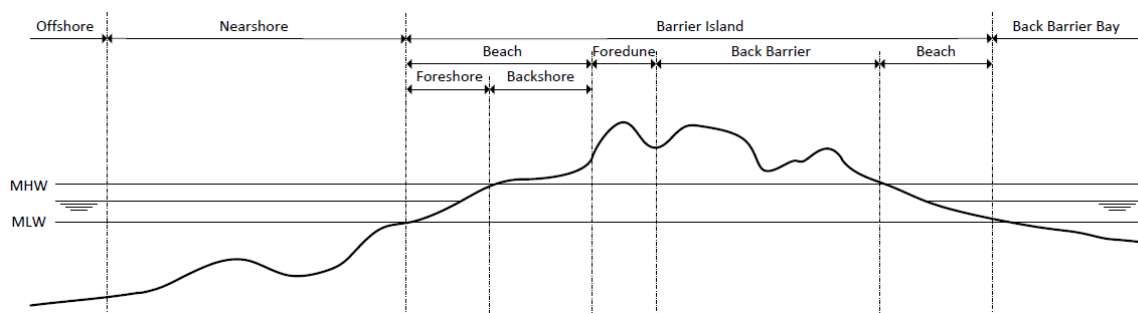


Figure 1: The coastal zone and their relevant terms, adapted from U.S. Army Corps of Engineers (2003).

The nearshore zone is the area between the beach and the offshore region. It starts where wave breaking begins. Typically found features in this region are breaker bars. It can be also referred to as the **surf zone**

The foreshore zone is bounded by the Mean Low Water (MLW) and Mean High Water (MHW) lines. The beach is the area seawards of the coastline that remains regularly subaerial, i.e. from the coastline to the low water mark

The backshore zone, lies between the MHW line and the toe of the fore-dune. The toe of the fore-dune is defined (in the Netherlands) as +3 m N.A.P (Dutch datum, approximately MSL). Together with the foreshore zone it forms the beach.

The fore-dune is the most seaward dune, located directly behind the backshore. Generally, the fore-dune has a height (in the Netherlands) around 10 m above the MHW.

The back barrier lies landward of the fore-dune. It can contain different features, including dunes, dune ponds, supratidal marshes, vegetated barrier flats and washover fans.

2.2 Sediment transport processes

Many natural processes play an important role in coastal sediment transport. There is a mutual adjustment of morphology and hydrodynamics that is involved in the dynamic character of transport of sediment.

The wave spectra in the surf zone (Figure 2) often contain large amounts of energy at frequencies equal and lower than the incident swell and wind waves (Masselink et al., 2003). Typically, the wave periods related to these frequencies range from approximately 10 seconds to several minutes. These are referred to as long waves (the lower frequency waves) and short waves (higher frequency waves) (Elfrink et al., 2002; Masselink et al., 2006; Reniers et al., 2010; Roelvink et al., 2009; Ruessink, 1998; Ruessink, Houwman, et al., 1998). The sediment transport processes are predominantly triggered by these two wave types.

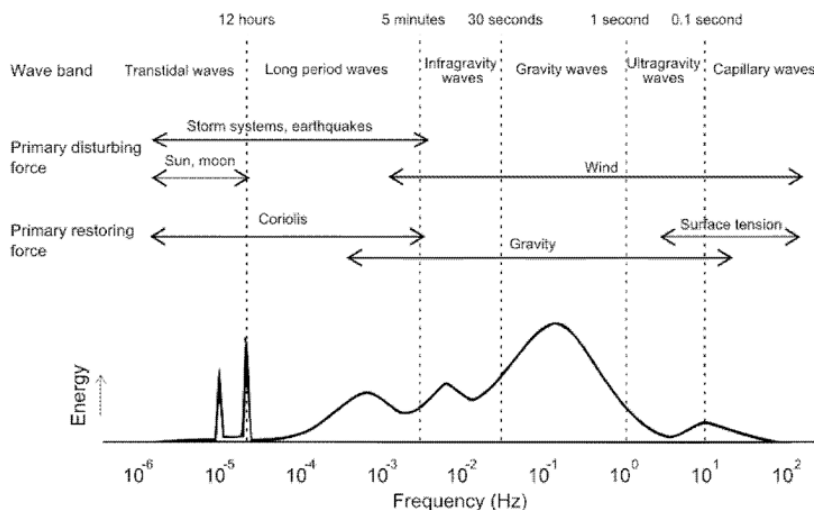


Figure 2: Wave classification by frequency (Kamphuis, 2000).

2.2.1 Short waves

Commonly used for describing short waves, is the linear wave theory. In the nearshore zone, linear wave theory is not applicable anymore. This is because waves deform due to the influence of the sea bed.

Wave asymmetry it is caused by the shoaling of waves in the nearshore zone, resulting in asymmetry around both the horizontal (skewness) and vertical axes (asymmetry). Due to wave asymmetry, the maximum onshore orbital velocity is higher than the maximum offshore velocity. Vertical asymmetry is the pitching forward of the waves, caused by the fact that the wave crest travels with a higher velocity than the wave trough (because wave celerity is related to water depth). This shape changes the vertical orbital velocities and accelerations.

Sediment transport is proportional to an exponent of the water velocity, such that there is a wave averaged net shoreward transport under skewed waves.

Undertow is an offshore directed return flow. The flow velocities in cross-shore direction have a depth average mean of zero, because of the balance between radiation stress and wave setup, this does not mean that there is no mass flux in the water column. The presence of waves creates an onshore directed mass flux above wave trough level, which is compensated for by the offshore directed undertow. Within the wave bottom boundary layer, bottom friction

dominates the flow; an additional mean shear stress is generated by the interaction of horizontal and vertical orbital velocities. This stress leads to an onshore directed mean flow, which is dominated under normal conditions.

Under storm conditions, the largest contribution to the net cross-shore sediment transport is most often made by the off-shore wave-driven undertow created by the short waves (Ruessink et al., 1998b).

The longshore current is caused by the incoming short wave groups. Besides this wave-induced forcing also wind and tidal forcing can contribute significant to the longshore current (Ruessink et al., 2001).

Due to wave dissipation in the nearshore zone there is a transfer of momentum from the wave motion to the mean flow which gives rise to a longshore current. This is the result of obliquely incoming waves, or a gradient in the wave height along the shore, that induces this longshore current. In most situations the current is predominantly induced by breaking waves which approach the coast at an angle.

The longshore current induces transport of sediment in the alongshore direction. This transport is parallel to the shoreline and the depth contour lines.

2.2.2 Long waves

Bound long waves are caused by incoming short wave groups (Longuet-Higgins et al., 1962). These wave groups are accompanied by a bound long wave. Spatial variation of the short wave amplitude causes spatial variation in radiation stresses. This variation in radiation stress induces water level variations, whereby it effectively forming a long wave, bound with the wave group (see Figure 3). In this report, these waves will be referred to as infragravity waves but are sometimes in literature also referred by the name surf beat. These infragravity waves are of importance in the dune erosion process.

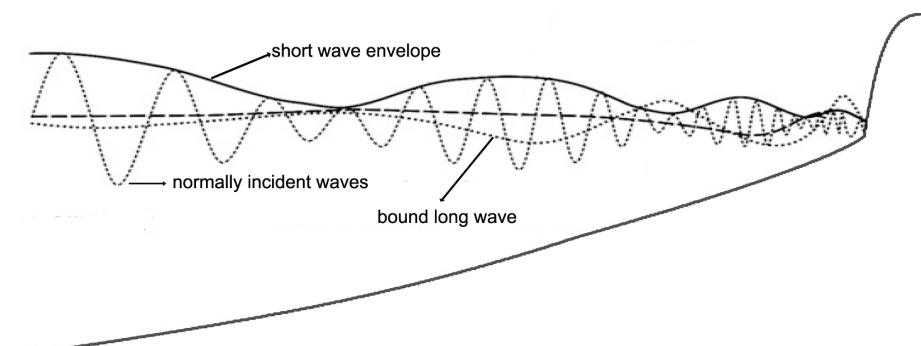


Figure 3: Schematic representation of the bound long waves, adapted from Williams et al. (2012).

Bound waves are enhanced when the incoming short wave groups start breaking in the nearshore. The bound long waves are released and enhanced upon shoaling, because they have longer wave lengths and are therefore less likely to break (Masselink & Puleo, 2006) in the contrast to short waves.

These long waves are found to have significant amplitude growth as they shoal. This is due to a net energy transfer from the grouped short waves to the accompanying long waves, owing to a phase lag of the group-induced long wave behind the envelope of the incident short-wave groups that develops as the waves shoal over the sloping bottom (Janssen et al., 2003).

These infragravity waves who have small wave heights in deep water, can induce run-up on beaches as much as several decimeters to one meter (Ruessink, van den Beukel, et al., 1998). They are generally in the order of 20-60% of the offshore wave height (Masselink & Hughes, 2003; Ruessink, 1998; Ruessink, van den Beukel, et al., 1998). At the beach these waves are (partially) reflected as free waves or dissipated because of collision with dunes.

Free waves are released bound long waves. In addition, free waves can be generated by varying radiation stress gradients due to incident wave groups leads to time-varying wave set-up. Then the temporal variation of the breakpoints acts as a wave maker, generating also free waves, both seaward and shoreward (Symonds et al., 1982).

If the generated free waves propagate farther into the surf zone they can be reflected or dissipated. Reflected waves induce a standing wave pattern in the surf zone due to the combination of incoming and outgoing wave motions and will either propagate out of the surf zone or become trapped in the surf zone.

Leaky waves are generated free waves which travel into the surf zone, and get reflected at the beach and then propagating outside of the surf zone.

Edge waves are similar to leaky waves but they don't travel out of the surf zone and are trapped inside and travel along the beach.

The research presented in this report investigates the behavior of the infragravity waves for bathymetric conditions representative for the Dutch coast; a mild-slope regime. this regime is defined as $\beta < 0.3$ (Battjes et al., 2004) calculated using:

$$\beta = (h_x/\omega)\sqrt{g/h} \quad (2.1)$$

in which h_x is the bed slope, ω the sub harmonic frequency, a h characteristic depth in the shoaling zone and g the gravitational acceleration.

In the mild-slope regime it is known that the incident bound waves are found to have significant amplitude growth as they shoal and surpassing that of generated free waves. Therefore, the breakpoint of the incoming wave groups moves over a relatively large distance. As a consequence, it makes this mechanism of generation of free waves proposed by Symonds et al. (1982) ineffective due to phase cancellation (Battjes et al., 2004). This means that the enhanced bound wave is dominant over the breakpoint-generated waves in the mild-slope regime. In addition, in the mild slope regime, the degree of reflection of waves is relatively low.

2.3 Storm impact

A storm surge is generally defined by the long gravity ocean surface elevation generated by low atmospheric pressure and high wind speeds during a storm (Olbert et al., 2010). When storm surges arrive at the beach, many different processes occur. Different sediment transport processes causes dunes to erode. The different sediment transport processes that take place during a storm are explained in this section. In additions, it is explained how these processes are modeled nowadays.

2.3.1 Impact scale regimes

Sallenger (2000) defined four scales for assessing storm impact, namely (i) swash regime, (ii) collision regime, (iii) overwash regime, and (iv) inundation regime. These regimes will be used for describing the erosion processes and are shown Figure 4. The regimes are described by the maximum wave run-up level, R_{high} , and the wave run-down level, R_{low} . The dune profile is described using the height of the primary dunes, D_{high} , and the height of the base of the dune, D_{low} . Figure 5 shows the definitions used to define different regimes.

Although these regimes do not provide quantitative answers to many morphological problems, it does provide insight into the stages of dune system morphology that occur during storms. The four regimes are described in more detail below.

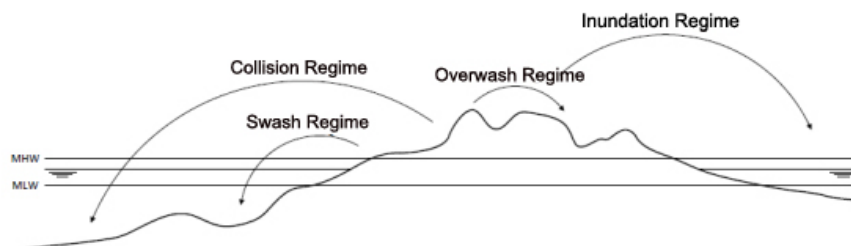


Figure 4: Sediment transport during the different regimes within a storm event (U.S. Army Corps of Engineers, 2003).

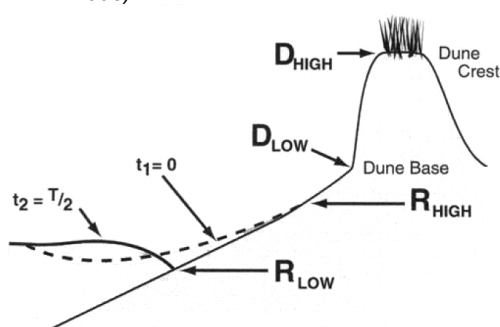


Figure 5: Definitions sketch describing variables used in scaling the impact of storm on barrier island, adapted from Sallenger (2000).

Swash occurs when there is the lowest storm impact. In this regime run-up is confined to the dune foot. The swash regime represents relatively common low energy storm conditions. As stated by Sallenger (2000), such conditions lead to sediment being transported offshore from the foreshore and beach. Infragravity waves are responsible for undercutting the dunes in the swash regime (Thornton et al., 2007). The swash regime is defined as:

$$\frac{R_{high}}{D_{high}} < \frac{D_{low}}{D_{high}} \tag{2.2}$$

Collision occurs when wave run-up reaches the base and face of the dune and transport sediment offshore and alongshore. In this regime, transport of sediment is directed from the dry dune face to the wet swash, i.e. slumping or avalanching is present. Slumping is predominantly triggered by a combination of infragravity wave run-up on the previously dry dune face and the (smaller) critical wet slope (Roelvink et al., 2009). Sediment transported in this way does generally not return to the original location and thus net dune erosion occurs (Figure 6). These processes occur when the threshold of equation 3.2 is exceeded.

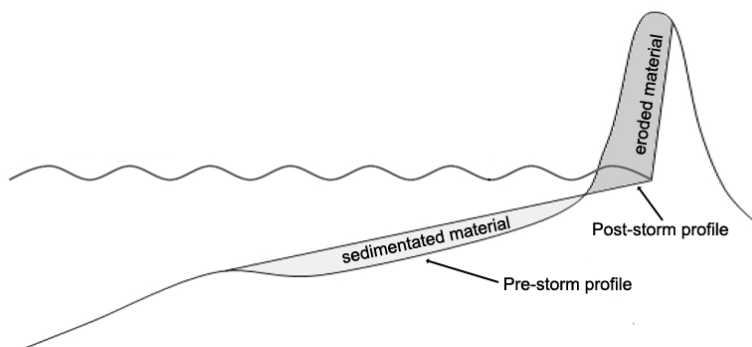


Figure 6: Simplified illustration of dune erosion caused by collision, adapted from (McCall, 2008).

$$\frac{R_{high}}{D_{high}} \leq \frac{D_{low}}{D_{high}} < 1 \quad (2.3)$$

Overwash is defined as the transport of sea water and associated sediment/drift from the beachface to the back barrier. The overwash regime is defined as:

$$\frac{R_{high}}{D_{high}} \geq 1 \text{ and } \frac{R_{low}}{D_{high}} < 1 \quad (2.4)$$

During the overwash regime the flow is dominated by low frequency motions on the time scale of wave groups, carrying water over the dunes. This onshore flux of water is an important landward transport process where dune sand is being deposited on the island and within the shallow inshore bay as overwash fans (Almeida et al., 2012). After overwash occurred, seven different cross shore profiles can be identified as possibility (Figure 7):

- *Crest accumulation* occurs when wave run-up just reaches the crest of the dune;
- *Landward translation* is hypothesized that the translation may be caused by a period of dune lowering, followed by crest accumulation during less severe conditions;
- *Dune lowering*; In this case sediment is transported from the seaward side of the crest landward;
- *Dune destruction* happens when the dune lowering continues until there is no discernible dune remaining after the storm;
- *Barrier accretion* is the case when sediment is eroded from the foreshore and deposited on the back barrier;
- *Barrier rollover* occurs If sediment is transported from the nearshore across the island and deposited in the back barrier bay, the entire barrier island translates landward;

- *Barrier disintegration* can happen if hydrodynamic conditions are severe enough. Sediment is eroded from the barrier island and deposited subaqueously in the back barrier bay or offshore.

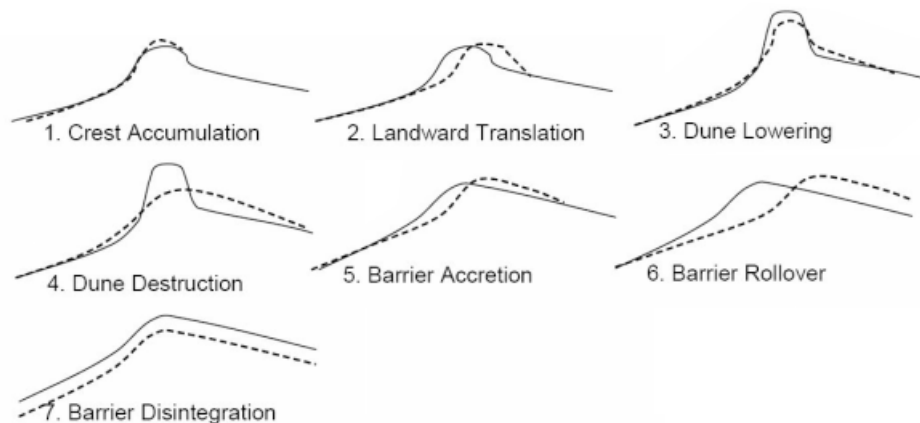


Figure 7: Different cross shore profiles after an overwash event. The solid line indicating the pre-storm profile, the dotted line indicates the post storm profile, adapted from Donnelly (2007).

Inundation regime, describing where the surge is sufficient to completely and continuously submerge the island (equation 2.5). Breaching of barrier islands occurs during the inundation regime, where a new channel is formed cutting through the island. This happens when a storm surge is sufficient to completely and continuously submerge the barrier. Limited evidence suggest the quantities and distance of transport are much greater than what occurs during the overwash regime (Sallenger, 2000). When beaches are completely inundated, the related morphological processes are not so clear.

$$\frac{R_{low}}{D_{high}} \geq 1 \quad (2.5)$$

2.3.2 Modeling storm impact

To model processes in the regimes described by Sallenger (2000) different approach can be found. In this section, most commonly used modeling approaches in these different regimes are presented.

Swash regime sediment transport has remained difficult to predict accurately by models. This is due to the complex hydrodynamic conditions in the swash zone, combined with the difficulty in making in-situ measurements necessary for calibrating and validating of models.

Different types of models are available to predict morphodynamic conditions close to the shoreline. There can be three broad types of model distinguished: probabilistic models, parametric model and time domain models.

The probabilistic and parametric models generally only provide information on wave heights and wave height distributions in the nearshore, whereas the time-domain models allow a detailed representation of non-linear wave motions and kinematics. Despite the prominence of infragravity energy in the swash zone, many of these models do not explicitly include infragravity waves.

Collision regime modeling approaches can be found in three types of analytical dune erosion models. The three types of models are those based on the equilibrium profile theory, based wave impact approach or physically-based.

Most existing models to predict the response in the collision regimes of dunes, tend to be based on the equilibrium theory which include doesn't include all physical processes. The equilibrium profile theory assumes that the beach profile strives toward an equilibrium state, defined by the wave and water level conditions. An equilibrium beach profile is defined as cross shore profile of constant shape that is reached after a long period of constant hydrodynamic forcing. This results most of the response of the dune is geometrically determined. The concept of equilibrium profiles under constant laboratory conditions was found valid by many researchers as long ago as 1939 (van de Graaff, 2006). Nowadays, design methods for dunes on the Dutch coast are based on an equilibrium-type of model.

The wave impact approach estimates the sediment transport from the dune and associated profile change by the waves directly hitting it. The total storm erosion is a function of the frequency and intensity of the impacts. Wave impacts can be described mathematically by a change in momentum flux of the waves as they hit the dune face. The wave impact theory has been empirically validated using small- and prototype-scale wave tank data (Larson et al., 2004).

Finally, the third type of model in the collision regime the physically-based models. Such models are defined by the fact that they attempt to accurately model all the physical processes involved, without assumptions modifying the physics of the processes (McCall, 2008).

Overwash and inundation modeling is relatively new. The first attempts were predictions of 1D cross-shore models. More recently, quasi-2DV cross shore profile modeling approaches were followed to predict overwash and inundation. The latest models are based on a depth and time dependent 2DH modeling approach.

One validated model with the capacity to simulate washover one dimensional numerical model SBEACH 1D (Larson et al., 1989). More recently, in the model UNIBEST-TC an adaptation was include for predicting overwash in flume experiments (Tuan et al., 2006).

Although these models provide useful predictions of 1D washover morphology, they are limited by the assumption of longshore. Field studies have shown that overwash is highly influenced by spatial variations in forcing and dune strength (Morton and Sallenger, 2003). Therefore it is important for any model to incorporate such longshore variation in order to successfully simulate overwash.

In addition, all these overwash models may limit their applicability because they do not account for infragravity waves. Near dune hydrodynamics are affected by the infragravity waves (van Thiel de Vries et al., 2008). Therefore, Roelvink et al. (2009) developed a new process-based and time dependent 2DH model of the nearshore and coast. The 2DH model XBeach has been successfully applied to simulate erosion and overwash on two sandy barrier islands in the United States (McCall et al., 2010). In this research it is tried to simulate observed overwash at the barrier Island Ameland during the Allerheiligenstorm.

3 Research conditions and data

In this chapter research conditions and data will be outlined and presented. In the first paragraph the research area is presented. The second section will elaborate about the hydrodynamic conditions during the Allerheiligenstorm. The final paragraph will present the different available bathymetric datasets.

3.1 Research area

Ameland ($53^{\circ}26'51''\text{N}$ $5^{\circ}47'33''\text{E}$) shown in Figure 8 and Figure 9 is a barrier island situated between the southern part of the Wadden Sea and the North Sea. The physical processes in this area are governed by semidiurnal tide which has a mean tidal range about 2.0 m and propagates from west to east with a speed around 1.5 m/s.



Figure 8: Map of the Netherlands with location of Ameland.

The island of Ameland has a length of 25 km and the widest cross-section on the island is around 4 km. Ameland is characterized by beaches with gentle slopes (β is less than 0.3). Its north side is protected against storms by coastal dunes. On the southern side the island is protected by a 17 km long dike. The maximum elevation on the island is +23 m N.A.P.

The Wadden Sea at the south side of the island is an area which stretches more than 500 km from Den Helder (The Netherlands) in the south to the peninsula Skallingen (Denmark) in the north. The Wadden Sea area is about 8000 km². The North Sea is located north of the island and can be described as a semi-enclosed, epi-continental sea with a surface area of 750 000 km² and a mean depth of 90 m.

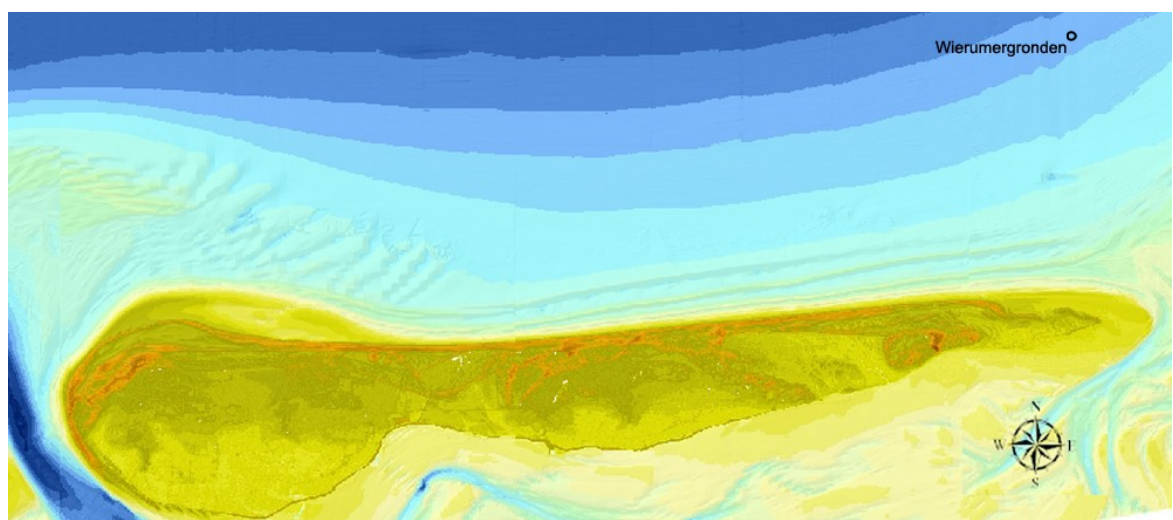


Figure 9: Map of Ameland derived from AH06. The length from west to east is approximate 25 km and the measured from north to south at maximum 4 km.

3.2 Storm conditions

Allerheiligen (All Saints' Day) at the 1st of November 2006 presented an historical storm, accordingly named the 'Allerheiligenstorm'. During this storm, high water levels were broke records more than 180 years old. Even despite the fact It was neap tide and the wind speed was not extreme. These storm conditions are expected to occur once every 65 year.

Moreover, if this storm occurred during spring tide, an additional rise of the water level of 30 cm is expected (den Heijer et al., 2007). Fortunately, it was neap tide and only some minor storm damage was reported. During this storm, some cars parked close to the ferry on Ameland were washed into the Wadden Sea. Also, it was reported that salt water, due to overwash, entered fresh water supplies at Ameland.

How was it possible that the water level reached this height? These water levels were caused by a fast moving low-pressure centre that moved in eastward direction over the North Sea. On the 31th of October 2006, the wind direction was southwest with wind speeds of 15 m/s. As the storm moved over the North Sea, the wind direction turned to more northerly directions and the wind speed increased to about 23 m/s, as measured at Huibertgat. At the peak of the storm the wind direction was northwest.

These details are known because the storm surge conditions used for this study were measured at Wierumergronden, by Data-ICT-Dienst Rijkswaterstaat. The measurement station was located off-shore at coordinates RD_x 192882 and RD_y 614562, relatively close to Ameland (see Figure 9). The water levels are represented by a maximum water level of +2.7 m N.A.P at 05:00 hr (Figure 10). The wind and pressure fields at the beginning (00:00 hr) and at the peak of the storm are shown in Figure 11.

Some additional information about the hydrodynamic conditions during the Allerheiligenstorm is presented in Appendix D. These hydrodynamics were obtained using a validated hindcast. A more elaborated explanation can be found in the rapport "Hydro-dynamics in the Wadden Sea during storm conditions" (Alkyon Hydraulic Consultancy & Research, 2007).

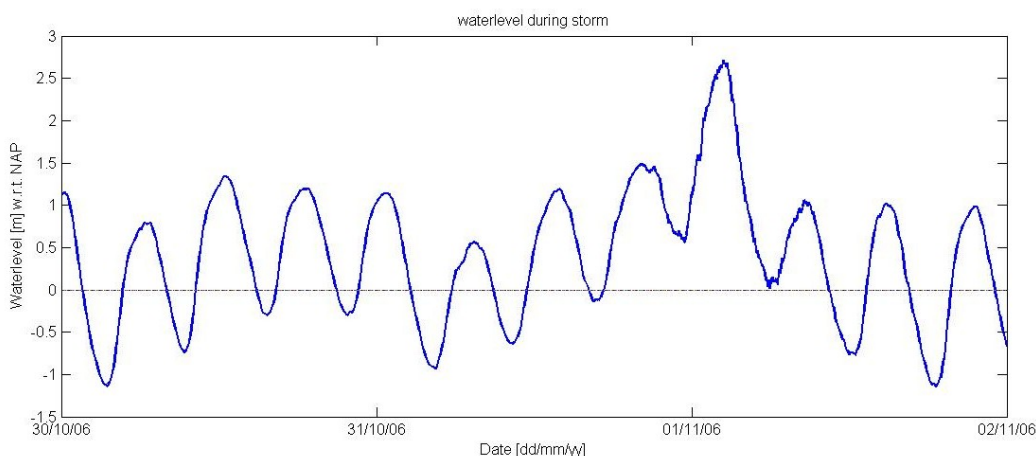


Figure 10: Water level during the Allerheiligenstorm at Wierumergronden (Rijkswaterstaat, 2006).

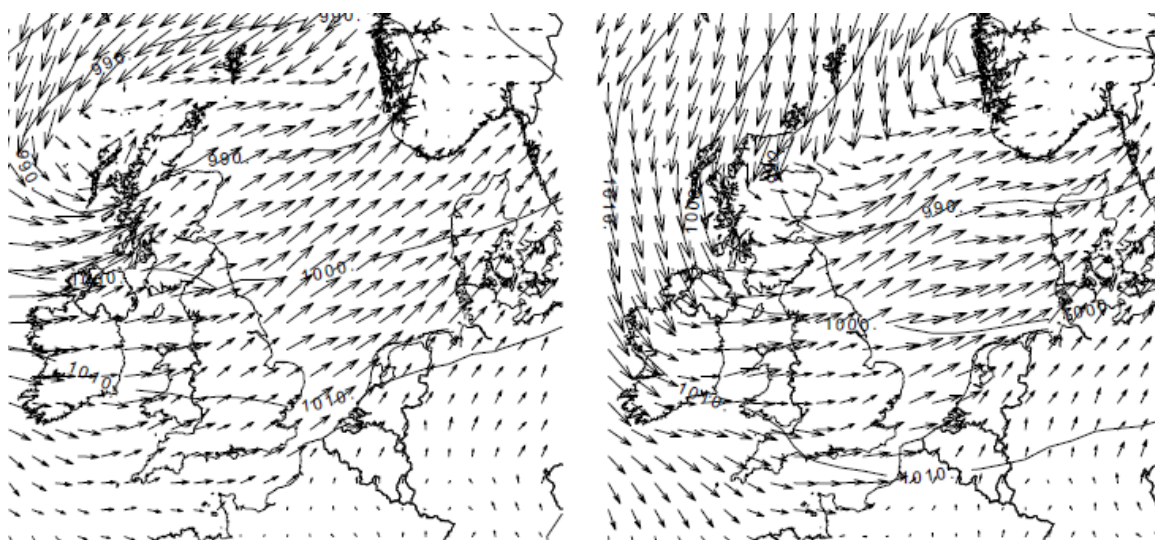


Figure 11: Wind en pressure fields 1st of November 2006 at 00:00 hr and at the peak of the storm at 05:00 hr. 1 cm is representing a wind of velocity 30 m/s (den Heijer et al., 2007).

3.3 Available data

The data used for this research is collected by the Adviesdienst Geo-informatie en ICT (AGI). In Table 1 the different data sets are shown. In Table 2 and Table 3 descriptive statistics, obtained from the report Rijkswaterstaat (2007), are shown. The statistics are showing the (expected) reliability of the data.

Table 1: Overview of available datasets.

Abbreviation	Data	Collected	Used technique	Resolution [m]
AHN	Actueel Hoogte Kaarten	2001	LIDAR	5x5
AH06	Elevation map of Ameland	15/04/2006, 18/04/2006 and 06/05/2006,	LIDAR	1x1
AH07	Elevation map of Ameland	27/03/2007	LIDAR	1x1
VAK	Vaklodingen	2000:2010	GPS-LRK ⁴	20x20
STORM	Elevation map of Ameland	29/11/2006	LIDAR	1x1
PHOTO	Birds eye prospective photo's	29/11/2006	-	-
AERIAL	Aerial prospective photo's	29/11/2006	-	-

Table 2: Statistics of available datasets (Rijkswaterstaat, 2007).

Data set	min N.A.P. [cm]	Max N.A.P. [cm]	Mean N.A.P. [cm]	SD [cm]
AHN	-27	2314	146.30	224.89
AH06	-177	1761	161,31	255.20
AH07	-59	2332	303.03	263.43
VAK	-2707	1643	-776.81	688.80
STORM	-155	1781	161.54	257.18

⁴ GPS - Long Range Kinematic (GPS-LRK) technology is a kinematic method used by vessels to measure water depth.

Table 3: Results from two control areas used for validation of the LIDAR data from datasets AH06 and AH07 (Rijkswaterstaat, 2007).

Data set	Place	Collected year	Number of points	Mean Deviation [m]	SD [m]	RMS [m]
AH07	Hollum	2007	118	0.010	0.017	0.02
AH07	Nes	2007	121	0.002	0.043	0.043
AH06	Hollum	2006	122	-0.025	0.015	0.029
AH06	Nes - Ameland	2006	129	0.01	0.067	0.067

AHN: For the purpose of this study this dataset is used for obtaining a general overview of the island of Ameland. Other available datasets only contain the elevation data of the coastal area. This dataset included also elevation data of other areas at Ameland.

This is one of the first measurements in the Netherlands using the LIDAR technique. The data has a grid size of 5x5 m. The collected data used only one laser point per grid cell, resulting according to the specification stated in accuracy with the maximum precision of 15 cm (Rijkswaterstaat, 2007).

AH06: This dataset is used to determine the position and shape of the dunes prior to the storm. In addition, it is also used to determine the (Jarkus) transects of 2006. The data were collected by AGI and has 1 m resolution. The results of the validation of the dataset can be found in Table 3. The dataset requirements were set by Rijkswaterstaat on a maximum deviation of -5 and +5 cm for 50% of the data, 67% of the data between the -10 and +10 cm and 95% of the data between -15 and +15 cm.

AH07: This dataset is used to determine the position and shape of the dunes prior to the storm. With this data also (Jarkus) transects of year 2007 are calculated by Rijkswaterstaat. The data is collected by AGI. The results according to the report of AGI (Rijkswaterstaat, 2007) of the validation of the dataset can be found in Table 3. The dataset requirements were set by Rijkswaterstaat on a maximum deviation of -5 and +5 cm for 50% of the data, 67% of the data between the -10 and +10 cm and 95% of the data between -15 and +15 cm.

VAK: This dataset contains the data of submerge bathymetry, measured in 2006. The resolution of the dataset is 20x20 m. These data are also used to construct the submerged bathymetry of the (Jarkus) transects of 2006.

STORM: This dataset is used to determine the position and shape of the dunes after the storm measured 28 days after the occurrence of the storm. LIDAR data was collected of the coastal zone. This was an extra measurement, due to the extraordinary Allerheiligenstorm, so that morphological effect of the storm could be analyzed later on. Statistics about the reliability of the data are not available.

PHOTO: Photographs taken from an airplane where collected simultaneously with the STORM data. This resulted in photographs with a bird's eye view of the coastal dunes.

AERIAL: during the collection of the data of STORM also areal pictures of the dunes were made what can help to analyze the storm impact more in detail. These photos were georeferenced to the dataset of the coordinate system and can be used to obtain dimensions of morphological features.

4 Data analyses

The Allerheiligenstorm resulted in overwash and breaching of the dune system of Ameland. In this chapter, data of this extraordinary event will be analyzed. The first paragraph outlines the methodology. The second paragraph will consist of an investigation of the quality of the data. Next, results of the observed overwash will be presented for two different locations and will be completed by a conclusion.

4.1 Methodology

The intended goal of this data analyses is to relate visible morphological changes to different storm impact regimes defined by Sallenger (2000). For the presented research, locations of interest are those where overwash and breaching of the dunes took place. The goal is to model these in XBeach and validate the simulated results with observed data.

To have confidence in our observations and predictions, a prerequisite is to have accurate data. Therefore, an assessment of the data will be performed and secondly, (if necessary) a quality improvement.

- **Data quality assessment** will be used to establish whether or not the required accuracy of LIDAR is met to use it for (i) quantifying morphological storm impact and (ii) use the data for the validation of predicting overwash occurrence by XBeach.
- **Data quality improvement** is necessary if the data quality assessment reveals that the data is of insufficient quality for (i) validating overwash occurrence and (ii) retrieving morphological storm impact due to the Allerheiligenstorm.

The next phase in the data analyses is to identify the overwash locations. At these overwash locations, different parts of the bathymetry are affected by also different (sometimes multiple) storm impact regimes. These impact regimes ((i) swash, (ii) collision, (iii) overwash and (iv) inundation), defined by Sallenger (2000) do provide insight into dune erosion processes that can occur during a storm. Within each different regime, patterns and relative magnitude of net erosion are unique. The border between regimes represents thresholds, defining where processes and magnitudes of impact change significantly (Sallenger, 2000).

This allows for some of these patterns and magnitude, caused by the different impact regimes, to be quantified with the available data. To quantify these morphological features some criteria are defined. These criteria are used to obtained results from datasets AH06 in combination with the AERIAL and PHOTO data. These data can be used together due to the fact that the aerial photographs were georeferenced with AH06. These georeferenced photos allow morphological impact induces during different impact regimes to be quantified.

The morphological impact (i.e. the magnitude and patterns) caused by these different impact regimes allows to compare observed and measured results with simulated results. The used criteria in relation to different impact regimes are shown in Figure 12 and will be explained next.

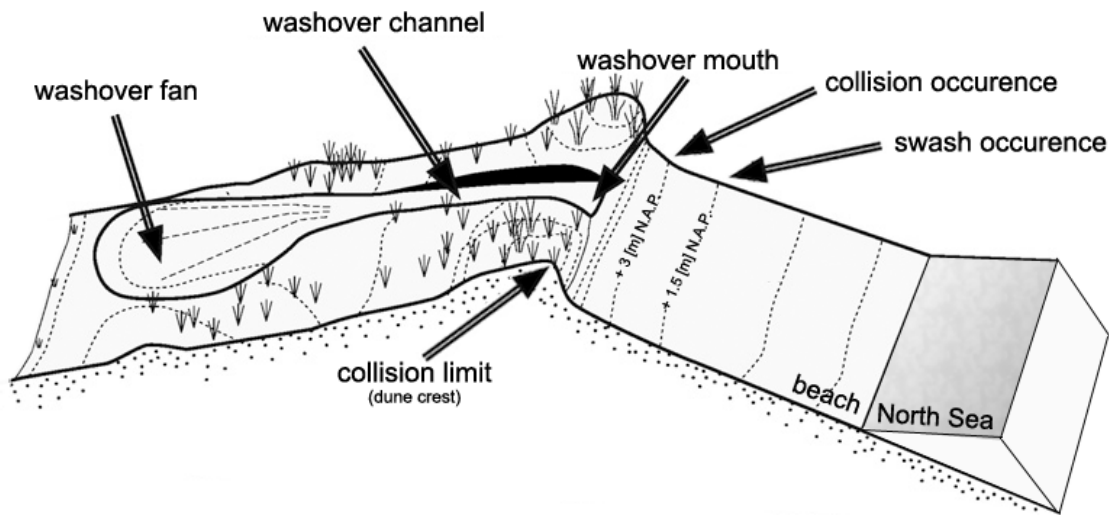


Figure 12: Terminology used for identifying morphological storm impact, adapted from Matias et al. (2008).

The swash regime represents relatively low energy conditions, resulting in small morphological changes. Photo-interpretation of morphological impact during the swash impact regimes represented difficulties, either in distinguishing it from other morphological occurrence, or to relate it to the recent storm swash. (i.e. photos were taken one month after occurrence, morphological impact might already be washed away). Therefore, criteria were defined to identify the extent of the area impacted by the swash regime, (i) swash occurrence and (ii) swash limit:

- **Swash occurrence** is assumed to start if the storm surge level exceeds an elevation above +1.5 m N.A.P. Above this normal maximum mean tidal range, morphology is normally less disturbed due to wave impact. Therefore, +1.5 m N.A.P. is assumed to be the threshold of occurrence of swash impact.
- **Swash limit** is the height, from where on the storm surge level starts undercutting the dunes. The dune foot in the Netherlands is defined at +3 m N.A.P. (Van de Graaff et al., 2006). It is assumed in our analysis to be the limit of the swash regime.

Morphological impact during the collision impact regime results in the transport of sediment in a direction it generally does not return from to the original location. Transport of sediment is directed from the dry dune face to the wet swash. Thus net dune erosion occurs in this regime. Eroded sediment due to the collision impact regime can be identified using two criteria's (i) collision occurrence and (ii) collision limit:

- **Collision occurrence** is defined where swash impact is confined to its maximum limit. Morphological impact due to collision occurrence can be recognized above the +3 m N.A.P. line.
- **Collision limit** is assumed to be at the crest height of the dune. If run-up exceeds this limit, overwash occurrence should be visible.

When overwash occurs, the onshore flux of water is an important landward transport process. Dune sand is being deposited on the island and within the shallow inshore bay creating overwash fans. Photo-interpretation can be used to distinguish these depositions of sand in the coastal morphology. Specific criteria were used to determine the extent of the washover: (i) washover occurrence; (ii) washover mouth; (iii) washover intrusion:

- **Washover occurrence** is determined by: sandy surface, absence of vegetation, and adjacency to the beach.
- **Washover mouth** is defined as an imaginary line that connects two longshore shoreline positions.
- **Washover intrusion** is defined as the maximum sand excursion distance in relation to the washover mouth.

Inundation can be recognized by a submerged bathymetry behind the dune barrier. Furthermore, when dune areas are completely inundated, the related morphological processes are not so clear and they are difficult to distinguish. Quantities and distances of sediment transport are much greater due to the inundation regime than that of the occurrence of overwash. Therefore, inundation can be distinguished based on the severity of morphologic impact.

4.2 Data quality investigation

For understanding and predicting the behavior of dune systems, observational data is an important source of information. The data will be used for quantifying morphological storm impact and validation of predicting overwash occurrence by XBeach. A prerequisite for obtaining these objectives is to have accurate data. To this end, in this section the data accuracy from the Allerheiligenstorm will be investigated and if necessary, improved.

4.2.1 Results quality assessment

Beach and dune areas are dynamic physical features. Morphological storm impact can occur at different spatial scales. In this research (small scale) overwash (fans) will be identified and simulated. The expected overwash occurrence is in the order of meters. The needed accuracy of the LIDAR data is correlated to this research goal. Therefore, in the next part, it will be established whether or not the accuracy required (i.e. accuracy to represent accurately small overwash fans) to obtain the research objectives is met.

The approach followed to assess the LIDAR data, is based on comparing elevations obtained from the different datasets with reference data. The accuracy that is being assessed is the absolute accuracy. The absolute accuracy of data accounts for all systematic and random errors. Absolute accuracy requires high vertical accuracy (z-direction). Also, a high horizontal accuracy is required (x- and y-direction). Especially, due to the fact that horizontal in LIDAR data can contribute significantly to errors detected in vertical accuracy. Therefore, both horizontal and vertical accuracy is investigated. The assessment is started with an investigation of the horizontal accuracy, followed by investigation of the vertical accuracy.

First, the horizontal accuracy of the LIDAR data is addressed. Horizontal errors in are more difficult to identify in LIDAR than vertical errors. This is because the bathymetry often lacks well-defined topographic features, which are required for such tests. To indentify errors without well-defined topographic features, contour mapping can help. Contour lines can portray a form of the surface that helps to compare different datasets. To assess the horizontal accuracy, the offset is measured between contour lines from the dataset (STORM) with reference data (AH06).

Deltares

The following observations are made by plotting the contour lines (Figure 13):

- The dataset (STORM) nowhere coincides with reference data (AH06);
- At the eastern part of Ameland, the data is shifted w.r.t. the reference data, with approximately a 2 m land inwards (south);
- North-west, the dataset is shifted towards sea (north);
- West, at the dike at Ameland the displacement is around 1 m toward sea (west).

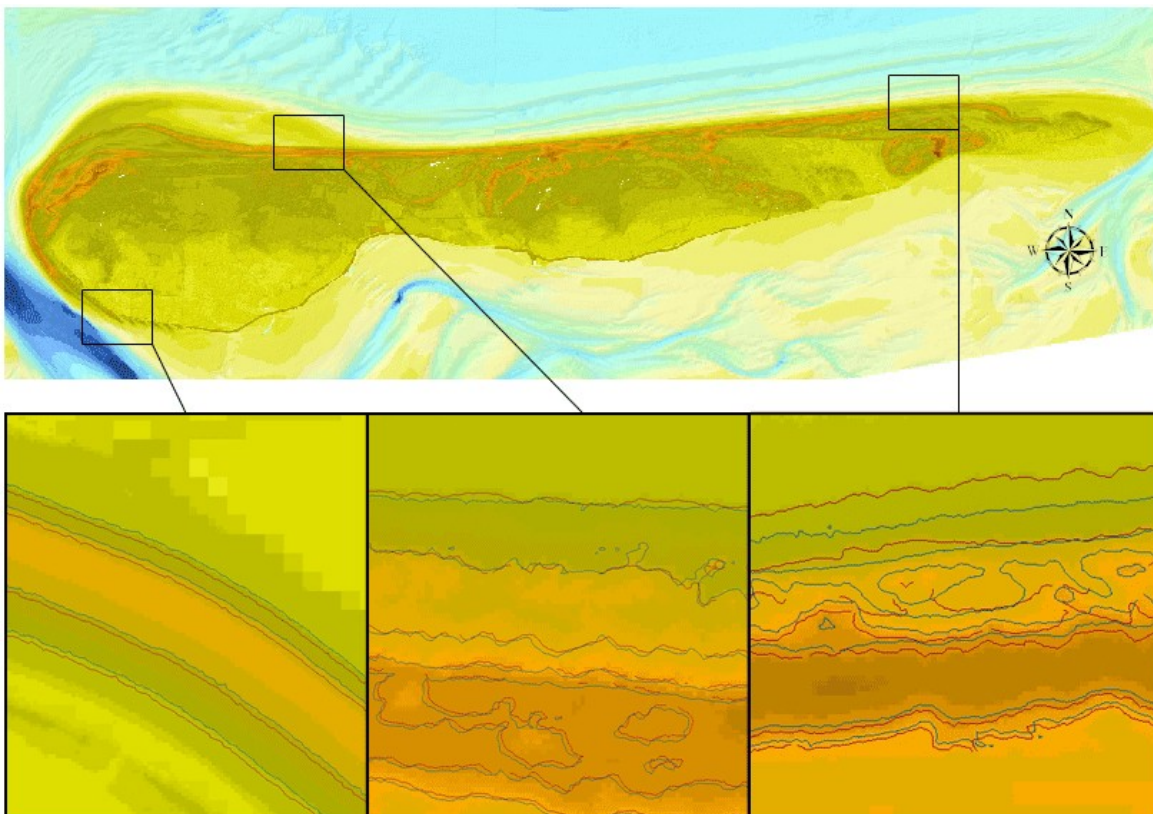


Figure 13: Contour lines of Ameland at enlarged areas of data STORM (red) and AH06 (blue). Contour lines are plotted at 3, 5, 7, 9 and 11 m N.A.P.

Secondly, for assessing the vertical accuracy, and investigated more in-depth the horizontal accuracy cross-sections are investigated. It is chosen to investigate surfaces that do not move in time and space. These locations are in literature referred to as ground control points (GCP). Dataset (STORM) GCPs cross-sections are compared on horizontal and vertical inaccuracies with cross-sections of reference data (AH06). Accurate dataset should show matching cross-sections at these GCPs. By measuring the off-set between the cross-sections, the observed inaccuracy can be quantified.

The locations of the selected GCPs are found in Figure 14. The cross-sections of the GCPs lead to the following observations (Figure 15):

- At most GCPs the off-set in the z-direction ranges between 10 and 30 cm;
- At one GCP (DikeCV), there little to no indication of elevation off-set;
- Horizontal off-set measured between cross-sections are approximately 2 m.

In addition, with the same procedure as comparing the GCPs, transects (based on dataset AH07) are compared (Figure 17). As reference year 2006 is taken and compared to year 2007 (see Figure 16 for their locations). The interpretations that are made from the results are:

- Data from transects 2006 nowhere, coincide with 2007;
- Transects from the year 2006 are approximately 20 cm lower compared to 2007;
- Horizontal off-set, measured between transect 2006 and 2007 are approximately 2 m.

Finally, from 2003 until 2010 a transect that is also a GCP (i.e. a dike) is assessed. It is used to investigate if an error is also present in different years, or the found inaccuracies can be related to only the data from the Allerheiligenstorm. The results are showing:

- No matching transects from 2003 until 2010 are found;
- Maximum horizontal shift between two transects is at maximum 4 m;
- Minimum horizontal shift between two transects is 5 cm;
- Vertical shifts ranges between 10 and 40 cm with an average of approximately 20cm.

Overall, results show that errors in the different data of AH06, AH07 and STORM at GCPs and transects. The data indicated inaccuracies in elevation with an average of 20 cm. The horizontal off-set showed to be around 2 m.

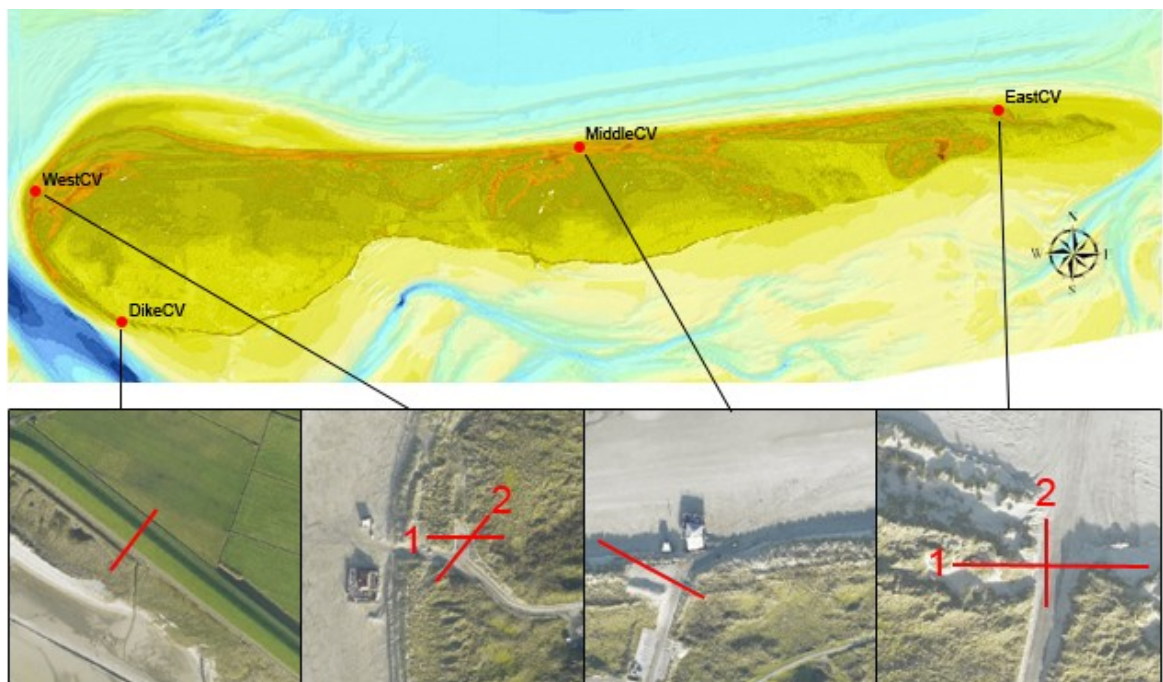


Figure 14: Locations at Ameland of GCP: 'DikeCV', 'West 1 and 2', 'MiddleCV, and 'East 1 and 2'.

Deltares

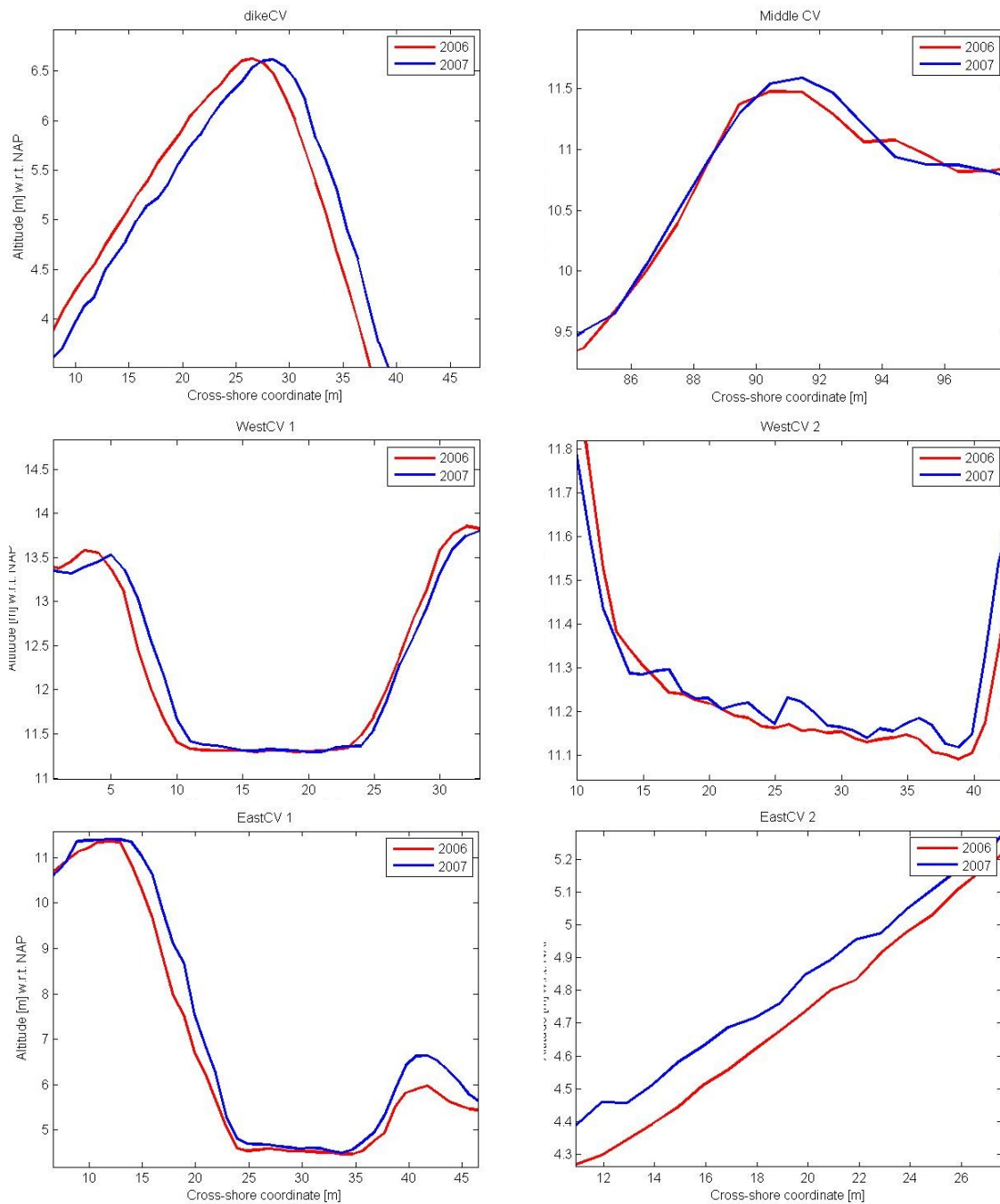


Figure 15: Cross-sections at Ameland, cross-sections AH06 (red) and STORM (blue).

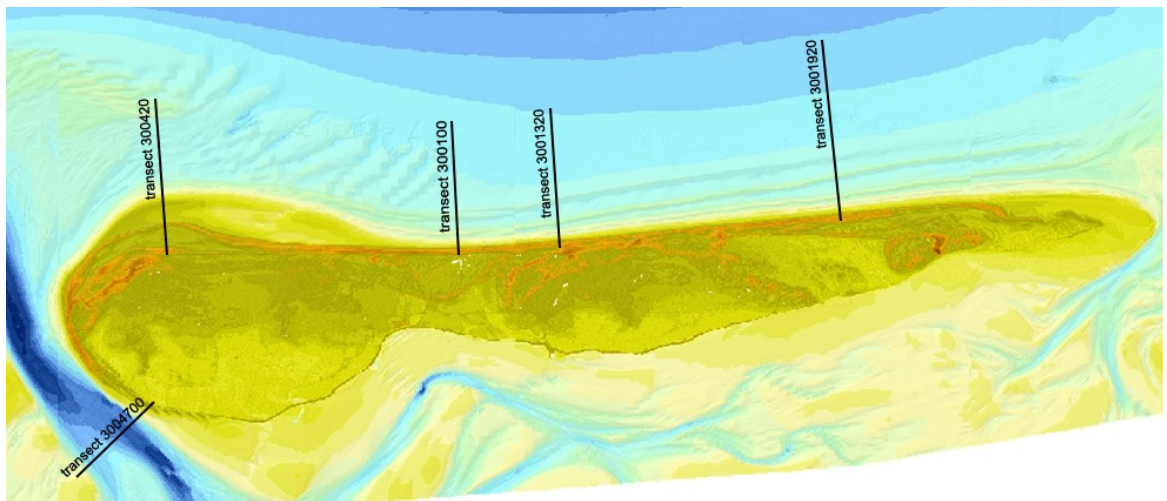


Figure 16: locations of used transects at Ameland.

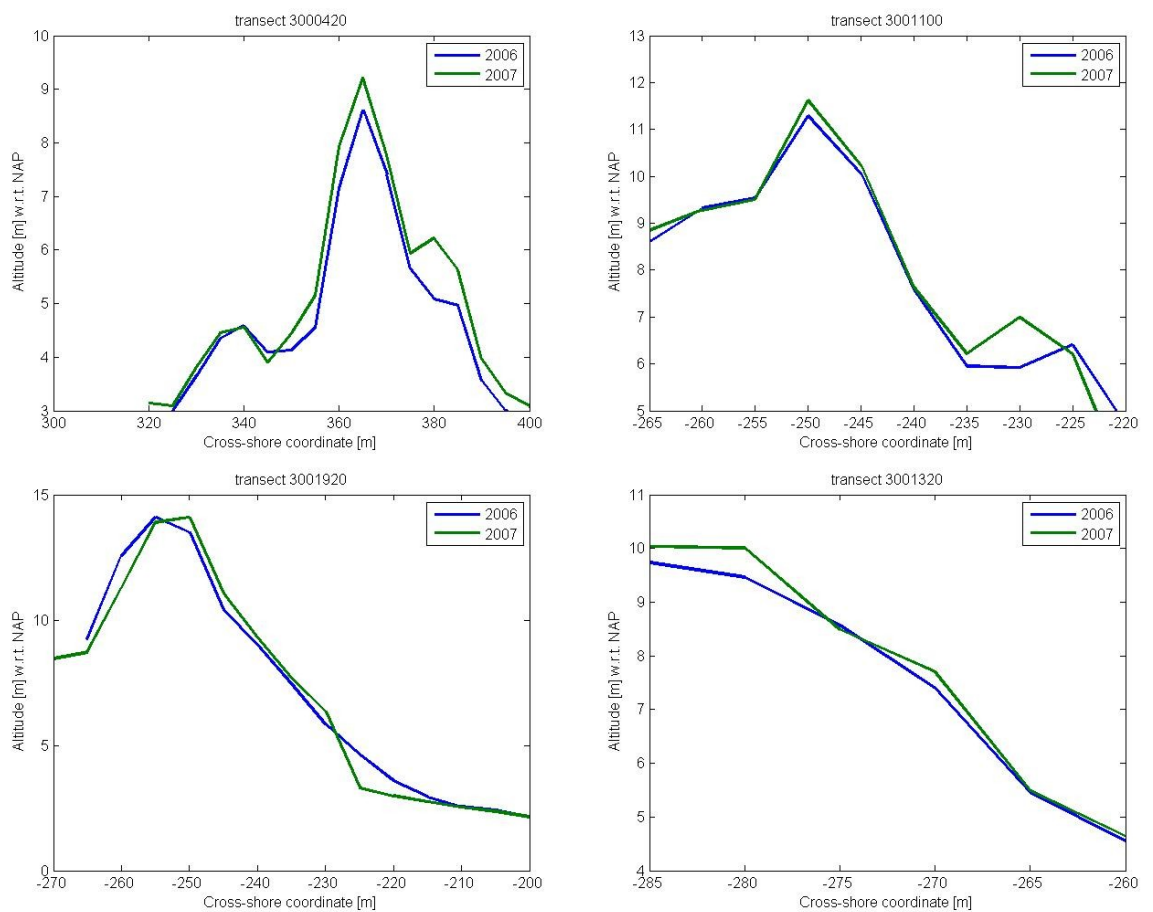


Figure 17: Transects 3000420, 3001100, 300190 and 3001320 for year 2006 (blue) and year 2007 (red).

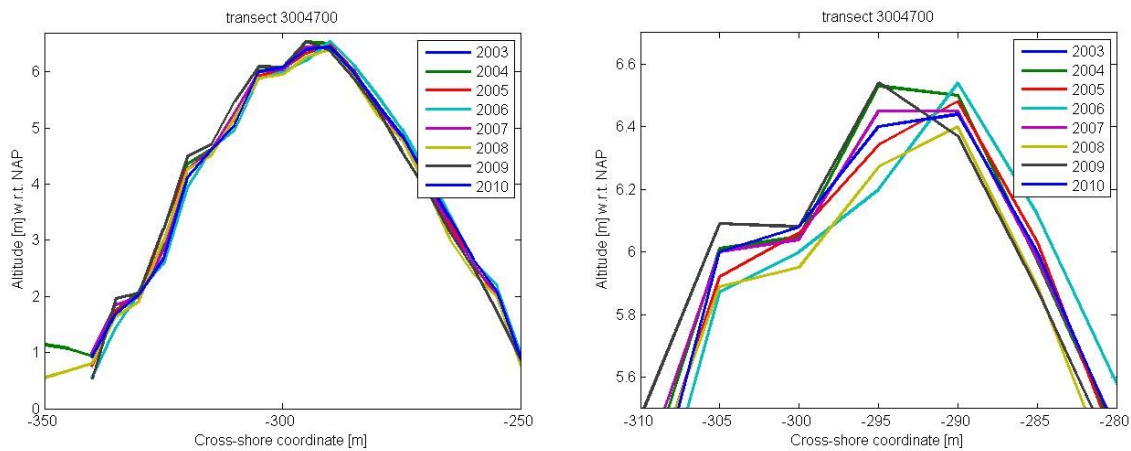


Figure 18: Transect 3004700 of a dike on Ameland. With the right figure showing an enlargement of this transect.

4.2.2 Results quality improvement

The accuracy level required by this research related to the spatial scale of identifying (small scale) overwash is relatively high (in the order of meters). Therefore, if the LIDAR will be used for qualitatively validating XBeach, improvement of accuracy of the LIDAR data is necessary.

The following actions are performed on the AH07 and STORM data trying to improve the accuracy of the data:

- Changing vertical z- direction;
- Shifting horizontal x- and y-direction;
- Combined together changing of x-, y- and z-directions.

The changed AH07 and STORM data is investigated to establish whether or not the accuracy improved. For assessing the data, an approach followed that is based on comparing elevations obtained from the changed datasets (AH07 and STORM) with reference data (AH06). The used approach has been elaborately explained in chapter 4.2.1.

This assessment resulted in the observation that accuracy was not improved. Only for limited parts of topographic areas of approximately 100x20 m showed that (better) matching data could be achieved (i.e. less average off-set in x- y- and z-direction). Overall, the average off-set measured at the contour lines, cross-sections and GCPs, increased compared to the off-set found without any performed actions.

In the assessment of the 'improved' data, it was found that at some locations better matching data could be achieved. Therefore, improving the quality of the data, based on only parts of the LIDAR data, is tried. The same operations on these separate parts of LIDAR data were executed as what was done to the total datasets of AH07 and storm. The separation of the LIDAR data parts are based on:

- Recorded flight paths during collection of the LIDAR data;
- The four different GCPs present at Ameland (see Figure 14).

The induced actions were assessed on how they affected the accuracy. The results showed accuracy was not improved. There are not enough GCPs available in Ameland to improve the accuracy of the data. Furthermore, performed improvement actions based on flight paths did

not seems the help. Overall, it can be said that the current operation did not improve accuracy of the LIDAR data of STORM and AH07. The data indicated that the errors are the result of a (not linear) shift, whereby shifting data only (partly) in x- y- or z-direction is insufficient.

4.2.3 Discussion

A prerequisite to validate a model, is to have accurate data. Results of the data investigation showed this prerequisite was not met. What is realistic to expect from LIDAR data if it is used for validation of the numerical models such as XBeach?

First of all, what in general can be expected from large-scale mapping using LIDAR? It is known that vertical accuracies for LIDAR of 0.15 m root-mean-square error are very difficult to achieve (Aguilar et al., 2010; Sallenger et al., 2003). A few comparable empirical studies have been conducted to investigate the accuracy that can be expected from LIDAR. These studies suggesting to expect vertical accuracies of 0.14–1.50 m root-mean-square error for large-scale mapping applications (Adams et al., 2002; Hodgson et al., 2004; Raber et al., 2007). The horizontal accuracy is to be expected less than several meters (Sallenger et al., 2003). Nevertheless, Rijkswaterstaat (2007) claims that the data used in this research much more accurate. It is stated by Rijkswaterstaat that vertical accuracy of the current LIDAR data consist for more than 50 % of the data with a maximum error of 5 cm, 67 % of the data with a maximum error of 10 cm and 95 % of the data with a maximum error of 15 cm. The presented results of the data investigation showed on average vertical inaccuracies larger than 15 cm. The horizontal accuracy of the data showed sometimes offsets as large as 2 m.

What could have been the reason of the found inaccuracies in used LIDAR data? Sources affecting LIDAR accuracy have been enumerated and discussed in many papers (Baltsavias, 1999 and Behan et al., 2000). We expect that errors in the data originated from various sources; the collection, calibration, interpretation and storage of the data.

Because of public tendering regulations, companies collecting LIDAR data can change on a yearly basis. Despite regulations for the collection of LIDAR data, these companies are allowed to use different (measurement) equipment and methods. This can affect the range, platform position and altitude, and laser beam direction (Baltsavias, 1999).

Furthermore, calibration of the LIDAR data on Ameland for the position and altitude is based on a local soccer field used as reference area (i.e. GCP). The x- and y-direction cannot be accurately calibrated (horizontal) with such an area. Results are not affected by a shifting position due to the flat nature of the area. The altitude measurements contain a small error due to this calibration method. Grass length and unevenness in the field might affect the calibration in the order of centimeters.

Moreover, Rijkswaterstaat uses visual interpretation to improve the accuracy, maps are aligned with reference layers. Our experience in this research with visual correction showed that it was time consuming and difficult to apply correctly, especially for obtaining sufficient accuracy to validate XBeach on our required detailed level. It might be to this time consuming and difficult nature that visual correction was not applied correctly.

Rijkswaterstaat (2007) also stated in their report that correction factors for processing the LIDAR data were used. It is unknown how these were applied and affect the present data. It is known that correction factors can (if applied correct) improve the accuracy of LIDAR data, but can also can have an error enhancing effect (Hladik et al., 2012). Formulae using

correction factors, exist for both horizontal and vertical accuracy improvement (Baltsavias, 1999),

Finally, the errors can originate from the large amount of data. Yearly, large amounts of data have to be transformed to the local (RD) coordinate system and checked by visual observation for inconsistencies. These sources of errors could have resulted in the observed inaccuracy in the LIDAR data used for the research presented in this report.

As a consequence of the observed inaccuracies, it has been difficult to derive three dimensional measurements of beach change with sufficient resolution and accuracy to validate XBeach. For quantitative analyses, using the current data, similar research by Hodgson and Bresnahan (2004) suggested that a resolution of 20x20 m. Their results showed that for numerical simulations of dune evolution based on sediment volumes on a 20x20 m scale showed an acceptable deviation from its true value. Hence, this resolution could be used for qualitatively validating XBeach for volumetric sediment changes.

In this research the necessary accuracy of the LIDAR is confined by the resolution required to represent the topographic complexity of overwash dynamics. To represent the (small) scale overwash features at Ameland, an 20x20 m resolution would be too coarse to simulate the distinguish overwash feature. A more suitable resolution for the intended research would be in the order of a few meters.

4.2.4 Conclusion

After an elaborate data investigation, it leads to the following conclusions regarding the data quality:

- Contour lines showed a shift of the back of the dune towards sea. This observation cannot be explained due to natural processes;
- Different cross-sections at GCP showed a shift of approximated 2 m in x- (longitude) and y-direction (latitude);
- Data indicated a error of on average approximately 20 cm in the z-direction;
- The different transects are confirming the observation of shift in the x- and y-direction also revealing;
- Errors can be found independently from the year they are collected;
- transect data can be found The inaccuracies are larger than the stated measurement errors by Rijkswaterstaat (2007). The data requirements set by Rijkswaterstaat are not met.

The results found can only be explained by a (systematic) error in measuring, collecting and processing of the data. The LIDAR data is of insufficient quality (at the moment) for the required (small scale) spatial resolution in the order of meters necessary for validating XBeach quantitatively. Therefore, a qualitative approach to identify overwash is followed.

4.3 Results observations

This section will present the results of the data analyses for identifying overwash locations. Two locations where overwash was present are identified. These two locations will be referred to as Paal22 and DeHon. Paal22 is named accordingly to 'Strandpaal' number 22 and is described in the first paragraph. DeHon is named after the nature reserve where it is located. It will be described in the second paragraph. The section will end with conclusions.

Both locations are situated at the east side of Ameland (Figure 19). These locations have considerable lower coastal dunes compared to remainder dunes at Ameland. The dune crests are around or lower than +5 m N.A.P. at Paal22 and DeHon, whereby at other places dune crests ranges above +10 m N.A.P. At DeHon, there where overwash fans present due to previously induced storm impact. At Paal22, all the observed morphological overwash impact is due the Allerheiligenstorm event.

Paal22, with corresponding coordinates RD_x 189.300 and RD_y 609.100 is shown in Figure 20. The total area of morphological interest is 300 m wide. DeHon is approximately located 1.5 kilometers more eastward from Paal22 at RD_x 191.500 and RD_y 610.000 (Figure 21). The extent of the overwash area is much larger than at Paal22 and is around 1500 m wide.

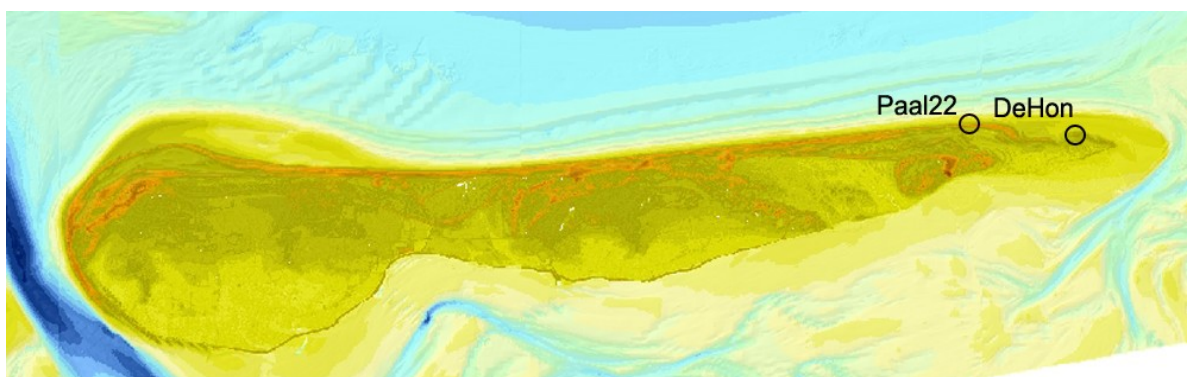


Figure 19: Location Paal22 and DeHon at Ameland.

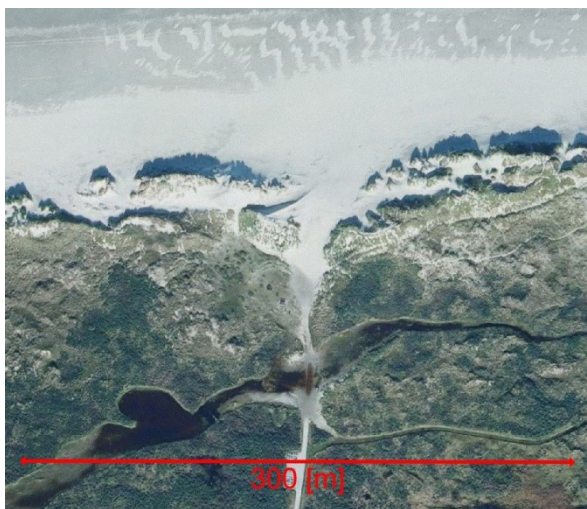


Figure 20: Location Paal22 at Ameland.

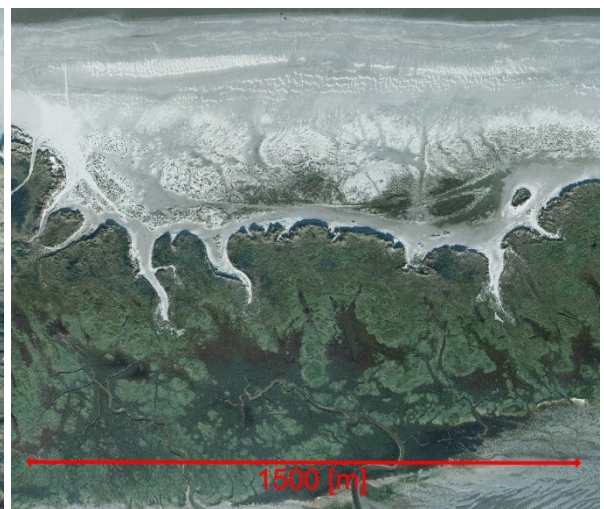


Figure 21: Location DeHon at Ameland.

4.3.1 Location Paal22

Location Paal22 is an access route through the foredune, to the beach (Figure 22). It can be seen that behind the foredune ridge an inundated area is present. At this location, Ameland is around 2 km wide at and morphodynamics are governed by the North Sea.

Notable, after the Allerheiligenstorm employees from the water company detected that salt water had entered the inundated fresh water area. This observation can be explained due to the fact that storm impact resulted in an extensive amount of overwash. Because of this, transported sand and salt water could contaminate the fresh water supply.

Deltares

Moreover, washover could also be observed from PHOTO and AERIAL data. A sandy surface with absence of vegetation is observed (Figure 22). Washover occurs at the washover mouth. The maximum distance between the intermittent dune ridge measures approximately 25 m. The intrusion of the washover (i.e. the extent in relation to the mouth of the overwash), can be observed until the inundated area at the back barrier. The overwash occurrence has an extent of 100 m. The dune crest at washover occurrence is approximate +5 m N.A.P. The narrowest part of washover occurrence is 5 m wide. The highest dunes that enclose the washover around the passageway is +/- 16 m. Overall, these measured dimensions results into the overwash occurrence presented in Figure 23.

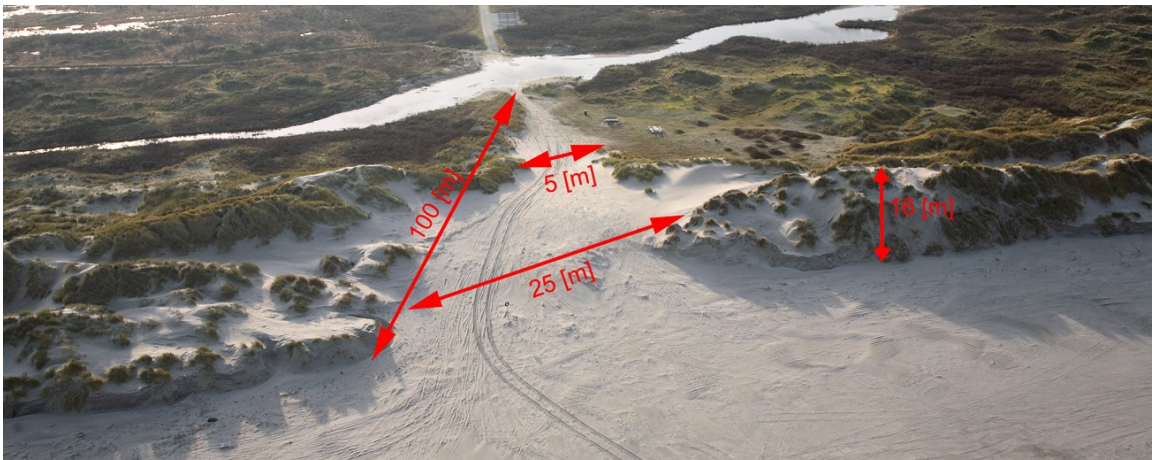


Figure 22: Paal22 shortly after the Allerheiligenstorm, with the dimensions of overwash occurrence.



Figure 23: Observed overwash occurrence during the Allerheiligenstorm at Paal22.

Next, the extent of the collision regime at Paal22 is identified. Collision starts occurring when the storm surge has sufficient magnitude to erode sand from the dune foot. This morphological feature is visible on photographs. Unfortunately, at location Paal22 no photograph was taken to illustrate this morphological impact. In addition, the AERIAL data represented difficulties to distinguish (and illustrate) collision occurrence. As an illustration of collision occurrence, a photograph taken close by to Paal22 is shown (Figure 24). It shows a dune ridge located 2 km west of Paal22.

Similar morphological collision behavior can be expected at Paal22 because the occurred collision is similar at these locations. Collision occurrence is defined when morphological

storm impact can be observed above the reference of +3 m N.A.P. Using this criteria, LIDAR data of AH06 and STORM can show this collision occurrence. A displacement of around 10 m of the dune foot is measured at Paal22 (Figure 35), similar as measured at the location of Figure 24. This is more than at (most) other locations where it is around the +6 m. It should take into mind that this is only an indication of the dimensions of the collision occurrence, due to inaccuracies in the data measurement errors.

The maximum extent of the collision can be easily derived from LIDAR data. In this identified area the observed morphological impact, it is related to collision impact.



Figure 24: Aerial photograph taken after the storm at 29/11/2006 at Ameland.

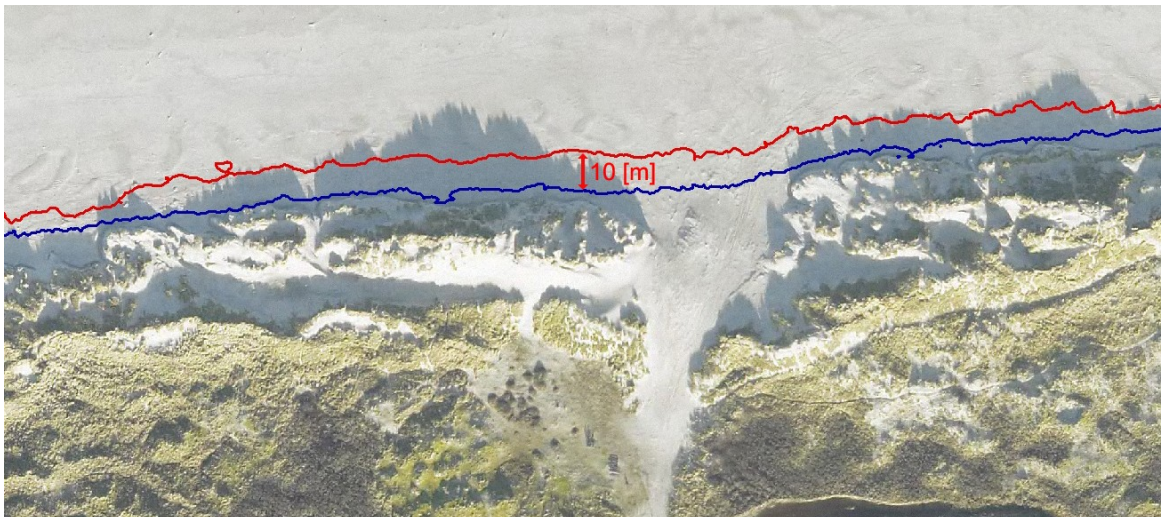


Figure 25: AH06 data (red) and STORM data (blue) contour line at +3 m N.A.P.

Finally, the area affected by the morphological impact due to swash is identified. The occurrence of swash is defined to be above +1.5 m N.A.P. and can directly be derived from AH06. The limit of the swash regime is based on the presumption that swash run-up is confined from the beach, seaward until the dune foot. The dune foot is based on LIDAR data AH06 and used as criteria to limit if the morphological impact by the swash regime.

Summarizing, the different maximum extent of swash, collision and overwash occurrence are identified based on criteria's of limit and maximum extent. These results are combined and a

delineation of the areas affected by these regimes during the Allerheiligenstorm is made (Figure 26). The figure shows where different regimes governed morphological impact, until the severity of the storm increased sufficient to enter the next impact regime. It can help to interpret the visible and simulated morphological impact and relate to different processes that are associated with the identified regimes.

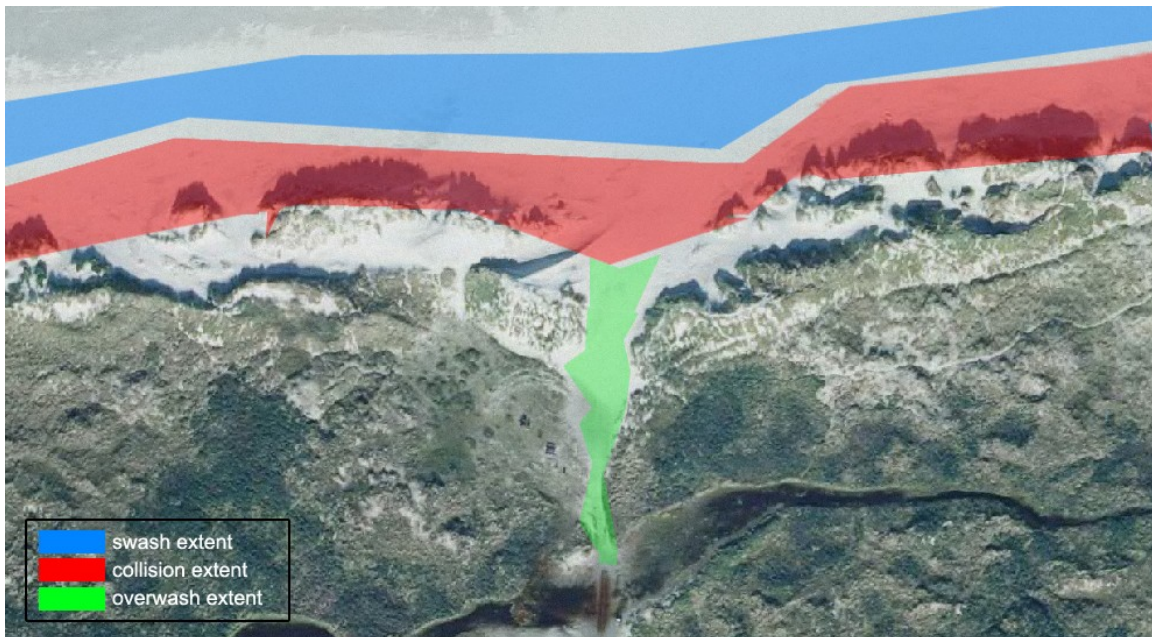


Figure 26: Delineation of different regimes present at de Allerheiligenstorm.

4.3.2 Location DeHon

DeHon is nature reserve that is subject to much morphological changes. There are new dunes developing and salt water marches are forming at the back barrier. Multiple washover fans can be found at location DeHon (see Figure 21).

Many morphological changes can be related to the physical processes governed by the North Sea. In addition, it is important to consider some processes are influence by the Wadden Sea. The Wadden Sea is located south (left in Figure 27) at a distance of less than a kilometer. Therefore, when a high storm surge is presented, some areas can be inundated and can influence water fluxes due to storm impact induced by the Wadden Sea. Furthermore, field research at this location revealed that within these fans peat layers are present. These peat layers form a hard surface and are difficult to erode.

The photo of the washover fan clearly shows a sandy surface with absence of vegetation, associated with washover processes. The washover mouth of the fan, the length of the imaginary line that can connect the two longshore shoreline positions, is 70 m long. The intrusion of water fluxes due to overwash in relation to the mouth, had an extent of 230 m. The narrowest part of the washover occurrence is around 15 m wide and it is surrounded by dunes with a height of around +20 m N.A.P. at the front and +10 m N.A.P. at the back. Behind the structure (in the middle of Figure 27) it can be seen that there is some unvegetated area covered with sand, indicating overwash.

This section presents only results for washover occurrence at one fan (the middle picture of Figure 28). Photos, and obtained dimension of overwash occurrence of the other fans are found in Appendix A. All the results combined together are presented in Figure 28.



Figure 27: DeHon shortly after the Allerheiligenstorm, with dimensions of overwash occurrence.



Figure 28: Observed overwash occurrence during the Allerheiligenstorm.

Figure 29 shows the +3 N.A.P. lines from before and after Allerheiligenstorm. At several places, the dune foot is eroded away. On the contrary to Paal22, there is also some indication of severe sedimentation below the dune foot. At some locations the dune foot shifted towards the sea. This might also be the effect of avalanching occurring. Overall the collision occurrence at DeHon does not show to have a large impact. From the data, the (maximum) collisions extend is directly obtained. Likewise, the swash impact limit was retrieved from the data. The swash extend is based on the +3 N.A.P. lines from before the Allerheiligenstorm (see also Figure 29).

Deltares

These dimensions can be used to make a delineation of the areas that are affected by different storm regimes (Figure 30). Within each regime, patterns and relative magnitude of net erosion are unique. The border between the regimes represents thresholds that defining when water level is of sufficient height, processes and magnitudes of impact change significantly. This figure can help be identified and compared these (the still visible after storm) significant changes during the different impact regime.

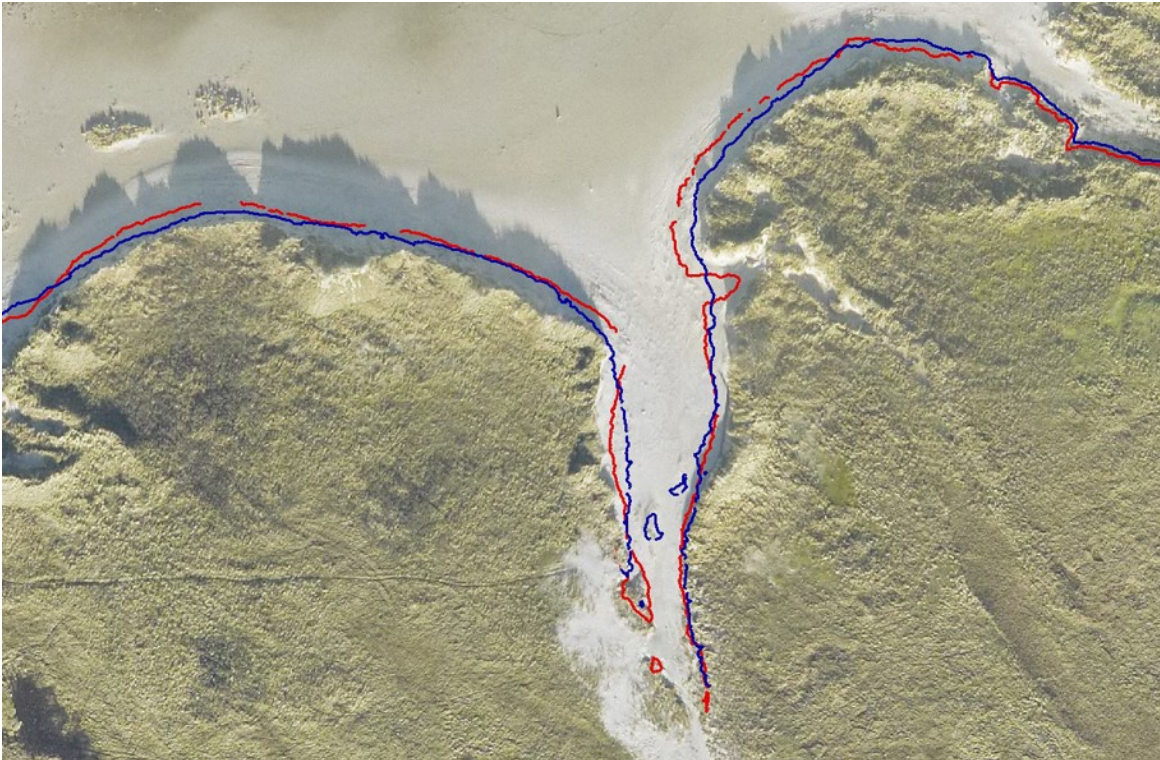


Figure 29: AH06 data (red) and STORM data (blue) contour line at +3 m N.A.P. Most right overwash fan at DeHon (see Figure 28).

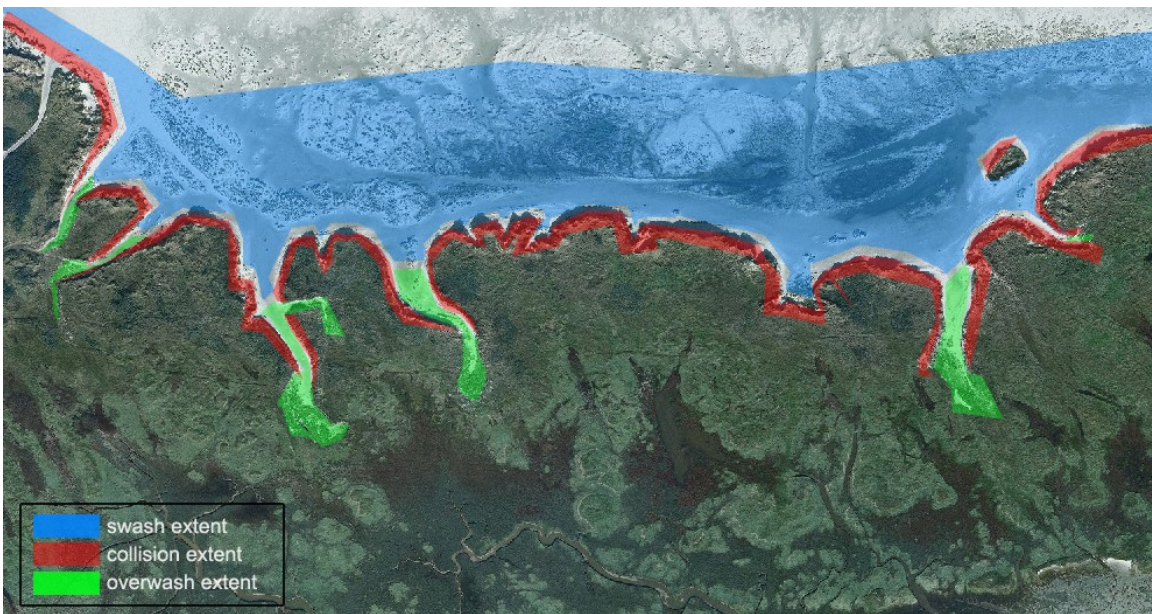


Figure 30: Delineation of different regimes present at de Allerheiligenstorm.

4.4 Conclusions

The collected data of the coastal dunes of the barrier island Ameland during storm surges of 1 November 2006 show two overwash locations: Paal22 and DeHon. The locations where threshold is exceeded to the subsequent impact morphological impact regime were identified

No conclusions about the (net) amounts of transport related to different storm impact regimes could be made due to insufficient quality of data. Therefore, criterias are used to quantify morphological storm impact.

The criteria of collision occurrence at Paal22 and DeHon could be observed. As a consequence storm impact, sand was transported offshore (or longshore), what resulted in net erosion of the dune front. The induced erosion was observed due to a shifted dune foot (mostly) land inward approximately 10 m and 5 m at respectively location Paal22 and DeHon.

The presence of the overwash regime during the Allerheiligenstorm was identified at Paal22 and DeHon by identifying overwash fans, which are characteristic features of the overwash regime. In this regime the sand undergoes a net landward transport starting at the overwash mouth, through the overwash channel.

Between these two locations there is a notable difference in magnitude of the observed overwash. At location DeHon the overwash is observed to be of larger magnitude than at location Paal22. The observed and measured data indicates that overwash intrusion reached as far as 90 and 230 m land inwards, at respectively location Paal22 and DeHon.

Summarizing, two overwash areas could be identified at Ameland. At other locations not indications were found that overwash was present during the Allerheiligenstorm.

5 Modeling in XBeach

We simulated the morphological behavior at two different locations. In this chapter, the results of these simulations by XBeach are presented. Firstly, the approach to obtain results with XBeach is presented. Next, the results are presented of the two different locations, Paal22 and DeHon. Finally, this chapter will conclude about the accuracy of the obtained overwash predictions.

5.1 Methodology

To simulate the morphological changes during the Allerheiligenstorm, XBeach is used. In this paragraph, firstly the mathematical methodology of the program is explained. Next, the approach to set up the model simulation is laid out. Finally, the approach to obtain the necessary results from XBeach simulations to fulfill the research goal is explained.

5.1.1 Model background

In this part a short description is given of mathematical background of the physics in the XBeach. Most physical processes are qualitatively described in the literature review (see chapter 2), in this part different processes are mathematically described. A more elaborated explanation can be found in the XBeach manual (Roelvink et al., 2010).

XBeach is an open source, process based, morphodynamic, numerical model (Roelvink et al., 2010). The model solves coupled 2D horizontal equations for wave propagation, flow, sediment transport and bottom changes, for varying (spectral) wave and flow boundary conditions. Because the model takes into account the variation in wave height in time it can resolve the long wave motions created by this variation (Roelvink et al., 2010).

Short wave-action equation

The wave forcing in the shallow water momentum equation is obtained from a time dependent version of the wave-action balance equation. Similar to Delft University's (stationary) HISWA model (Holthuijsen et al., 1989):

$$\frac{\partial A}{\partial t} + \frac{\partial c_x A}{\partial x} + \frac{\partial c_y A}{\partial y} + \frac{\partial c_\theta A}{\partial \theta} = -\frac{D_w}{\sigma} \quad (5.1)$$

With the wave A action given by:

$$A(x, y, t, \theta) = \frac{S_w(x, y, t, \theta)}{\sigma(x, y, t)} \quad (5.2)$$

Where the formula represents wave-action propagation speeds by C_x and C_y , θ represents the angle of incidence with respect to the x-axis, s_w represents the wave energy density in each directional bin and σ the intrinsic wave frequency and D_w is the wave energy dissipation calculated according Roelvink (1993),

Finally, given the spatial distribution of the wave action and therefore wave energy the radiation stresses (important for the modeling the bound long wave) can be evaluated (using linear wave theory):

$$\begin{aligned}
 S_{xx}(x, y, t) &= \int \left(\frac{c_g}{c} (1 + \cos^2 \theta) - \frac{1}{2} \right) S_w d\theta \\
 S_{xy}(x, y, t) &= S_{yx,w} = \int \sin \theta \cos \theta \left(\frac{c_g}{c} S_w \right) d\theta \\
 S_{yy}(x, y, t) &= \int \left(\frac{c_g}{c} (1 + \sin^2 \theta) - \frac{1}{2} \right) S_w d\theta
 \end{aligned} \tag{5.3}$$

Roller energy balance

The roller energy balance is coupled to the wave action/energy balance, where dissipation of wave energy serves as a source term for the roller energy balance. The roller energy balance is then given by equation 5.4:

$$\frac{\partial S_r}{\partial t} + \frac{\partial c_x S_r}{\partial x} + \frac{\partial c_y S_r}{\partial y} + \frac{\partial c_\theta S_r}{\partial \theta} = -D_r + D_w \tag{5.4}$$

The roller energy in each directional bin represented by $S_r(x, y, t, \theta)$, The total roller energy dissipation D_r according to Reniers et al. (2004). The roller energy The propagation speed in c and D_w the wave energy dissipation are the same as used for the wave energy density propagation as used in short wave equation.

The roller contribution to radiation stress is given by:

$$\begin{aligned}
 S_{xx,r}(x, y, t) &= \int \cos^2 \theta S_r d\theta \\
 S_{xy,r}(x, y, t) &= S_{yx,r}(x, y, t) = \int \sin \theta \cos \theta S_r d\theta \\
 S_{yy,r}(x, y, t) &= \int \sin^2 \theta S_r d\theta
 \end{aligned} \tag{5.5}$$

Roller induced shear stresses are calculated from the spatial distribution of roller energy:

$$\begin{aligned}
 F_x(x, y, t) &= - \left(\frac{\partial S_{xx,w} + S_{xx,r}}{\partial x} + \frac{\partial S_{xy,w} + S_{xy,r}}{\partial y} \right) \\
 F_y(x, y, t) &= - \left(\frac{\partial S_{xy,w} + S_{xy,r}}{\partial x} + \frac{\partial S_{yy,w} + S_{yy,r}}{\partial y} \right)
 \end{aligned} \tag{5.6}$$

Shallow water equations

For the low-frequency and mean flows the shallow water equations are used. To account for the wave induced mass-flux and the subsequent (return) flow these are cast into a depth-averaged Generalized Lagrangian Mean (GLM) formulation (Andrews et al., 1978; Walstra et al., 2000)

$$u^L = u^E + u^S \quad \text{and} \quad v^L = v^E + v^S \tag{5.7}$$

Here u^S , v^S represents the Stokes drift in x- and y-direction respectively (Phillips, 1978):

$$u^s = \frac{E_w \cos \theta}{\rho h c} \quad \text{and} \quad v^s = \frac{E_w \sin \theta}{\rho h c} \quad (5.8)$$

Where the wave-group varying short wave energy and direction are obtained from the wave-action balance. The resulting GLM-momentum equations are given by:

$$\begin{aligned} \frac{\partial v^L}{\partial t} + u^L \frac{\partial v^L}{\partial x} + v^L \frac{\partial v^L}{\partial y} + f u^L - \nu_h \left(\frac{\partial^2 v^L}{\partial x^2} + \frac{\partial^2 v^L}{\partial y^2} \right) &= + \frac{\tau_{sy}}{\rho h} - \frac{\tau_{by}^E}{\rho h} - g \frac{\partial \eta}{\partial y} + \frac{F_y}{\rho h} \\ \frac{\partial u^L}{\partial t} + u^L \frac{\partial u^L}{\partial x} + v^L \frac{\partial u^L}{\partial y} - f v^L - \nu_h \left(\frac{\partial^2 u^L}{\partial x^2} + \frac{\partial^2 u^L}{\partial y^2} \right) &= \frac{\tau_{sx}}{\rho h} - \frac{\tau_{bx}^E}{\rho h} - g \frac{\partial \eta}{\partial x} + \frac{F_x}{\rho h} \\ \frac{\partial \eta}{\partial t} + \frac{\partial h u^L}{\partial x} + \frac{\partial h v^L}{\partial y} &= 0 \end{aligned} \quad (5.9)$$

Here τ_{bx}, τ_{by} are the bed shear stresses, η is the water level, F_x, F_y are the wave-induced stresses, ν_h is the horizontal viscosity and f is the Coriolis coefficient. The bottom shear stress terms are calculated with the Eulerian velocities as experienced by the bed

$$u^E = u^L - u^s \quad \text{and} \quad v^E = v^L - v^s \quad (5.10)$$

Also, the boundary condition for the flow computations are expressed in functions of (u^L, v^L) and not (u^E, v^E).

Sediment transport formulations

The sediment transport is modeled with a depth-averaged advection diffusion equation (Galappatti et al., 1985):

$$\frac{\partial hC}{\partial t} + \frac{\partial hCu^E}{\partial x} + \frac{\partial hCv^E}{\partial y} + \frac{\partial}{\partial x} \left[D_h h \frac{\partial C}{\partial x} \right] + \frac{\partial}{\partial y} \left[D_h h \frac{\partial C}{\partial y} \right] = \frac{hC_{eq} - hC}{T_s} \quad (5.11)$$

Where C represents the depth-averaged sediment concentration which varies on the wave-group time scale, and D_h is the sediment diffusion coefficient. The entrainment of the sediment is represented by an adaptation time T_s , given by a simple approximation based on the local water depth, h.

Transport formulations

For calculating the sediment transport formulation of Soulsby - van Rijn (Soulsby, 1997) has been implemented.

$$C_{eq} = \frac{A_{sb} + A_{ss}}{h} \left(\left(|u^E|^2 + 0.018 \frac{u_{rms}^2}{C_d} \right)^{0.5} - u_{cr} \right)^{2.4} (1 - \alpha_b m) \quad (5.12)$$

Where sediment is stirred by the Eulerian mean and infragravity velocity in combination with the near bed short-wave orbital velocity, u_{rms} , obtained from the wave-group varying wave energy using linear wave theory.

The combined mean/infragravity and orbital velocity have to exceed a threshold value, u_{cr} , before sediment is set in motion. The drag coefficient, C_d , is due to flow velocity only (ignoring shortwave effects). To account for bed-slope effects on the equilibrium sediment concentration a bed-slope correction factor is introduced, where the bed slope is denoted by m and α_b represents a calibration factor. The bed load coefficients A_{sb} and the suspended load coefficient A_{ss} are functions of the sediment grain size, relative density of the sediment and the local water depth

5.1.2 Model setup

The grid that will be applied is a rectilinear, non-equidistant, staggered grid. XBeach allows the grid size to vary in cross shore and longshore direction. Depending on the size and the geometry of the interest area, corresponding resolutions for computational grids are chosen.

The spatial resolutions of two computational grids are chosen to accurately represent the scale and dimension of the observed overwash processes. At location Paal22, the overwash occurrence is in the order of meters. The smallest possible grid resolution at the area of interest (60 m) in XBeach is chosen to represent this area, a 1x1 m grid (Figure 32). The magnitude of overwash at DeHon showed to be in the order of 10 m and the area of interest is much wider (1250 m), therefore a coarser resolution for the area of interest is chosen, a 5x5 m grid (Figure 33).

More details of the processing of LIDAR to represent the grids of the different locations XBeach are shown in Appendix B. In Appendix C the used model setup parameters are shown.

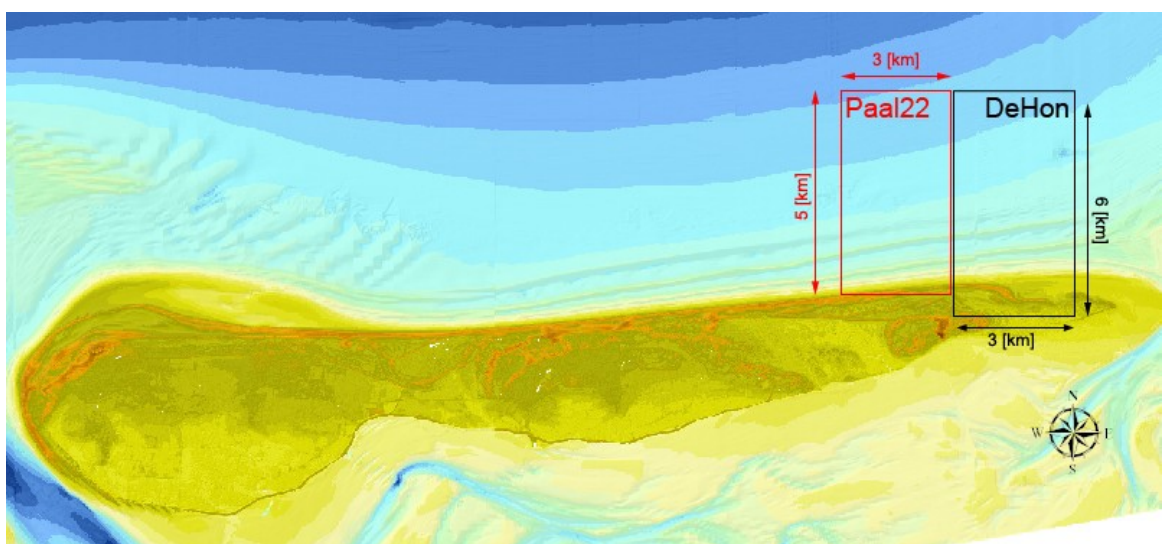


Figure 31: location of grid Paal22 and grid DeHon modeled in XBeach.

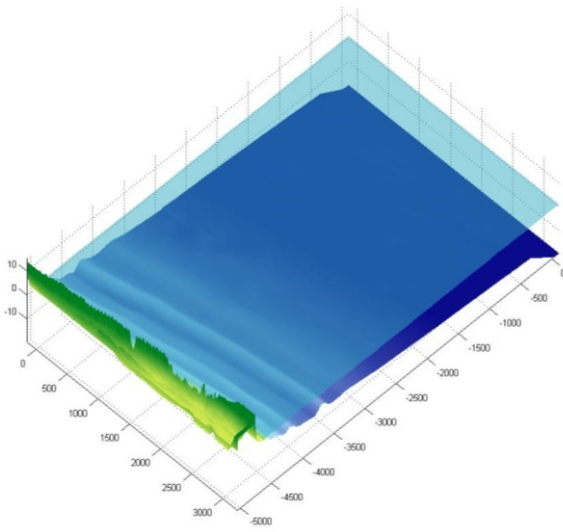


Figure 32: Grid in XBeach of Paal22.

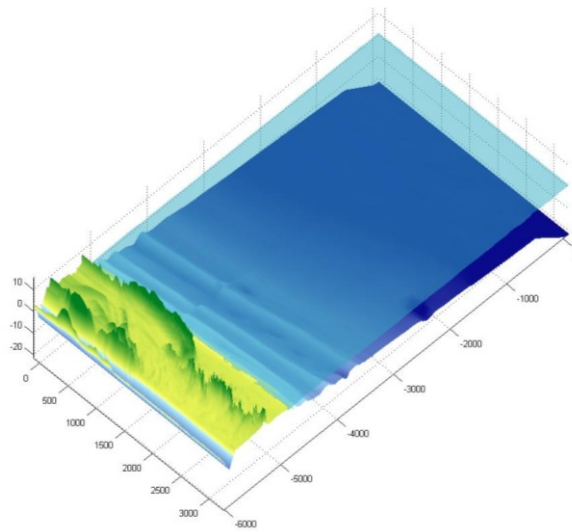


Figure 33: Grid in XBeach of DeHon.

The boundary conditions required to inform the interior of the numerical model about the world outside the model are in the next section described. Because of the strong influence of boundary conditions on the result of the model, it is essential to have properly defined boundaries

Offshore boundary is an artificial boundary which has no physical meaning. Flow boundary conditions in XBeach are represented by the absorbing-generating boundary condition of Dongeren et al. (1997) is applied on the offshore boundary. This boundary condition is based on the Method of Characteristics and allows outgoing long waves to pass through the boundary with minimal reflection, irrespective of the angle of the long wave. At the same time the boundary can be used to generate long waves. Also short wave forcing occurs at the offshore boundary.

The spectrum is determined by the peak period, wave height, spectral peakedness, mean angle and directional spreading. The routine follows the procedure as outlined by Van Dongeren et al. (2003) (see Appendix C for the wave input conditions). The amplitude of each wave component at each grid point along the offshore boundary is determined by linear interpolation of the variance density corresponding to the frequency and direction of the wave component in the two neighboring input spectra.

Lateral boundaries are the boundaries perpendicular to the coastline. It is assumed that the longshore wave energy gradient is zero across the lateral boundaries and a Neumann boundary condition is applied to the wave energy. It is assumed that the wave energy gradient along the crest of the wave groups is zero. The local mean wave direction is used to determine the angle of the crest of the wave group on the boundary. The wave energy on the lateral boundary is then found by interpolation of the wave energy.

At the **Back bay boundary**, wave energy is allowed to propagate freely out of the model domain. As in general there is no propagation of wave energy in the negative x-direction, the back boundary has no influence on the results of the model.

5.1.3 Simulating results

XBeach allows us to generate large amount of data by simulating morphodynamic processes at Paal22 and DeHon. In order to understand, examine and compare the various modeling outcome and outputs, there is a need for a clear method to analyze the XBeach data. This method is described in the following paragraph.

Morphological impact predictions by XBeach of the 1st of November, 2006 storm for overwash locations Paal22 and DeHon are investigated. Predictions by XBeach of the cumulative sediment changes are used for this.

The simulated results by XBeach are investigated on overwash features that can be compared later on with the measured and observed data from the data analyses. Three different criteria are used: (i) Washover occurrence, (ii) Washover mouth and (iii) Washover intrusion. An elaborate explanation of the used criteria can be found in chapter 4.2.1.

Morphological impact regimes predictions using results of XBeach are calculated at 5 different time steps during the Allerheiligenstorm (at 01:00, 03:00, 05:00, 07:00 and 09:00 hr). Values for D_{high} , D_{low} , R_{high} and R_{low} are obtained from the XBeach model result. They are based on locations where thresholds to subsequent regimes are first exceeds. Next, it is analyzed how the preceding morphological impact regimes to overwash affect the occurrence and magnitude of simulated overwash.

The analyses will focus on how impact of the morphological regimes during the Allerheiligenstorm affected the morphological evolution of the bathymetry at Paal22 and DeHon. Whether or not overwash is occurring in XBeach can be relate to induced erosion processes in these different storm impact regimes. Overwash can occur if enough sand is eroded after continuous swash and collision storm impact. The impact regimes can either result in overwash due to dune lowering because of avalanching, or due to the fact that crest is eroded away by the prolonged attack of waves. Furthermore, another factor that can result in overwash occurrence is the storm surge level. If the storm surge level of sufficient height, it exceeds the overwash threshold (without the necessity of erosion, the above described dune crest lowering or avalanching).

The magnitude of overwash occurrences can be related to different factors. Factors can be the (sufficient) water level height, the duration or intensity of overwash occurrence, or it is related to topographic nature of the area.

Summarized, the above factors that can influence overwash occurrence and magnitude are water level height and bed level (changes). Therefore, at the five different calculated impact regimes these factors are investigated by simulating the predicted water and bed level changes in XBeach. In addition, the volumetric sediment changes between the five subsequent storm impact regimes are obtained from XBeach model simulations.

Hydrodynamic conditions during the Allerheiligenstorm on the barrier island with a gentle beach slope at Ameland are analyzed. Therefore, it will be investigated what the infragravity waves height is when overwash occurs.

The simulated total wave height by XBeach will be used to calculate infragravity wave height. To calculate infragravity wave height, equation 5.13 is used:

$$H_{rms,low} = \sqrt{8 \int_{fl}^{fh} S df} \quad (5.13)$$

It is assumed that one cross-shore profile represents the complete area of interest. Even though alongshore variability is present, the effect on the infragravity response is generally limited (Reniers et al., 2002; van Dongeren et al., 2003).

5.2 Results simulation location Paal22

In this paragraph the results of the simulation by XBeach for the location Paal22 are presented. These results allows us to compare (later on) the XBeach model predictions with measured data of the Allerheiligenstorm. First, the morphological impact prediction results Secondly, simulated morphological impact during the storm event simulation is investigated. In addition, simulated hydrodynamic conditions during the peak of the Allerheiligenstorm are presented. Finally, a conclusion is given.

5.2.1 Morphological impact predictions

In this paragraph, the predicted results of the morphological impact simulation with XBeach are presented. The conditions represent the storm of the 1st of November 2006. The results of these simulations are used to predict total storm impact and the magnitude of overwash occurrence.

Simulated changes by XBeach in sediment volumes are plotted (Figure 34). Cross-shore coordinate 1.893×10^5 correspond with the location of lowest dune crest is measured (i.e. where D_{high} has the lowest value). Offshore, accretion occurs around $y = 6.092 \times 10^5$. Closer to the dunes, small amounts of sediment are deposited on the beach. At the dune front, the XBeach predicts severe erosion.

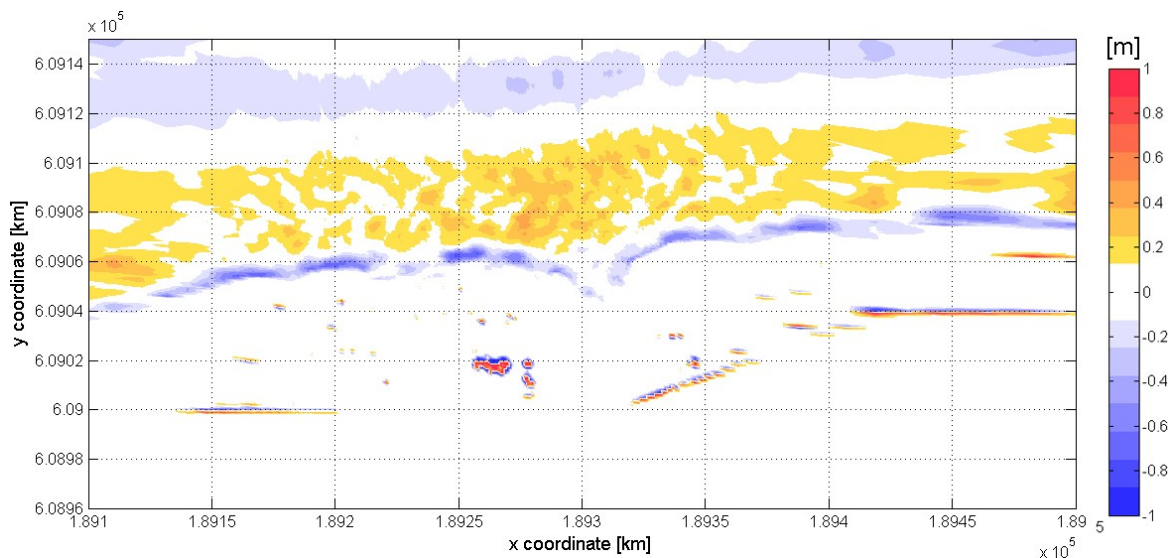


Figure 34: Erosion (blue) and sedimentation (red) prediction by XBeach, simulating the Allerheiligenstorm. The North Sea is located above.

The simulated morphological change behind the dune can be ignored. This is due the avalanching algorithm used in XBeach. This algorithm is accounting for the transport of sediment from the dry dune face to the wet swash, i.e. slumping or avalanching. In this algorithm, XBeach accounts for the fact that saturated sand moves more easily than dry sand, by introducing a critical wet slope and a dry slope. As a result, slumping should be

predominantly triggered by a combination of infragravity swash run-up on the previously dry dune face and the (smaller) critical wet slope. The modeled topography at Paal22 behind the dune exceeds the critical dry slope. Therefore, at the start of the simulation, when no morphological changes behind the dune barrier should occur, avalanching is simulated. In reality, this steep slope does not result in slumping. This is due to the presence of vegetation which retains the dune sand and prevents avalanching from occurring.

The results, ignoring the erroneous avalanching, show very low morphological impact behind the dune. The simulated changes of the bed level behind the dune barrier are very small. Nevertheless, these bed level changes are of importance to identify overwash. All this morphological impact behind the dune barrier is the result of simulated overwash by XBeach. Therefore, in Figure 35, simulated results by XBeach are presented and projected one aerial photographs, using two different scales. The first scale (1) representing morphological bed level changes at the foreshore. The second scale (2) shows the bed level changes at the back barrier.

Finally, the total extent of the overwash occurrence is obtained from the simulation by XBeach. Figure 36 accounts for the entire surface that is subject to overwash.

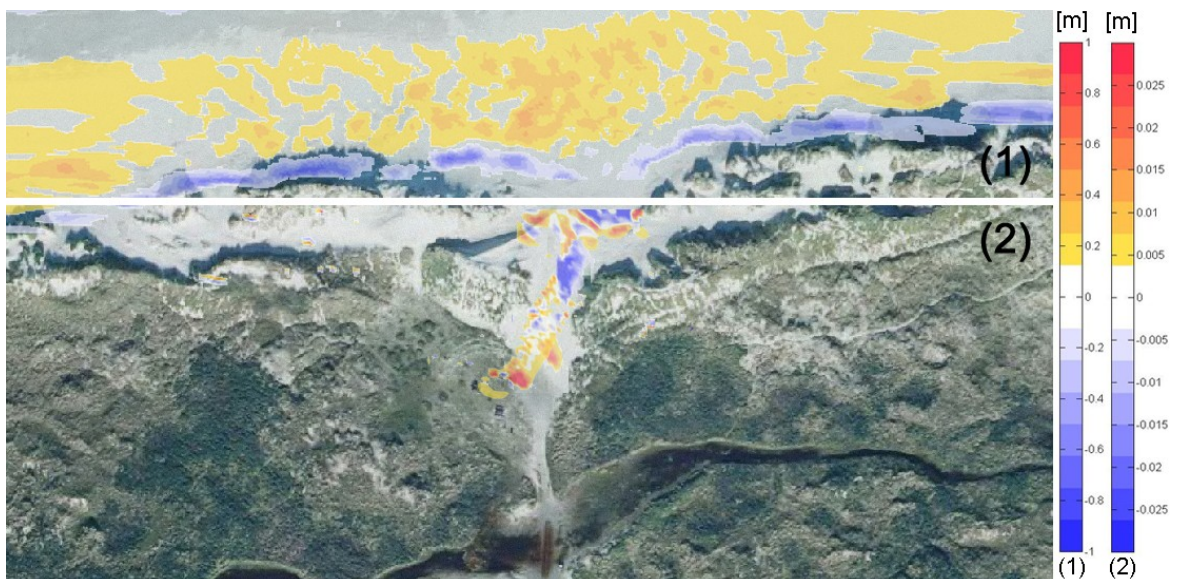


Figure 35: Erosion (blue) and sedimentation (red) prediction by XBeach, simulating the Allerheiligenstorm.



Figure 36: Overwash occurrence during the Allerheiligenstorm simulated by XBeach.

5.2.2 Morphological impact regimes

This paragraph presents results to investigate how XBeach simulates dune erosion during different storm impact regimes. For this purpose morphological evolution of the bed level profile during the Allerheiligenstorm is investigated.

Firstly, different values for D_{high} , D_{low} , R_{high} and R_{low} in time are derived from XBeach model results (Table 4). The cross-section used to obtain these value is located at x is 2495 m at Figure 38. With these values different storm impact regimes, using the definitions of chapter 3.2, were calculated. The results are shown in Figure 37. The results show different time steps and their associated impact regimes. It can be seen that at 01:00 hr the impact of the storm is swash. With the storm continuing in time the entering collision at 3:00 hr. The highest level of impact is reached at 05:00 hr. After the peak of the storm is reached, the impact decreases to the collision regimes.

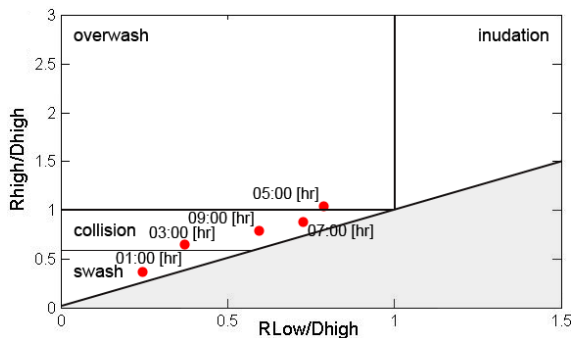


Figure 37: Delineation of the four different regimes at different time steps plotted for Paal22.

Table 4: variables at Paal22, used for Figure 37. Elevations are referenced in m to N.A.P.

Time hr	D_{high} m	D_{low} m	R_{high} m	R_{low} m	Surge
01:00	5.2	3	2.2	1.7	1.13
03:00	5.2	3	3.1	2.4	2.06
05:00	5.1	3	5.2	3.6	2.72
07:00	5.1	3	4.7	3.2	2.52
09:00	5.1	3	3.5	2.7	1.05

Next, the (maximum) simulated water level by XBeach is investigated (Figure 38). It shows the maximum water level during the Allerheiligenstorm. The model result shows overwash occurring at 05:00 hr. Water washed over the dune crest, behind the dune barrier. It is in agreement with the predicted storm impact scale (see Figure 37).

At these calculated time steps of the storm impact scales, dune erosion related to these impact scales are investigated. Results predicted by XBeach presented in Figure 39, can help to relate dune erosion to different storm impact scales. At top, the simulated profiles after the five time steps are projected. In addition, the according instantaneous water levels at these time steps are shown. The centre figure shows the sedimentated volumes between the subsequent time steps. The bottom graph shows bed level changes by showing the changes cumulative volumes of sediment in time.

From Figure 39 it can be seen higher water levels are associated with higher storm impact. Morphological impact at the first time step shows only at the foreshore some bed level changes occurred. The second time step, 03:00 hr associated with the collision regime, there is morphological impact until the distance of 4880 m. Between the 05:00 and 07:00 hr, the storm intensity is at highest and the extent of morphological changes can be observed far land inward.

The center graph shows storm impact is at 01:00 hr confined to the dune foot. At 03:00 hr XBeach results show that erosion at the dune foot increases. At the dune front erosion starts to occur. The result of the morphological impact difference between 05:00 and 07:00 hr can be explained by occurring overwash; sand is transported due to washover intrusion of 70 m

away from the dune crest. The overwash results in a maximum sedimentation due to overwash of less than 4 cm. The results are showing that induced erosion at the dune front and dune crest did not result into a sufficient lowering of the dune. The simulation shows overwash occurs due to the fact that the storm surge water level is of a sufficient height.

Furthermore, in the center graph, it can be seen that with continuation of the storm, the morphological changes flattens out. This is most clearly illustrated by the line of the last time step 09:00 hr. This is due to the fact that bed level variability smoothens out in time by the morphological storm impact. This is also resulting in morphological changes that are also smoothed out.

Finally, the total cumulative sedimentation/erosion (the lower graph of Figure 39) clearly shows that the dune front is increasingly eroded over time. At the dune base around elevation of 2 m, there is accretion occurring over time. Off shore at 4820 m, severer erosion appeared with continuing of the storm simulation.

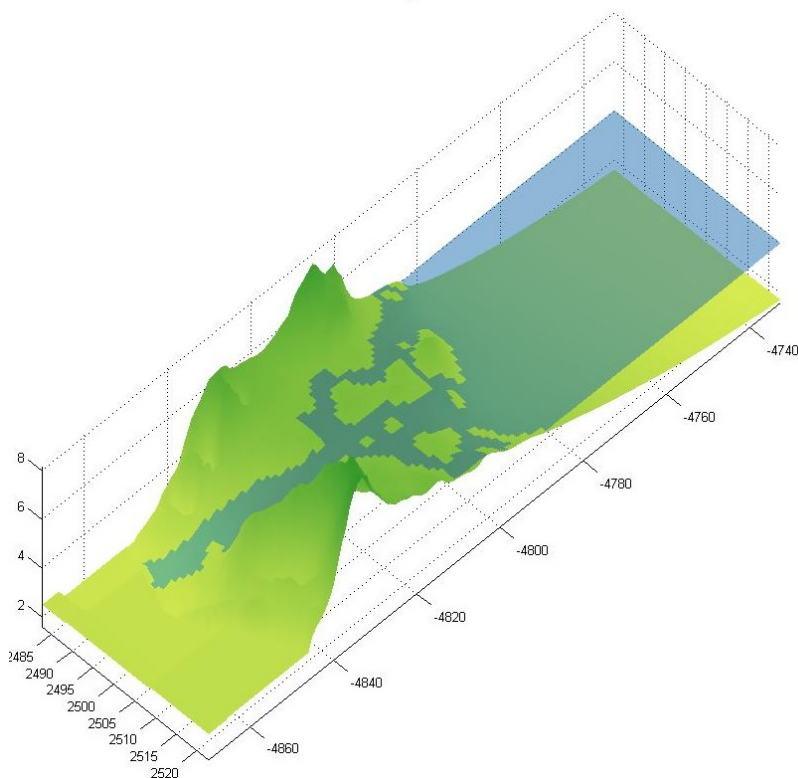


Figure 38: Overwash location at Paal22 showing predicted water level at 05:00 hr.

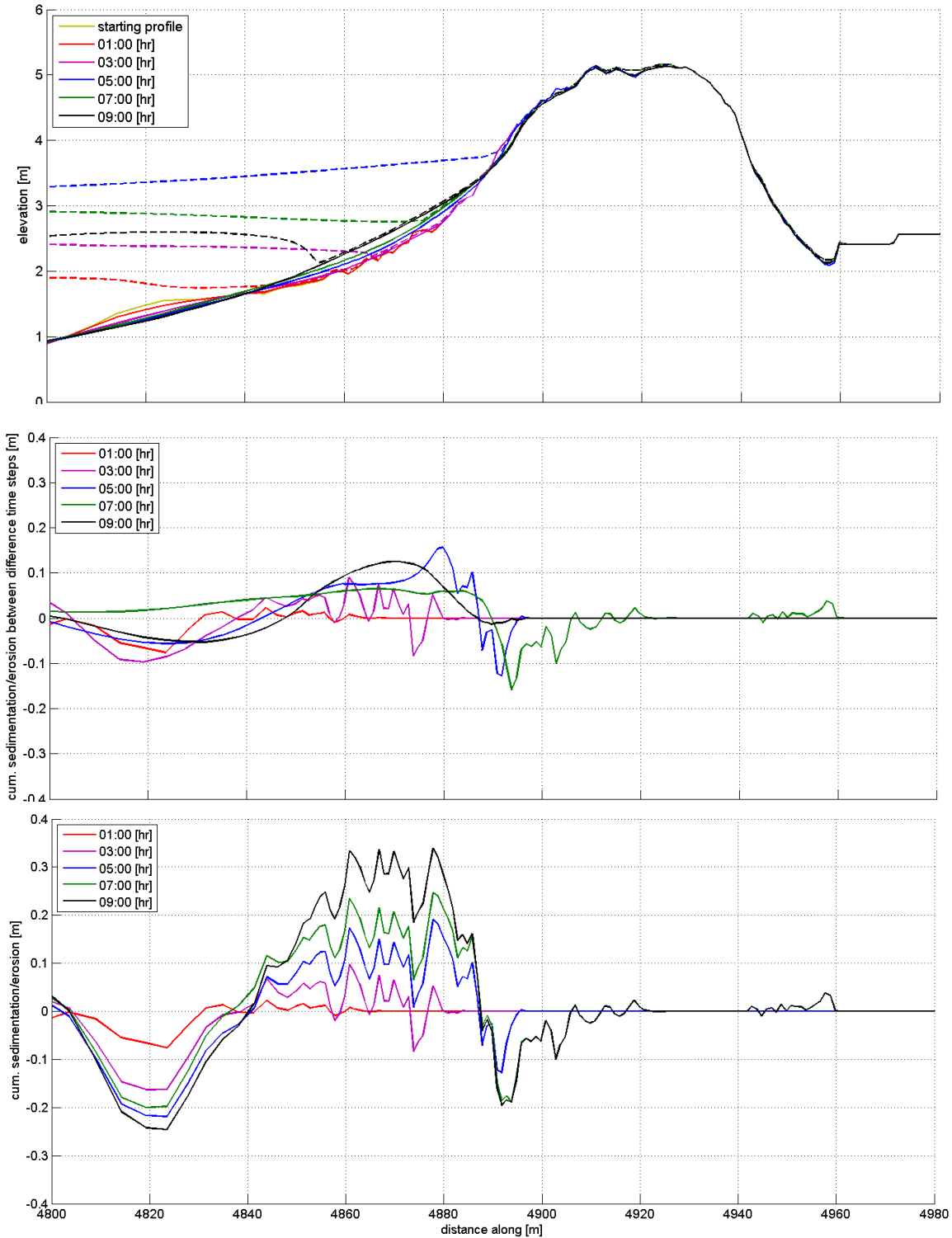


Figure 39: Morphological storm impact during the Allerheiligenstorm at Paal22. The upper graph showing storm profiles and their corresponding instantaneously water level at 5 different time steps. The middle figure shows volumes of sediment changes between these subsequent time steps. At the bottom, the cumulative sedimentation is shown.

5.2.3 Hydrodynamic conditions

Simulated hydrodynamic conditions by XBeach were represented by T_{rep} 12.2 s and H_{m0} 6.8 m. The simulated wave height and water levels when the storm surge level was at its maximum (05:00 hr) are shown in Figure 40.

The total wave height simulated by XBeach off-shore, consists mostly of high frequency waves. When approaching the shoreline, the low frequency waves become dominant over the high frequency waves. Furthermore, low frequency waves are increasing in wave height when approaching the shoreline, contrary to the high frequency waves, that are decreasing in height. The low frequency waves are close to the dune in the order of 0.5 m. High frequency waves are ranging about a 1,5 m height from 300 m away from the dune crest m until less than 0.3 m in height close to the dune.

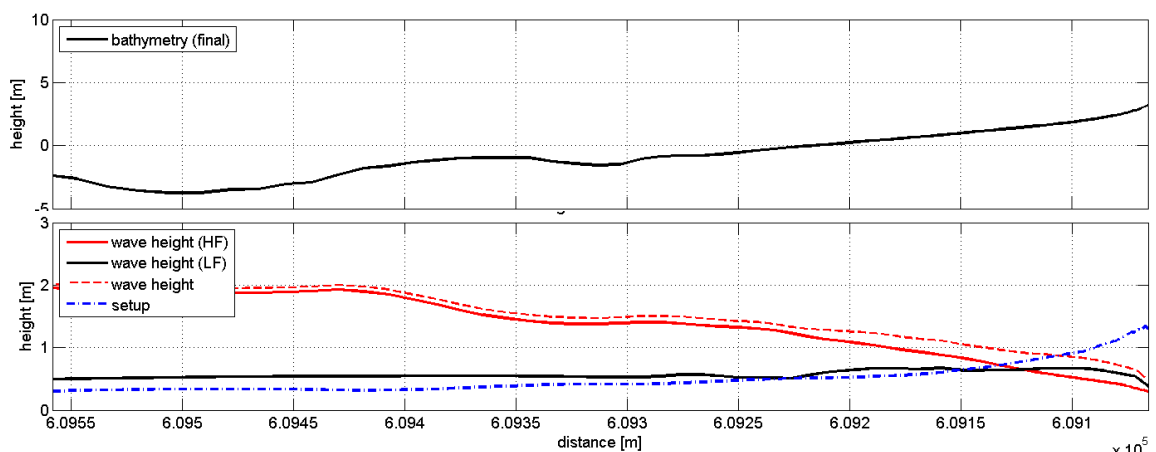


Figure 40: Hydrodynamics conditions predicted by, at the peak of the November 1st, 2006 storm. The upper graph shows the (post storm) bathymetry. The simulated maximum setup, low frequency, high frequency and tot wave height are shown below.

5.3 Results simulation location DeHon

Results obtained from XBeach by simulating the Allerheiligenstorm at DeHon are presented in this paragraph. The paragraph starts with the cumulative morphological impact predictions of XBeach. Secondly, simulated morphological impact during the different storm impact regimes is investigated. This paragraph is completed by presenting the predicted hydrodynamic conditions during the Allerheiligenstorm.

5.3.1 Morphological impact predictions

The results of the morphological impact simulation with XBeach are presented in the following part using conditions to represent the storm on the 1st of November 2006 at DeHon. XBeach predictions of bed cumulative sediment volumes are used to evaluate the performance of the model over the total duration of the storm.

Figure 41 shows results of the predicted volumetric sediment changes at location DeHon. It can be seen that at the foreshore, much morphological changes are visible. Some severe eroded locations, backed with areas where sand is deposited. Furthermore, a clear pattern can be observed where coastal dunes are present. The dune front is eroded, and at the dune accretion is occurred. Furthermore, the overwash fans that was present already before the Allerheiligenstorm shown severe impact. Especially at the back of the overwash fan, much severe erosion can be recognized.

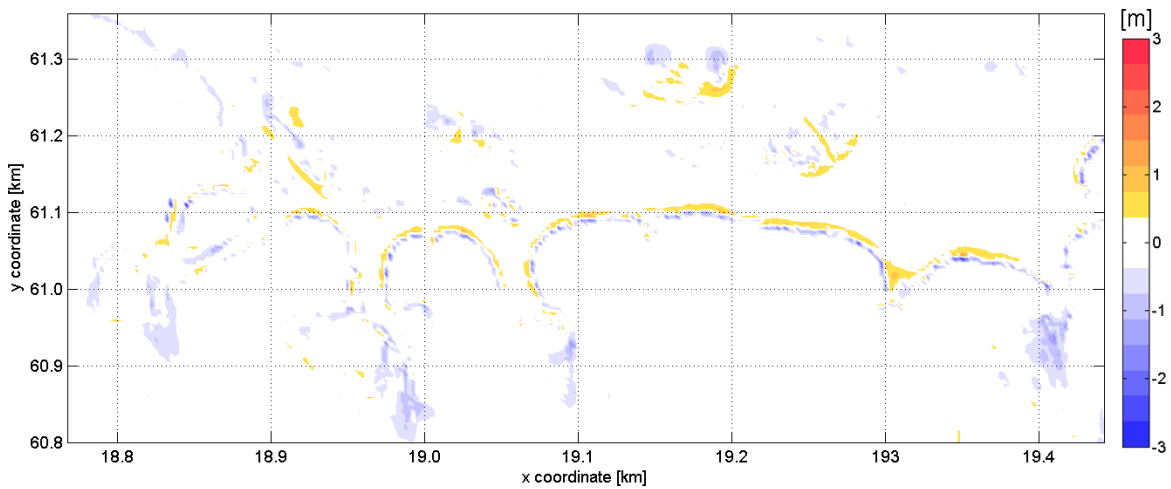


Figure 41: Sedimentation (red) and erosion (blue) of the Allerheiligenstorm predicted by XBeach at DeHon.

The simulated results are plotted upon aerial photographs (Figure 42). Severe erosion is predicted within and at the end of the overwash fans. Deposition is simulated at the back barrier, at the end of the eroded surface. This deposition can be related to the grid boundary conditions (for an explanation of selected grid boundary conditions see Appendix B) combined with topographic features at DeHon. These conditions resulted in stagnant water, where in reality it can be assumed water fluxes were present (i.e. because of tidal marshes and the Wadden Sea). Behind the dune barrier this stagnant water is not present in storm conditions, hence deposition would not occur in reality.

Therefore, when identifying overwash at this location sediment deposition related to these conditions is ignored. Furthermore, the dimensions of overwash, presented in Figure 43, are identified base on: (i) Overwash mouth, (ii) occurrence and (iii) intrusion (see chapter 4.1)

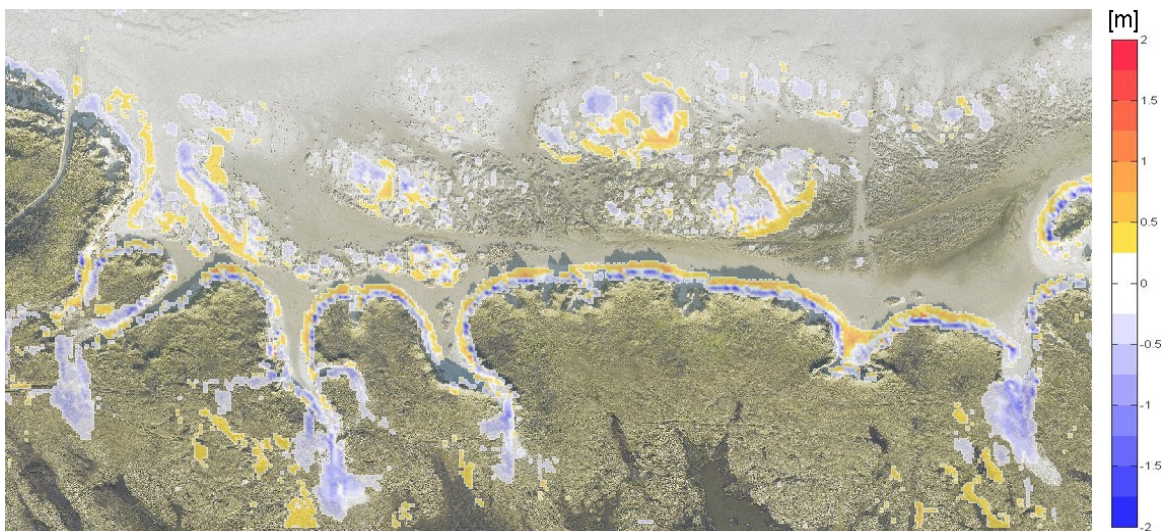


Figure 42: Sedimentation (red) and erosion (blue) of the Allerheiligenstorm predicted by XBeach at DeHon.

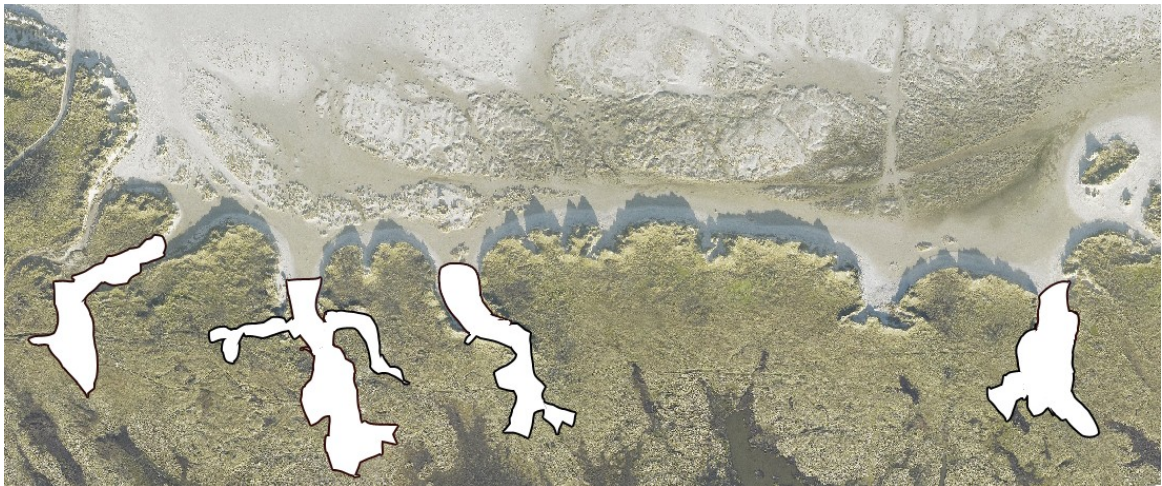


Figure 43: Overflow prediction by XBeach, simulating the Allerheiligenstorm.

5.3.2 Morphological impact regimes

This paragraph presents results to assess how XBeach simulates dune erosion processes during different storm impact regimes. To this end, morphological impact regimes and the evolution of the bed level profile during the Allerheiligenstorm will be investigated.

For five time steps, values of D_{high} , D_{low} , R_{high} and R_{low} at the 1st of November 2006 storm are obtained from XBeach and shown in Table 5. Figure 44 shows the calculated storm impact scale, based on the values of Table 5. It can be seen that storm impact first increases over time. The overflow regime is reached at 05:00 hr and after 07:00 hr storm impact decreases to collision. At these calculated time steps of the storm impact scales, related dune erosion in these impact scales are investigated. Results predicted by XBeach showing water levels and related dune erosion processes during the calculated different storm impact scales.

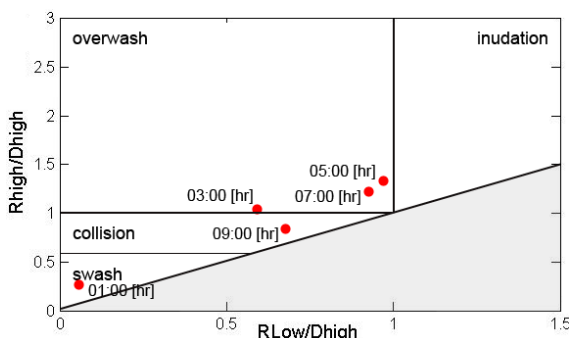


Table 5: Values of storm impact scale variables, Elevations are referenced to N.A.P.

Time hr	D_{high} [m]	D_{low} [m]	R_{high} [m]	R_{low} [m]	Surge [m]
01:00	3.5	3	1.6	1.3	1.13
03:00	3.5	3	3.6	2.4	2.06
05:00	3.4	3	4.3	3.2	2.72
07:00	3.3	3	3.6	3.0	2.52
09:00	3.3	3	2.5	2.7	1.05

Figure 44: Delineation of four different regimes at five different time steps is plotted for DeHon.

At 01:00 hr, almost no bed level changes can be observed (Figure 45). Minor bed level changes at the foreshore can be found. At 03:00 hr the first storm impact can be clearly observed (Figure 46). Especially at the foreshore, morphological impact can be seen. Some accretion occurs behind the first foredune ridge. Sedimentation can also be observed around 5525 m. Also at the dune foot some morphological impact can be seen. There is already water behind the dune presents, indicating limited overflow occurred.

At 05:00 hr, when calculated storm impact scale is at its highest, extensive morphological impact is simulated (Figure 47). At the back barrier, the area shows to be inundated.

Deltares

Furthermore, the storm surge is of sufficient magnitude to wash water over the dune ridge at y is -5450 m. At both sides at this location, XBeach simulates water washing over the dunes. Volumetric changes within the overwash fan are now, at the peak of the storm, clearly visible. Especially at the back, where the overwash fan is at its narrowest, much erosion is observed. Behind the observed erosion, accretion can be seen. At the overwash mouth, almost no morphological impact is observed.

After at 07:00 hr, the highest simulated storm surge peak has passed and water level decreases (Figure 48). The foreshore is still completely inundated. At the back barrier, water slowly flows away using the lateral boundaries. Due to the reduced capacity of water that can flow away to the lateral boundaries, water is still present at around x is 2100 m. In reality, the capacity is also reduced due high water levels present at the Wadden Sea. This high water level limits the flowing away of water fluxes through the tidal inlet marches. The severity of the observed erosion increased at this time step. It can be seen that erosion and sedimentation is limited to the already previously storm impact affected surfaces.

The last calculated time step of storm impact is at 09:00, when the impact scale classified the storm at this location as collision. The simulated results show (Figure 49) that the foreshore is still partly inundated. Also, some water is still present in the overwash fan. Behind the dune barrier, almost no water is presents. Most water is drained away to the lateral boundaries. Furthermore, it seems that the water in the overwash fan is retreating seawards. The observed volumetric changes do not seems to be increased in severity anymore.

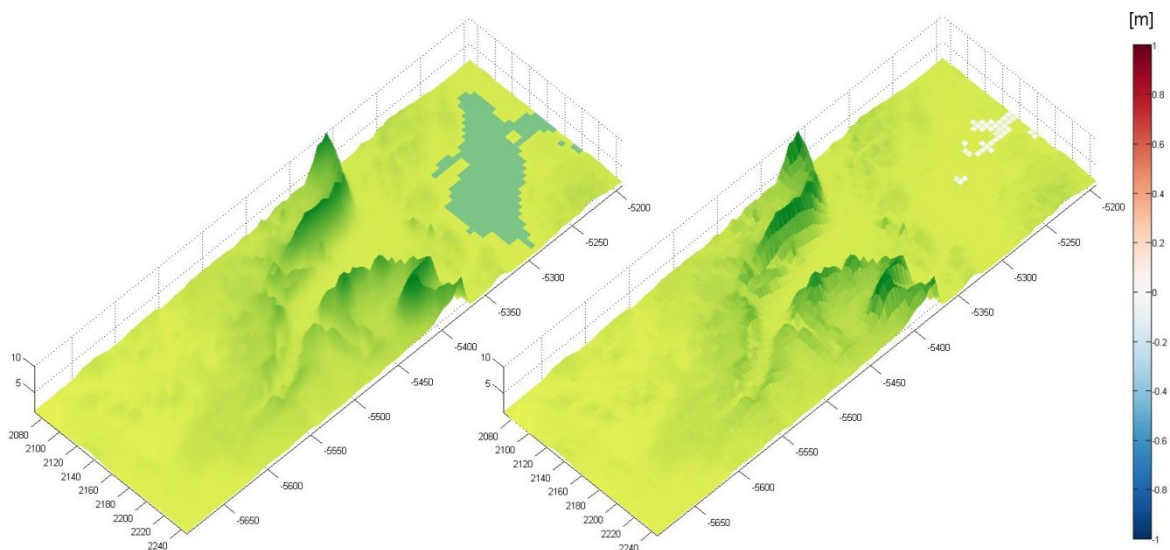


Figure 45: Overwash fan at DeHon at 01:00 hr, simulated water level (left) and cumulative sediment volume (right).

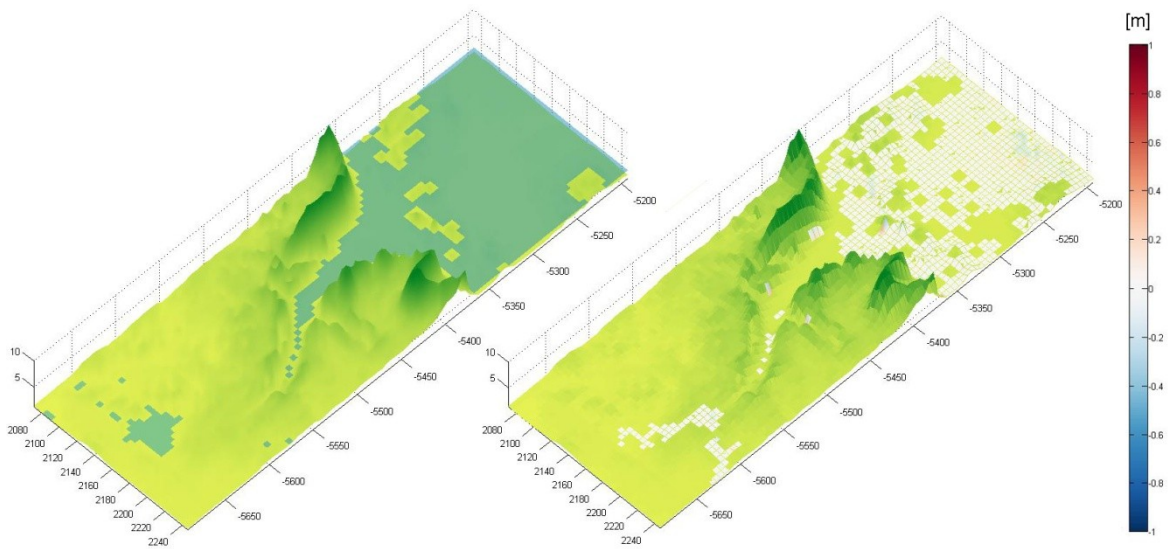


Figure 46: Overwash fan at DeHon at 01:00 hr, simulated water level (left) and cumulative sediment volume (right).

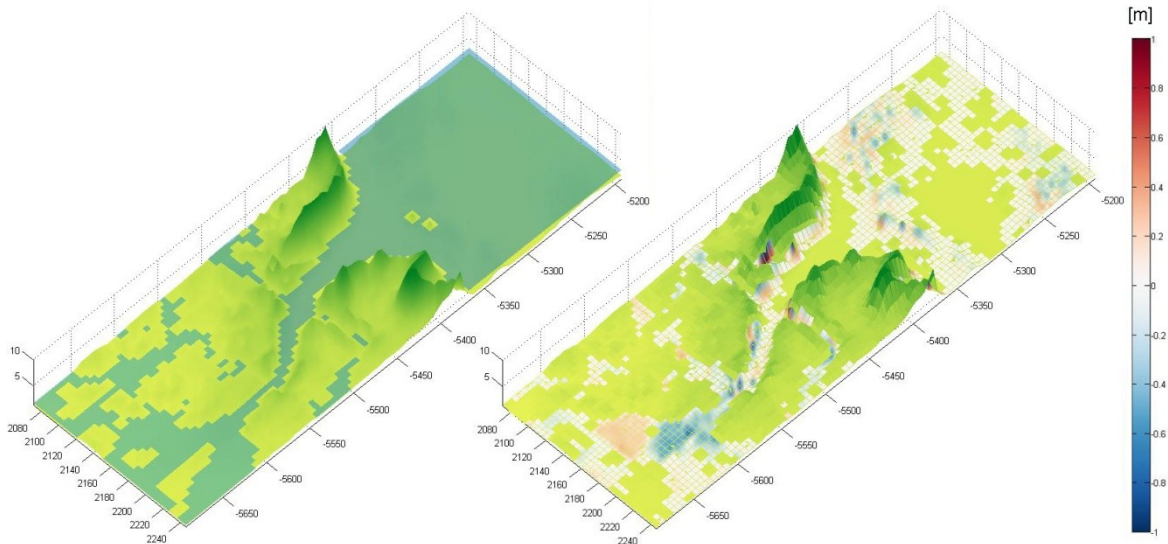


Figure 47: Overwash fan at DeHon at 05:00 hr, simulated water level (left) and cumulative sediment volume (right).

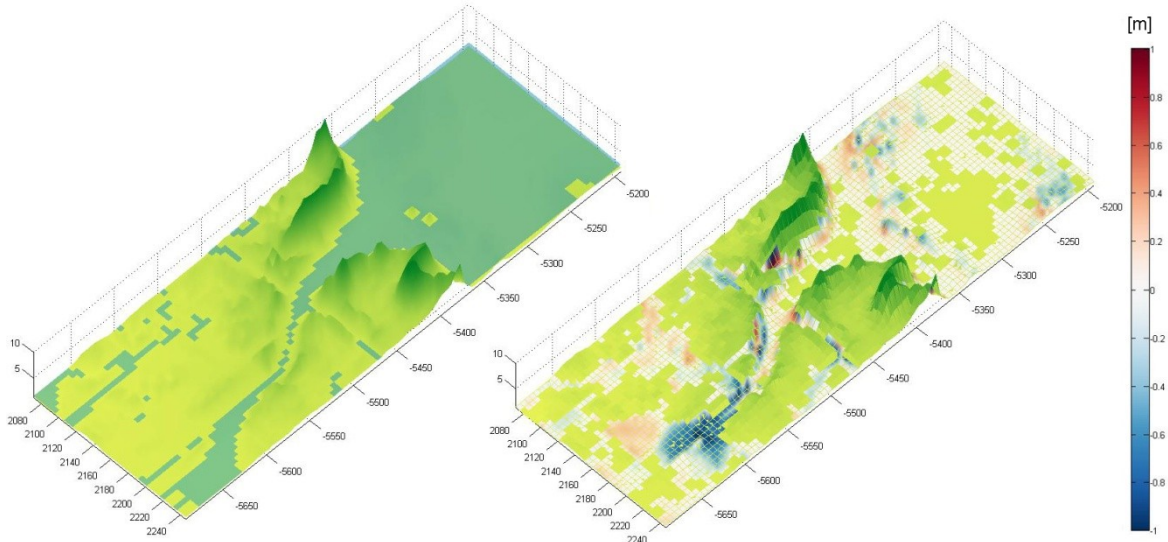


Figure 48: Overwash fan at DeHon at 07:00 hr, simulated water level (left) and cumulative sediment volume (right).

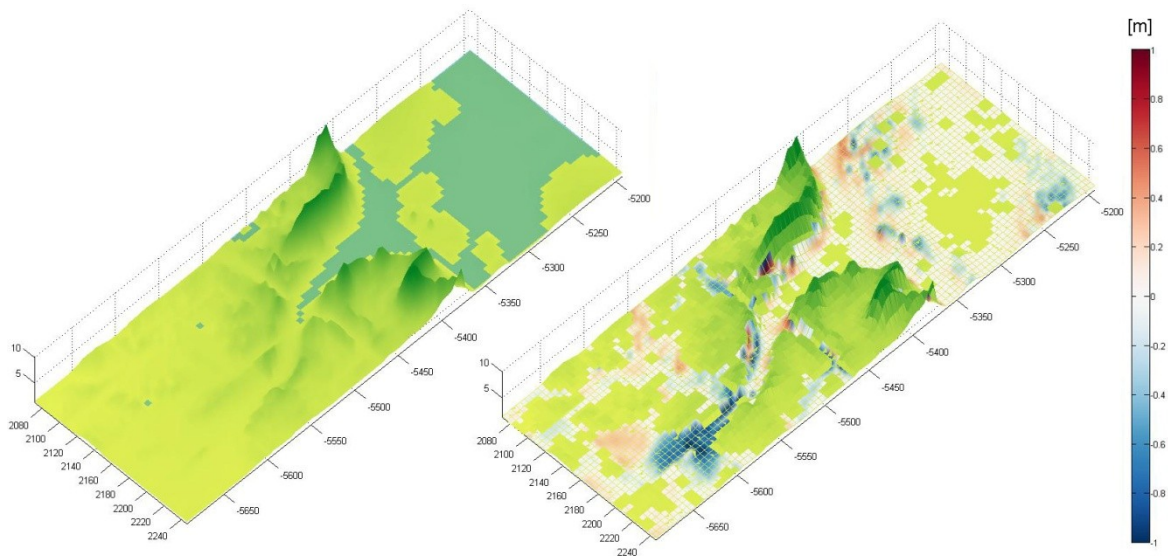


Figure 49: Overwash fan at DeHon at 09:00 hr, simulated water level (left) and cumulative sediment volume (right).

The volumetric sediment changes between the five subsequent storm impact regimes are retrieved from XBeach model simulations. The volumetric sediment changes between 01:00 were already previously shown (Figure 45). There was at this time step almost no morphological impact. The next time interval is between 01:00 and 03:00 and is shown in Figure 50. Some bed level changes can be seen at the foreshore. Also, a little of morphologic changes can be observed behind the dunes. At the dune foot, there are almost no signs of storm impact.

From 03:00 until 05:00 hr most clearly storm impact is observed (Figure 51). At the foreshore, much surface area is affected by erosion or sedimentation. Most distinguish during this time step, is the induced erosion in the overwash fan. Much erosion can be seen at the back of the overwash fan. Furthermore, at $y = -5450$ m at both sides of the overwash fan erosion takes place. At the dune foot there can be seen some sedimentation and erosion at the dune front.

The impact scale between 05:00 and 07:00 hr was scaled at the overwash regime. This is also showed by the results in Figure 52. The same pattern submerges as between 03:00 and 05:00, only less severe. During this regime it can be seen that at $x = 2100$ m there is relatively much sedimentation at this location. This can be again be related to the stagnant water due to the selected lateral boundaries. Moreover, sedimentation occurred at the dune base, and there is erosion of the dune front.

The final calculated time step is at 09:00 hr. Between this timestamp and 07:00 hr, the morphological changes are shown in Figure 53. It can clearly be observed that the storm impact decreases. The severity of morphological changes is diminishing.

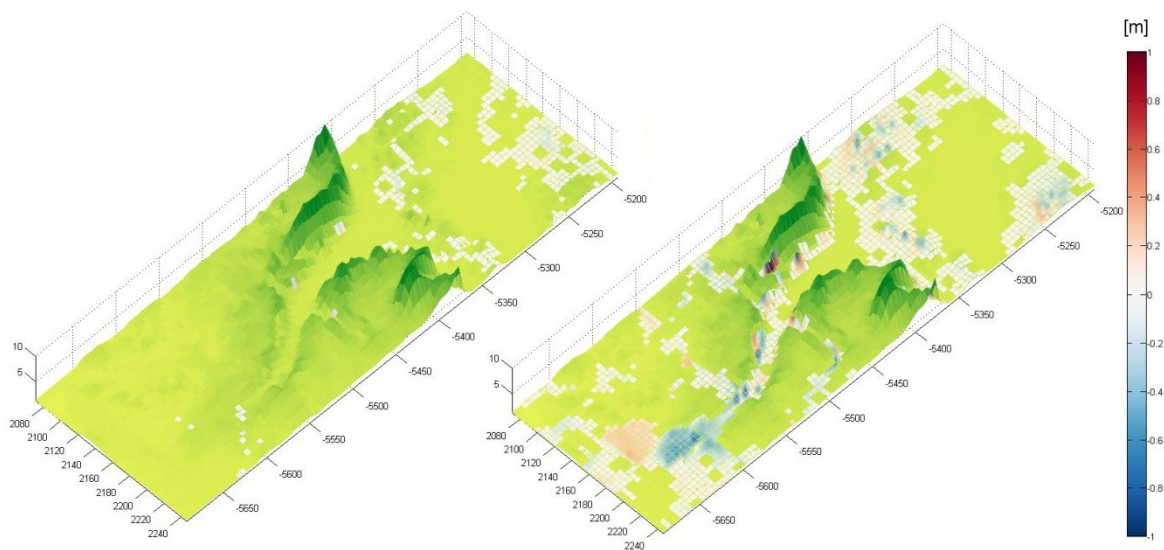


Figure 50: Overwash fan at DeHon with indicating predicted erosion (blue) and sedimentation (red) between time 01:00 and 03:00 hr.

Figure 51: Overwash fan at DeHon with indicating predicted erosion (blue) and sedimentation (red) between time 03:00 and 05:00 hr.

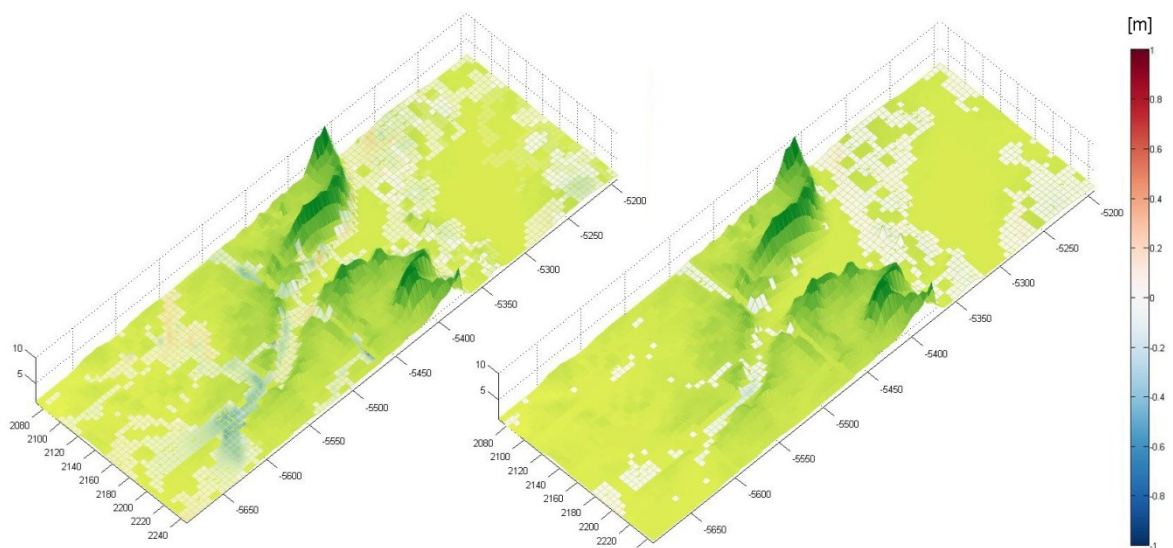


Figure 52: Overwash fan at DeHon with indicating predicted erosion (blue) and sedimentation (red) between time 05:00 and 07:00 hr.

Figure 53: Overwash fan at DeHon with indicating predicted erosion (blue) and sedimentation (red) between time 07:00 and 09:00 hr.

5.3.3 Hydrodynamic conditions

XBeach simulated the hydrodynamic conditions by a T_{rep} 12.2 s and H_{m0} of 6.8 m. The simulated wave height and water levels when the storm surge level is at maximum (05:00 hr) are shown in Figure 54.

Low frequency waves are increasing in wave height when approaching the shoreline, contrary to the high frequency waves. The low frequency waves are approximately 0.5 m, high frequency waves are ranging from 1.5 m 300 m away from the dune crest and below 0.5 m when they are close to the dune.

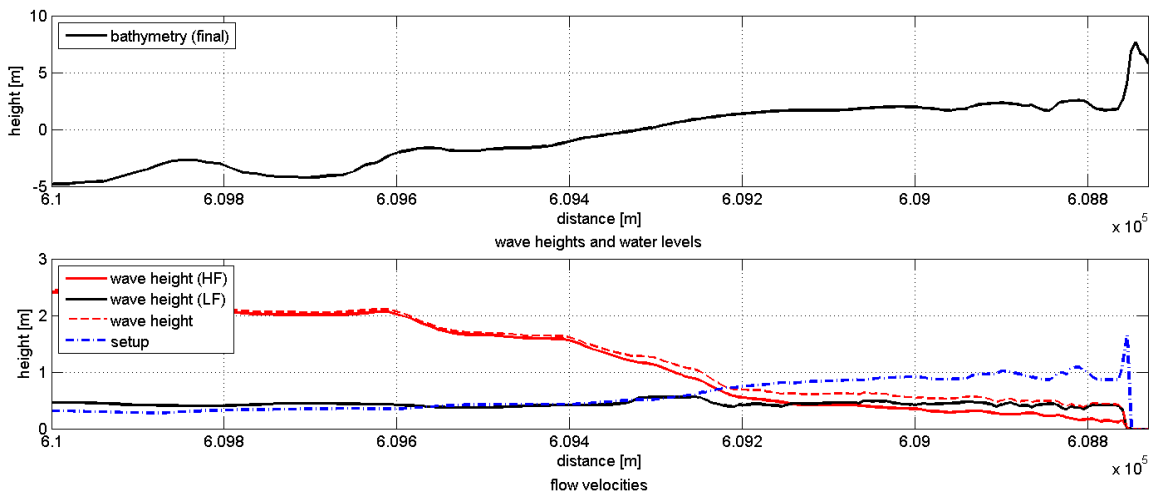


Figure 54: Hydrodynamics conditions predicted by, at the peak of the November 1st, 2006 storm. The upper graph shows the (post storm) bathymetry. The simulated maximum setup, low frequency, high frequency and tot wave height are shown below.

5.4 Conclusions

Two different grids were modeled in XBeach, to investigate how XBeach would simulate the morphological impact at these locations. The presented results from the simulations the Allerheiligenstorm at these locations have led to conclusions:

At both locations, the simulation of XBeach of the November storm shows that with continuing storm impact, the severity of the simulated morphological changes at the dune front increases. With the storm continuing over time, the total eroded sediment volume increases.

XBeach simulated overwash at observed overwash locations. When the storm conditions were represented by the overwash storm impact regime, overwash was simulated and transported sediment to the back barrier. At Paal22, the threshold to overwash was only slightly exceeded and only small amount of overwash occurrence could be observed. The overwash prolongs longer and the induced morphological changes due to overwash are abundantly.

At both locations, the threshold to overwash is exceeded due to storm surge induced a sufficient water level to wash water over the dunes. At both the overwash locations, results showed that the dune crest was not significantly lowered before overwash occurred. Hence, overwash occurred due to the magnitude of the storm surge level.

XBeach simulation showed that at the dune front, the total wave height, almost completely was determined by the wave height of infragravity waves. Furthermore, At DeHon, infragravity wave height was simulated slightly higher than at Paal22.

6 Sensitivity analyses

In this chapter will present two different sensitivity analyses. First, the threshold sensitivity overwash is investigated. Furthermore, XBeach will be tested for sensitivity to S_{max} (the transport limiter). The chapter will end with conclusions.

6.1 Methodology

Sensitivity analyses can be done to test and validate parameters and / or processes in a specific model. By varying the value of a parameter and comparing the results, the importance of that variable can be determined. If there are not many differences, the variable is not very important to the model result. Two parameters in particular are expected to be important for our model outcome: (i) bed level height and (ii) the use of S_{max} .

Bed level elevation sensitivity is investigated. Sensitivity analysis can increase confidence in model predictions. Exceedance of the threshold to overwash could be the result of the approximate 20 cm inaccuracy of the elevation height in the LIDAR data (see also chapter 4.2.4). To increase confidence in the model prediction, bed level is in- and decreased and it is investigated how this influences the outcome of the XBeach simulation.

The total bed level height at Paal22 is increased until in simulations by XBeach do not exceed the threshold to overwash. In addition, the sensitivity to a decrease of the bed level is investigated. This can reveal how the inaccuracies in the data might affect the magnitude of the overwash occurrence. The simulation time of the model was 2 hrs and the water level peak of the storm surge was imposed after 1 hr on these simulations.

S_{max} is a parameter that should only affect the model results if extensive overwash is predicted shown by (McCall, 2008; McCall et al., 2010). In our simulations S_{max} was activated only for location DeHon, because only extensive overwash was present at this location. It is important to know how this parameter affects other results, rather than overwash predictions.

Overwash is overestimated due to the empirical pick-up function in XBeach. This function results in overprediction of erosion rates in the case of high sediment concentrations and Shield numbers exceeding 1. This is also the case during overwash conditions. It can be explained by the fact that reduction in the suspended sediment transport capacity due to turbulence damping, which is caused by the sheet flow layer, is not included. Also, a reduced in the bottom shear stress in sheet flow conditions (which is present during overwash) may explain in part the overestimation of sediment transport rates by the pick-up function (McCall et al., 2010).

Therefore, a limitation is placed on the equilibrium sediment concentration by limiting the Soulsby–Van Rijn stirring velocity during sheet flow. By limiting this function, it should be ensured that sediment transport only under overwash conditions becomes a linear function of flow discharge. This will result in representing overwash conditions more accurately (McCall, 2008).

Investigation of this S_{max} parameter will be performed by running simulations of Paal22 with and without S_{max} activated. Location Paal22 is chosen because only small amounts of

overwash occurrence was observed and simulated. Therefore, the results should show a little difference between the two sensitive cases, with and without Smax.

6.2 Results sensitivity to bed level changes

In Table 6 the results for this sensitivity analysis of changing bed levels is shown. Figure 63 shows the effect of the bed level changes in sedimentation volume.

It can be seen that dune face retreat for all simulations is comparable. The developed shape of the dune after a storm surge level of two hours is similar. Although visible in all runs except run 8, simulated dune erosion increases behind the dune barrier with a lower bed level. It can be seen most obviously in run 4. Run 7, where the bed level is increased with 20 cm, there is only a small change in bed level simulated behind the dune. In run 8, there are no bed level changes observed behind the dune at all. Bed level changes behind the dune can only be explained by occurring overwash.

In Figure 63, the eroded volumes of the different runs are shown. It shows decreasing bed levels resulting in increased eroded volumes. Furthermore, when bed levels are lowered with an additional 30 cm, changes in simulated bed levels can be observed further land inwards. Offshore, differences between the Run 1 – 8 in simulated bed levels diminish after 4800 m where approximately the swash regime starts. As can be seen from, from 4800 m distance the predicted values of erosion and sedimentation start to coincide.

Table 6: Overview of effect of different simulations of 1 November 2006 with changed bathymetry input. The table shows the run number, the in- or decrease in the bed level, the corresponding figure where the result is showed and if overwash is simulated.

Run	Bed level change	Figure	Overwash
1	5 cm lowered	Figure 55	Yes
2	10 cm lowered	Figure 56	Yes
3	20 cm lowered	Figure 57	Yes
4	30 cm lowered	Figure 58	Yes
5	5 cm increased	Figure 59	Yes
6	10 cm increased	Figure 60	Yes
7	20 cm increased	Figure 61	Yes
8	30 cm increased	Figure 62	No

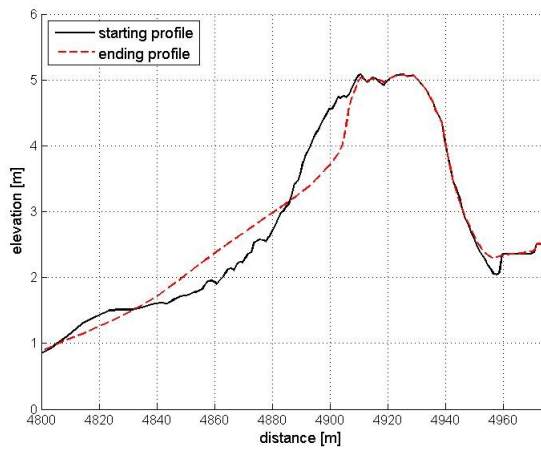


Figure 55: Run 1, decrease of bed profile with 5 cm.

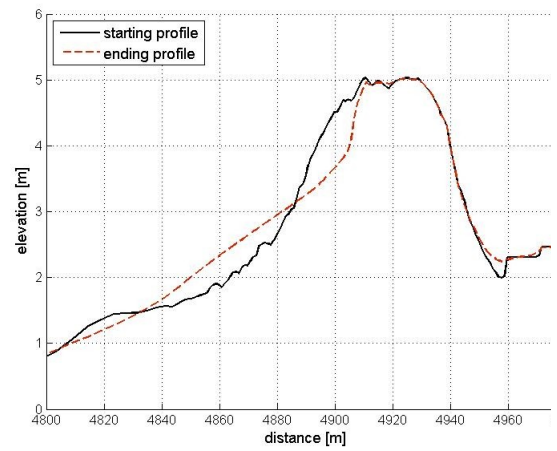


Figure 56: Run 2, decrease of bed profile with 10 cm.

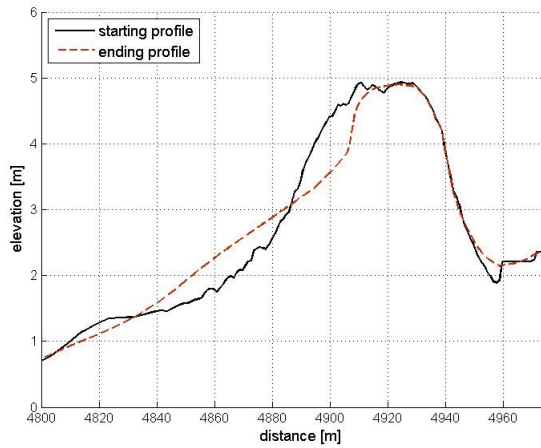


Figure 57: Run 3, decrease of bed profile with 20 cm.

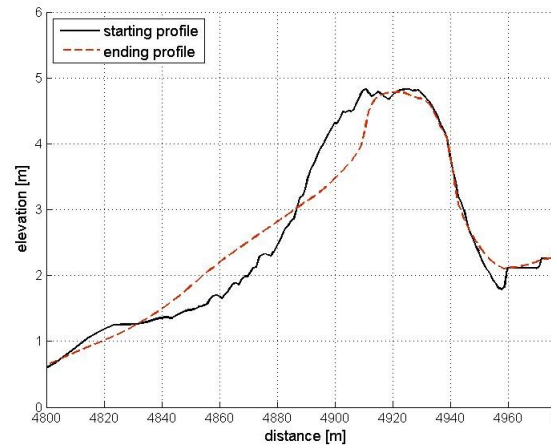


Figure 58: Run 4, decrease of bed profile with 30 cm.

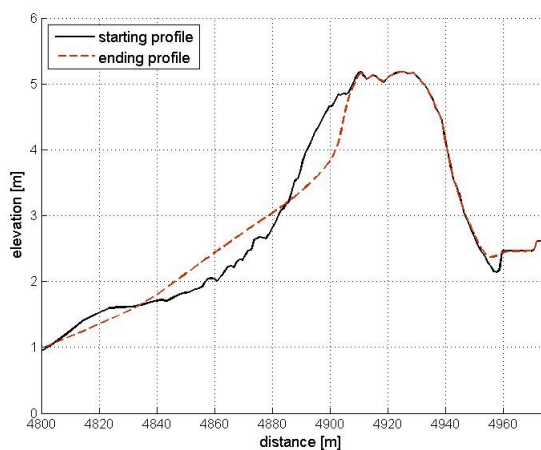


Figure 59: Run 5, Increase of bed profile with 5 cm.

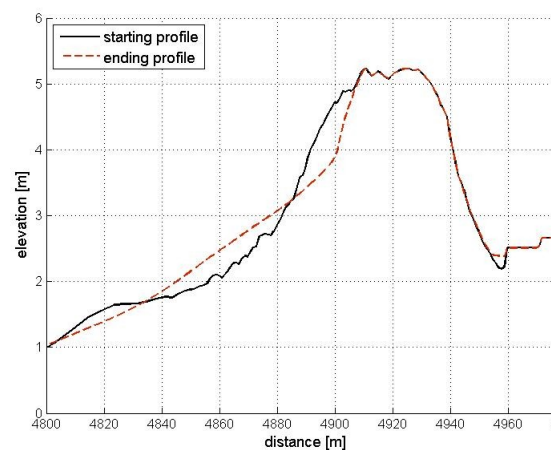


Figure 60: Run 6, Increase of bed profile with 10 cm.

Deltares

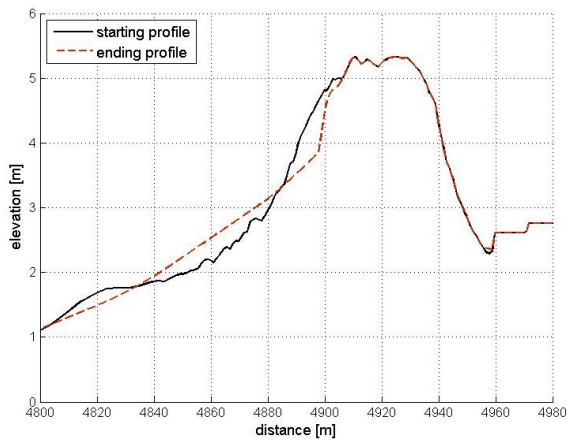


Figure 61: Run 7, Increase of bed profile with 20 cm.

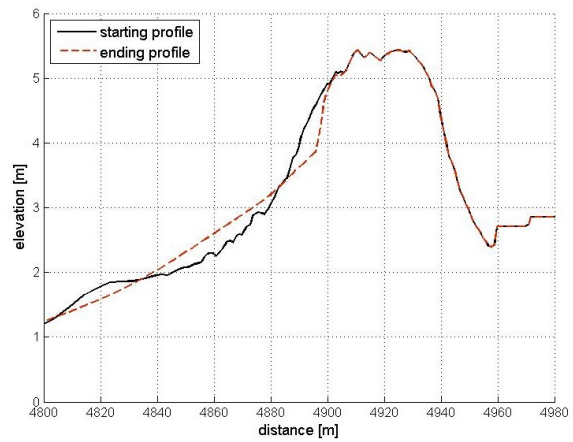


Figure 62: Run 8, Increase of bed profile with 30 cm.

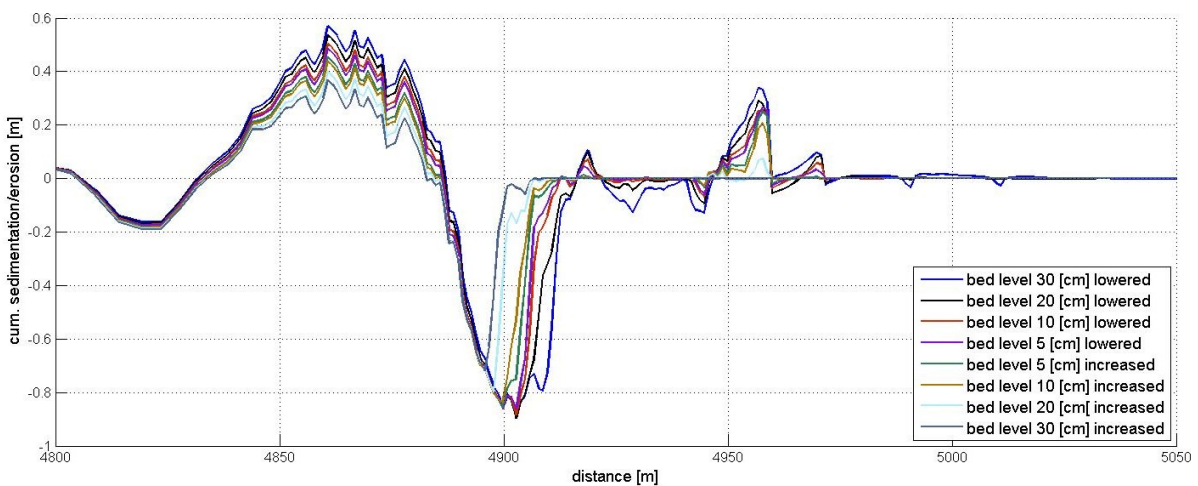


Figure 63: Showing the morphological impact of sensitivity simulation cases. At the top, the cross-shore profile is shown. The cumulative sedimentation and erosion of location Paal22.

6.3 Results sensitivity to Smax

Two simulations were performed to test the effect of Smax. One model run without the use of Smax and a model run with Smax. As locations to test the effect of Smax, location Paal22 is chosen.

The results of the sensitivity analysis are shown in Figure 64. The results show that if Smax is activated, indeed less sediment transport is predicted land inwards due to overwash. Unexpectedly, bed level changes at the dune front are also significantly affected by the transport limiter. Activating the transport limiter resulted in a decrease of erosion at the dune face and an increase of erosion at the dune base. The dune foot retreat is about 7 m less without Smax at location Paal22.

This sensitivity analyses did not include a detailed investigation of flow velocities near to the coastline. Averaged flow velocities over time showed in these simulations to be normal. It might be due to the fact that instantaneous flow velocities can be higher and therefore exceeding the value for activating the transport limiter. Hence, reducing sediment transport in front of the dune will cause lowering of the capacity to erode sediment from the foreshore.

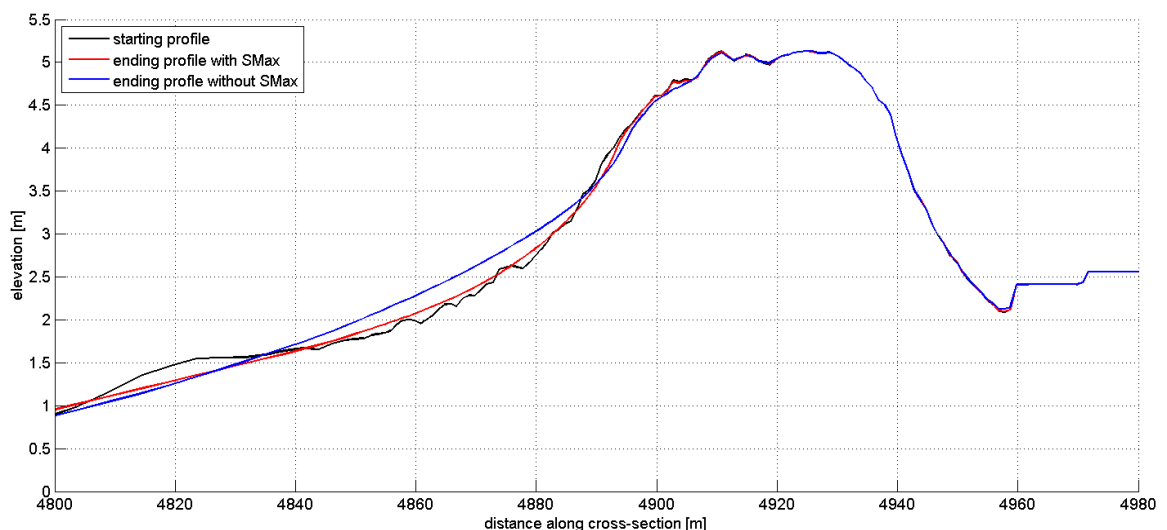


Figure 64: Predicted cross-shore profile at location Paal22 by XBeach with transport limiter on (red) and off (blue).

6.4 Conclusions

The following can be concluded due to the varying of the bed level and (de)activating Smax in XBeach.

Overwash was predicted for bed level changes between -30 cm and +30 cm. The threshold for predicting overwash at location Paal22 in XBeach was +20 cm. The severity of the erosion increased with a decreasing bed level, but the patterns of volumetric sediment changes were comparable. Offshore, simulated results were not (significantly) affected by bed level changes.

Smax results in an unexpectedly decrease of erosion of the dune face and an increase of erosion at the dune base, mostly associated with the collision regime. Off shore, the transport limiter showed to have limited effect on sediment transport rates. In addition, the results confirmed that Smax did limit sediment transport, if overwash occurred.

7 Analyses results and discussion

In this chapter, results from simulations by XBeach and the data analyses analyzed. First, results of location Paal22 are compared, followed by location DeHon. At both paragraphs it is also discussed where the observed difference can be related. Furthermore, this chapter presents a discussion regarding the research results.

7.1 Observed versus simulated results

This section will elaborate about the difference between the observations and simulations of location Paal22 and DeHon. It will explain the difference between the simulated and observed results. Most of the time, these differences can be related to physical processes, numerical parameters, model imperfections, etc.

7.1.1 Location Paal22

Location Paal22 is an access route through the fore dune, to the beach of Ameland. At this location, overwash was present during the Allerheiligenstorm. Another morphological change that could be clearly distinguished as Allerheiligenstorm impact was a significant dune foot retreat.

Eroding of the dune foot was established as criteria for collision occurrence. It can be used as an indicator of the accuracy of the observed versus the simulation collision storm impact. The predicted and observed shift of the dune foot can be seen in Figure 65. This result shows that the predicted erosion at the dune foot is reasonably comparable to the observed erosion. The observed dune foot shift measured approximately 10 m (-/+ 2 m) land inward. The simulated results showed a lower shifting, on average around 8 m land inwards.

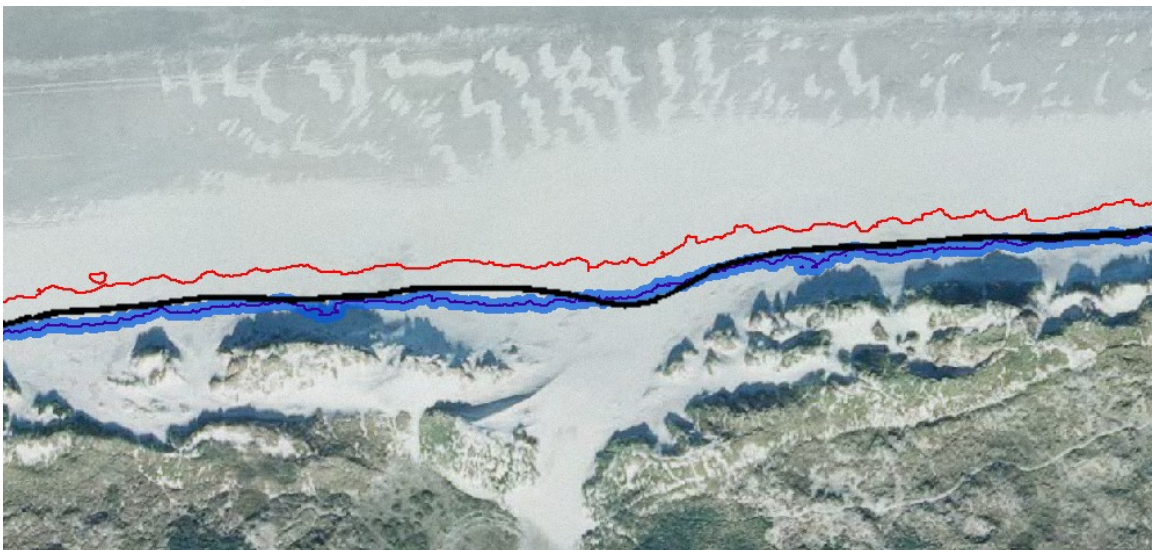


Figure 65: The pre (red), post (blue, with lighter blue shows the inaccuracy of 2 m) and predicted (black) by XBeach dune foot.

The research presented two results that affected erosion at the dune front. They might affect the accuracy of the simulated results. Sensitivity analyses showed that a decreasing the bed level increases erosion at the dune front (see chapter 6.2). Hence, the prediction of erosion at the dune foot might be more accurate if the bed level height was underestimated due to inaccuracies in the LIDAR data. On the other hand, at this location Smax was not activated.

Although this should not significantly affect erosion at the dune front, sensitivity analysis showed that activating S_{max} strongly decreased erosion at the dune base (see chapter 6.3).

Moreover, that XBeach simulated overwash at this location, is in agreement with observed results. Difference exists between the predicted and observed magnitude of the occurred overwash (Figure 66). The observed extent of the overwash occurrence was approximately 100 m, the simulated results showed a maximum land inward deposition (measured from the dune crest) of 80 m. The width of the overwash fans show to be similar.



Figure 66: Observation (red) and simulation by XBeach (black) overwash occurring during the Allerheiligenstorm.

There are no quantitative (accurate) observations available of the volumetric changes behind the dune. The predicted overwash by XBeach showed to be very small. Predicted morphological changes were sometimes less than a centimeter. Two sources of data suggest more overwash was present during the Allerheiligenstorm than predicted. The first sources are the photographs taken after the 1st of November 2006. With the limited predicted changes by XBeach, morphological overwash impact features would not have been visible on these photographs. The second sources are the observations of the water company of Ameland. The predicted limited overwash (of salt water) would not have lead to a complain of overwash, contaminating the fresh water supplies of the water company.

Small morphological predicted changes occur because the threshold for overwash is slightly exceeded in the simulation. Differences between observed and predicted storm impact at this location might originate because of missing physical processes of shortwave run-up. XBeach uses a shortwave averaged wave group resolving the model of surf zone processes. This is resulting in an underestimation of the maximum run-up at the dune front (Roelvink et al., 2010). Experiments by Deltares in the wave flume (van Thiel de Vries et al., 2008) showed that short wave run-up impact is especially important when (only slightly) exceeding the threshold from collision to overwash. If short wave run-up was simulated, it could increase severer overwash storm impact and prolong longer overwash occurrence. In addition, the differences in resemblance can be explained the fact that the dune crest only contains a small amount of sand. The dune crest can be easily eroded by the prolonged attack of short wave run-up, resulting in increasing overwash if short wave run-up is simulated. Hence, short wave run-up could be an explanation of the underestimated morphological storm impact.

7.1.2 Location DeHon

The research investigated morphological impact at the nature reserve 'De Hon'. Observational results established the presence of overwash occurrence during the Allerheiligenstorm. This was confirmed by the simulations with XBeach. To compare observations and simulations of collision, one (representing) result of an overwash fan is analyzed in detail. At this fan, the simulated and observed dune foot retreat is analyzed. Furthermore, the overall predicted and observed overwash occurrence is compared.

The simulated collision occurrence shows discrepancies with observed (Figure 67). The overall predicted dune foot shift shows a smaller retreat than observed. The maximum underestimation of the dune foot retreat is approximately 5 m. Within the overwash fan itself, it seems like more agreement is found between predicted and observed collision occurrence.

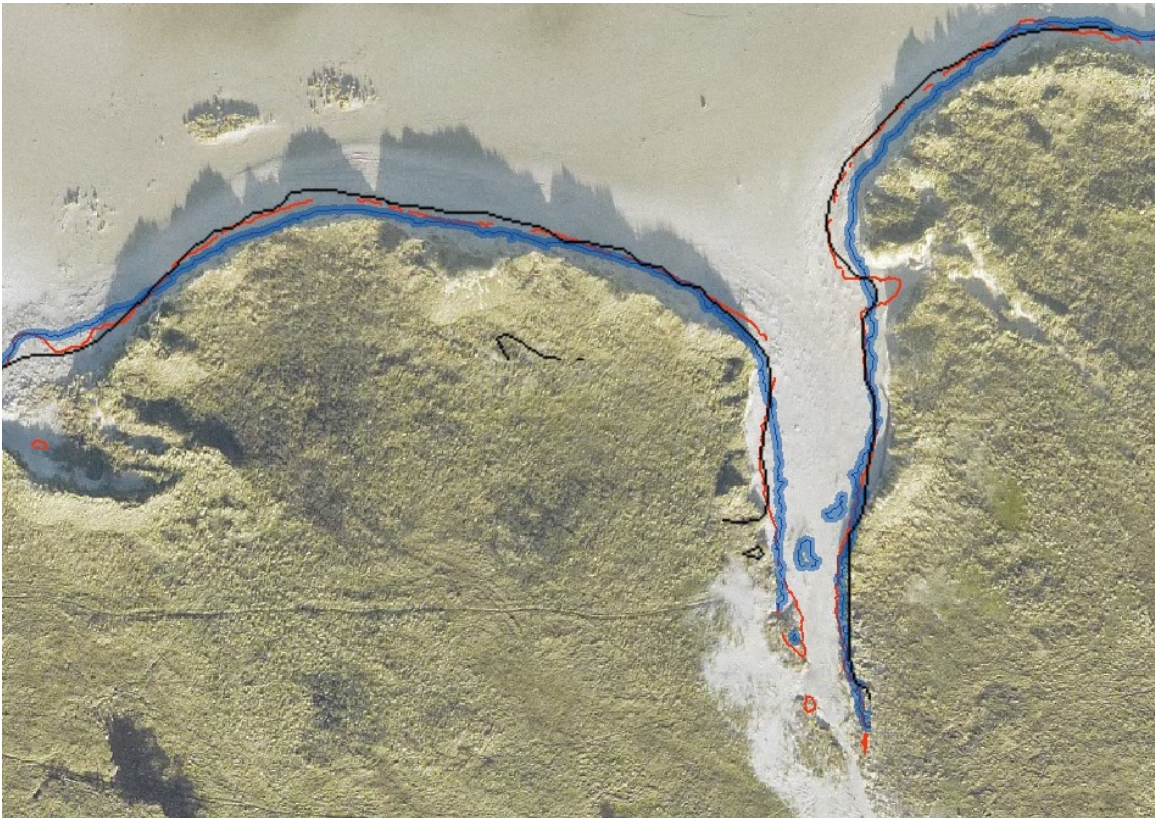


Figure 67: The pre (red), post (blue, with lighter blue shows the accuracy, +/- 2 m) and final predicted (black) by XBeach Allerheiligenstorm dune foot.

Overall, erosion at the dune foot occurred much less, both simulated as observed, in comparison to location Paal22. This can be explained due to the topographic nature of the area. The foreshore has more characteristics of dissipative beach. The beach is characterized by a wide and (relatively) flat sandy coastal zone with the dunes backed by a wide beach. At this dissipative beach, high energy waves start breaking far offshore. These high energy waves (and also short waves) are associated with erosion at the dune front.

XBeach simulates this dissipative behavior of the beach correctly. Nevertheless, the predicted collision occurrence at DeHon was underestimated. Therefore, two explanations can be given. First of all, at DeHon Smax is activated. As the results of the sensitivity analyses of Smax showed, it had significant reducing effects on predicting erosion at the dune front. At

Paal22, without Smax activated, more agreement between observed and predicted collision occurrence was found. Furthermore, less erosion at the dune foot might also be explained if the observed data inaccuracy resulted in overprediction of the elevation of the bed level.

The occurrence of overwash at DeHon was much more clearly observed than at Paal22. Multiple distinguishable overwash fans were observed and extensive overwash occurrence could be. Simulations by XBeach of the Allerheiligenstorm confirmed this observation. The predictions showed that the threshold to overwash was abundantly exceeded.

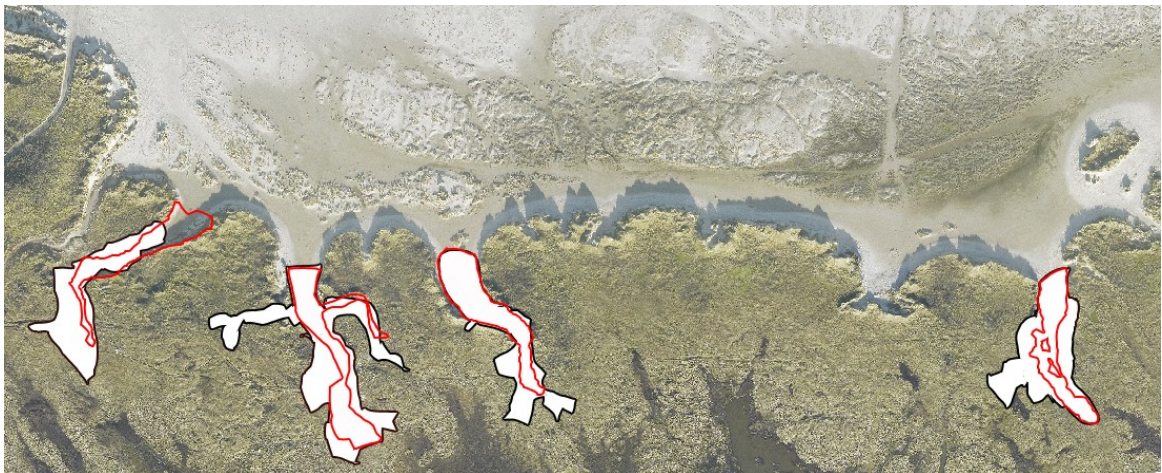


Figure 68: Observation (red) and simulation by XBeach (black) overwash occurring during the Allerheiligenstorm.

The simulated magnitude of overwash occurrence located at the back barrier is larger than the observed overwash. Especially, the width of the overwash occurrence is larger. The extent of the overwash occurrence of XBeach shows better agreement with the observations. Note that XBeach predicts an 'extra' overwash fan, located at the second overwash fan from left (Figure 68). This obtained difference might be related to the quality of the data. Sensitive analysis showed that overwash was sensitive to a few centimeters of decrease of bed level (see chapter 6.2.) This might be the reason of the overprediction of overwash. The extra overwash fan and the larger magnitude of simulated overwash occurrences can be explained due to model imperfections. Some physically important features and processes present at DeHon, are not simulated (accurately).

Smax was used because previously it was shown that XBeach will overpredict overwash-driven morphological changes. This is when large amounts of sediment are suspended in the water column and the Shields number is high during overwash conditions (McCall, 2008). Several other explanations can be given for overprediction, including the resistance effects of vegetation and soil cohesion and the choice of the sediment transport relation (McCall et al., 2010). Vegetation and peat might act in reality as a natural transport limiter and could explain the observed overestimation of dune overwash lowering at location DeHon.

The simulated result at DeHon shows that the threshold for overwash is largely exceeded. Therefore, explaining the difference at this location due to missing physical process of shortwave run-up is less likely. Short wave run-up is especially importance when exceeding only slightly the threshold to overwash. In addition, the dissipative effect of the foreshore at DeHon, reduces the effect of these short waves.

7.2 Discussion

7.2.1 Predicting storm impact with XBeach

What do the current obtained results say about how XBeach should be used for prediction of storm impact? Can XBeach predictions be used in order to manage overwash in areas where it is not desirable, or to reduce the consequences of overwash? Therefore, the model should be reliable predict overwash occurrence and magnitude. This research presented an assessment of two areas at Ameland (Paal22 and DeHon) during the Allerheiligenstorm. XBeach predicted at both of these locations accurately the observed occurrences of overwash. As a result of this, XBeach could also be used to accurately assess if overwash occurs in similar conditions. For example, assessing if overwash occurs at (other) areas of the Dutch Wadden Sea Islands.

The predicted magnitude of overwash showed still some discrepancies with observations. Results showed that multiple factors influenced the extent of the simulated overwash. Previously research by McCall (2008) showed that a transport limiter (S_{max}) has to be activated during overwash conditions. Still, with using this transport limiter, the results showed difference between the observed and simulated extent of the overwash. Nevertheless, the order of the magnitude of the overwash predicted by XBeach was comparable. In addition, difference between observation and simulation could be explained due to the missing of some physical processes in the simulation. This provides opportunities for improvement of predictive capacities of overwash by XBeach.

On the other hand, the results showed that collision impact at the dune front decreased with activating the transport limiter. When no overwash is expected, for example when coastal dunes are of sufficient height, more accurate predictions can be obtained without using the transport limiter.

XBeach can accurately predict occurrence of overwash in advance, but could it also be used as a real time forecast model for morphological storm impact? The model setup in this research used very detailed resolutions to predict overwash. Especially at Paal22 it was necessary to use the detailed resolution of 1x1 m in order to predict overwash. This resulted in very long compute times (+/- 8 days). It makes (real time) decisions on mitigation/adaptation strategies for forecasted storm impact with XBeach not (yet) possible. With increasingly advancements in compute power of computers, it could be soon a problem from the past.

Some advancement are already made last years. For example the use of MPI (Message Passing Interface) implementation in XBeach with automatic domain decomposition for parallel (multi-processor) computing. Also, halfway during this research, new computers came available. It reduced model time with about 30%. As a consequence of these advancements, some new model instabilities occurred. These should be solved first, if XBeach is to be used for real time forecasting storm impact. Therefore, at the moment XBeach can only be use to predict in advance, by using for example storm design events, morphological (overwash) storm impact.

7.2.2 Communicating predicted storm impact

To obtain results from XBeach an elaborate (time consuming) investigation and interpretation of the simulate model results were necessary. Using Sallenger's (2000) scale to present model predictions can serve managers to assess (quickly), without knowledge of XBeach, the expected magnitude of the morphological impact. This scale can help for making decisions on

mitigation/adaptation strategies and to allocate the required resources to those locations more prone to be affected by a predicted storm.

The unmodified form of the presented scale was used in this research. This results in that the highest dune at Ameland would determine the regime for the entire island (i.e. swash, collision, overwash and inundation). Simulations by XBeach showed that this was not representative for Ameland. With the presence of large alongshore variability, real differences in the magnitude of erosion processes along the coastal dunes significantly vary in terms of type of response and intensity at different spatial scales.

The unmodified form of the presented scale was used in this research. Hence, the highest dune at Ameland would determine the regime for the entire island (i.e. swash, collision, overwash and inundation). Simulations by XBeach showed that this was not representative for Ameland. With the presence of large alongshore variability, real differences in the magnitude of erosion processes along the coastal dunes significantly vary in terms of type of response and intensity at different spatial scales.

Also the simulation of morphodynamic behavior was incorporated in the storm impact scale. The dune crest at DeHon was lowered significantly during the storm. This predicted change in elevation of the dune crest in time was used for our storm impact scale calculations. Several authors (Gervais et al., 2012) already argued, but our results shows, that this is an important characteristic that needs to be included.

Nevertheless, the dune crest is not (always) suitable as a threshold to evaluate the vulnerability of a dune system. It can be very high above the reference level, but containing only a small amount of sand. The dune crest can easily be eroded by the prolonged attack of waves. Therefore it can be argued that taken the crest elevation for failure prediction of coastal dunes is not always valid; it is important to consider actual capacity of the beach to adapt to storm conditions (Bosom et al., 2010).

Thus, when communicating the predictions of the magnitude of overwash, another adaptation to the theory by Sallenger (2000) is proposed. Currently, the two dimensions of the storm impact scale consist of dune elevation characteristics and storm surge level. For a more representative storm impact scale, a third dimension should be added. This new dimension should consist of beach variables, characterizing its capacity to respond to the storm and adapt its shape. It will result in a more accurate storm impact scale to represent the predicted magnitude overwash. This scale can be used to prevent storm overwash in areas where it is not desirable, or where the magnitude of overwash needs to be reduced.

8 Conclusions and recommendations

The objective of this research was to validate XBeach for dune overwash at beaches with a gentle slope. This research was performed by analyzing data and simulation by XBeach the morphological impact on the coastal dunes at Ameland. This research has led to the conclusion and recommendations that will be presented in this chapter.

8.1 Conclusions

The overall motivation of this research was to improve the prediction of storm impact on coastal dunes with the numerical modeling program of XBeach. Therefore, it was investigated if XBeach could accurately predict overwash. This research presented a data analyses and compared it with simulations by XBeach. It has led to the conclusions presented in this section

The observed and measured data of dune erosion, at the barrier island Ameland during the Allerheiligenstorm showed that:

- The quality of the collected data was insufficient quality to use it for a quantitative validation of overwash processes;
- At Ameland during the Allerheiligenstorm overwash was observed at two locations: Paal22 and DeHon
- The two identified overwash locations where different in magnitude. At location DeHon a grid size of 5x5 m is sufficient to represent the observed overwash location, at location Paal22 a grid size of 1x1 m should is sufficient to simulate the overwash location;
- These two location were suitable to validate XBeach for the occurrence of overwash;

Comparing simulations with observations of the two different locations Paal22 and DeHon showed that:

- XBeach simulated overwash at observed overwash locations;
- There are discrepancies between observed and simulated magnitude of overwash. The indicated order of the magnitude of predicted and observed overwash is agreement;
- If the threshold to overwash in XBeach is only slightly exceeded, overwash is underestimated;
- Overestimation of the magnitude of overwash in XBeach is predicted if abundant overwash occurred;
- Overwash occurrence was predicted due to the severity of the storm surge water level;
- Morphological impact predictions of collision and overwash are sensitive to the use of the overwash transport limiter;
- At the dune front, total wave height is determined by infragravity wave height.

Overall, it can be said that our results indicates that XBeach was able to accurately represent the morphological overwash occurrences, present at beaches with a gentle slope.

8.2 Recommendations

There are a number of recommendations for improving the XBeach model predictions. The first recommendations are related to the data used for the simulation, followed by recommendations regarding the XBeach model itself. Finally, some recommendations for communicating predicted results are given:

- Improve the accuracy of LIDAR data, to validate presented model results for predicted volumetric sediment changes due to overwash occurrence;
- Use LIDAR preliminary to identify locations prone to overwash.

There are also possibilities to improve XBeach model performance:

- Add missing physical processes, e.g. short wave run-up is and the effect of vegetation;
- Investigate how transport limiter S_{max} effects XBeach model predictions during different storm impact regimes;
- Solve the problems with the anomaly regarding the wave force (see also appendix E);
- Simulate the hydrodynamic of the Wadden Sea, to investigated storm impact at location DeHon more accurately.

Furthermore, in the discussion it is argued to use some adaptations to communicate storm impact, which leads to the following recommendations to communicate future storm impact.

- To accurately represent storm impact, when assessing vulnerability at the Dutch coastal system, a third dimension should be added to the proposed scale by Sallenger (2000). This dimension should include the capacity of the dune to adapt to storm impact.
- With some adaptation to the storm impact scale of Sallenger (2000), than it could be efficiently used to allocate resources, to prevent/mitigate expected storm induced damages along the coastal zone.

9 Bibliography

- Adams, J., & Chandler, J. (2002). Evaluation of lidar and medium scale photogrammetry for detecting soft-cliff coastal change. *Photogrammetric Record*, 17(99), 405-418.
- Aguilar, F. J., Mills, J. P., Delgado, J., Aguilar, M. A., Negreiros, J. G., & Pérez, J. L. (2010). Modelling vertical error in LiDAR-derived digital elevation models. *ISPRS Journal of Photogrammetry and Remote Sensing*, 65(1), 103-110. doi: <http://dx.doi.org/10.1016/j.isprsjprs.2009.09.003>
- Alkyon Hydraulic Consultancy & Research. (2007). Hydro-dynamics Wadden Sea during storms. Emmeloord: Alkyon Hydraulic Consultancy & Research.
- Almeida, L. P., Voudoukas, M. V., Ferreira, Ó., Rodrigues, B. A., & Matias, A. (2012). Thresholds for storm impacts on an exposed sandy coastal area in southern Portugal. *Geomorphology*, 143–144(0), 3-12. doi: 10.1016/j.geomorph.2011.04.047
- Andrews, D. G., & McIntyre, M. E. (1978). An exact theory of nonlinear waves on a Lagrangian-mean flow. *Journal of Fluid Mechanics*, 89(4), 609-646.
- Baltsavias, E. P. (1999). Airborne laser scanning: basic relations and formulas. *ISPRS Journal of Photogrammetry and Remote Sensing*, 54(2–3), 199-214. doi: [http://dx.doi.org/10.1016/S0924-2716\(99\)00015-5](http://dx.doi.org/10.1016/S0924-2716(99)00015-5)
- Battjes, J. A., Bakkenes, H. J., Janssen, T. T., & van Dongeren, A. R. (2004). Shoaling of subharmonic gravity waves. *J. Geophys. Res.*, 109(C2), C02009. doi: 10.1029/2003jc001863
- Bosom, E., & Jiménez, J. A. (2010). Storm-induced coastal hazard assessment at regional scale: Application to Catalonia (NW Mediterranean). *Advances in Geosciences*, 26, 83-87.
- Daly, C., Roelvink, D., van Dongeren, A., van Thiel de Vries, J., & McCall, R. (2012). Validation of an advective-deterministic approach to short wave breaking in a surf-beat model. *Coastal Engineering*, 60(0), 69-83. doi: 10.1016/j.coastaleng.2011.08.001
- den Heijer, F., Noort, J., Peters, H., de Grave, P., Oost, A., & Verlaan, M. (2007). Allerheiligenvloed 2006: Rijkswaterstaat.
- Dong, G., Ma, X., Perlin, M., Ma, Y., Yu, B., & Wang, G. (2009). Experimental study of long wave generation on sloping bottoms. *Coastal Engineering*, 56(1), 82-89. doi: 10.1016/j.coastaleng.2008.10.002
- Dongeren, A. R. V., & Svendsen, I. A. (1997). Absorbing-Generating Boundary Condition for Shallow Water Models. *Journal of Waterway, Port, Coastal, and Ocean Engineering*, 123(6), 303-313. doi: [http://dx.doi.org/10.1061/\(ASCE\)0733-950X\(1997\)123:6\(303\)](http://dx.doi.org/10.1061/(ASCE)0733-950X(1997)123:6(303))
- Donnelly, C. (2007). *Morphologic Change by Overwash: Establishing and Evaluating Predictors*. Paper presented at the Proc. of International Coastal Symposium, Gold Coast, Australia.
- Elfrink, B., & Baldock, T. (2002). Hydrodynamics and sediment transport in the swash zone: a review and perspectives. *Coastal Engineering*, 45(3–4), 149-167. doi: 10.1016/s0378-3839(02)00032-7
- Engineers, U. A. C. o. (2003). *Coastal Engineering Manual*.
- Galappatti, G., & Vreugdenhil, C. B. (1985). A depth-integrated model for suspended sediment transport. *Journal of Hydraulic Research*, 23(4), 359-377. doi: 10.1080/00221688509499345
- Gervais, M., Balouin, Y., & Belon, R. (2012). Morphological response and coastal dynamics associated with major storm events along the Gulf of Lions Coastline, France. *Geomorphology*, 143–144(0), 69-80. doi: 10.1016/j.geomorph.2011.07.035
- Hladik, C., & Alber, M. (2012). Accuracy assessment and correction of a LIDAR-derived salt marsh digital elevation model. *Remote Sensing of Environment*, 121(0), 224-235. doi: <http://dx.doi.org/10.1016/j.rse.2012.01.018>
- Hodgson, M. E., & Bresnahan, P. (2004). Accuracy of airborne lidar-derived elevation: Empirical assessment and error budget. *Photogrammetric Engineering and Remote Sensing*, 70(3), 331-339.

- Holthuijsen, L. H., Booij, N., & Herbers, T. H. C. (1989). A prediction model for stationary, short-crested waves in shallow water with ambient currents. *Coastal Engineering*, 13(1), 23-54. doi: 10.1016/0378-3839(89)90031-8
- Janssen, T. T., Battjes, J. A., & van Dongeren, A. R. (2003). Long waves induced by short-wave groups over a sloping bottom. *J. Geophys. Res.*, 108(C8), 3252. doi: 10.1029/2002jc001515
- Kamphuis, J. W. (2000). *Introduction to Coastal Engineering and Management* (Vol. 16): World Scientific Publishing Co. Pte. Ltd.
- Larson, M., & Kraus, N. (1989). SBEACH: numerical model for simulating storm induced beach change. Report 1: Empirical Foundation and Model Development. Vicksburg, MS.: US Army Eng. Waterways Exp. Station.
- Lindemer, C. A., Plant, N. G., Puleo, J. A., Thompson, D. M., & Wamsley, T. V. (2010). Numerical simulation of a low-lying barrier island's morphological response to Hurricane Katrina. *Coastal Engineering*, 57(11-12), 985-995. doi: 10.1016/j.coastaleng.2010.06.004
- Longuet-Higgins, M. S., & Stewart, R. W. (1962). Radiation stress and mass transport in gravity waves, with application to 'surf beats'. *Journal of Fluid Mechanics*, 13(04), 481-504. doi: 10.1017/S0022112062000877
- Masselink, G., & Hughes, M. G. (2003). *Introduction to coastal processes and geomorphology*. London: Oxford University Press.
- Masselink, G., & Puleo, J. A. (2006). Swash-zone morphodynamics. *Continental Shelf Research*, 26(5), 661-680. doi: 10.1016/j.csr.2006.01.015
- Matias, A., Ferreira, Ó., Vila-Concejo, A., Garcia, T., & Dias, J. A. (2008). Classification of washover dynamics in barrier islands. *Geomorphology*, 97(3-4), 655-674. doi: <http://dx.doi.org/10.1016/j.geomorph.2007.09.010>
- McCall, R. T. (2008). *The longshore dimension in dune overwash modelling*. (Msc), Delft University of Technology, Delft.
- McCall, R. T., Van Thiel de Vries, J. S. M., Plant, N. G., Van Dongeren, A. R., Roelvink, J. A., Thompson, D. M., & Reniers, A. J. H. M. (2010). Two-dimensional time dependent hurricane overwash and erosion modeling at Santa Rosa Island. *Coastal Engineering*, 57(7), 668-683. doi: 10.1016/j.coastaleng.2010.02.006
- Olbert, A. I., & Hartnett, M. (2010). Storms and surges in Irish coastal waters. *Ocean Modelling*, 34(1-2), 50-62. doi: 10.1016/j.ocemod.2010.04.004
- Phillips, M. (1978). The Dynamics of the Upper Ocean. *Journal of Fluid Mechanics*, 88(04), 793-794. doi: 10.1017/S0022112078212396
- Raber, G. T., Jensen, J. R., Hodgson, M. E., Tullis, J. A., Davis, B. A., & Berglund, J. (2007). Impact of lidar nominal post-spacing on DEM accuracy and flood zone delineation. *Photogrammetric Engineering and Remote Sensing*, 73(7), 793-804.
- Reniers, A. J. H. M., Groenewegen, M. J., Ewans, K. C., Masterton, S., Stelling, G. S., & Meek, J. (2010). Estimation of infragravity waves at intermediate water depth. *Coastal Engineering*, 57(1), 52-61. doi: 10.1016/j.coastaleng.2009.09.013
- Reniers, A. J. H. M., Thornton, E. B., Stanton, T. P., & Roelvink, J. A. (2004). Vertical flow structure during Sandy Duck: observations and modeling. *Coastal Engineering*, 51(3), 237-260. doi: 10.1016/j.coastaleng.2004.02.001
- Rijkswaterstaat. (2007). Kwaliteitsdocument laseraltimetrie Projectgebied Kust. In D. T. beschrijving (Ed.): Adviesdienst Geo-informatie en ICT.
- Rijkswaterstaat, D.-I.-D. (2006). *Waterhoogte in cm t.o.v. normaal amsterdams peil in oppervlaktewater gemeten bij Wierumergronden*. Retrieved from: <http://www.waterbase.nl>
- Roelvink, Reniers, van Dongeren, van Thiel de Vries, Lescinski, J., & McCall, R. T. (2010). XBeach Model Description and Manual (6 ed.). Delft: Unesco-IHE Institute for Water Education, Deltares and Delft University of Technology.
- Roelvink, D., Reniers, A., van Dongeren, A., van Thiel de Vries, J., McCall, R., & Lescinski, J. (2009). Modelling storm impacts on beaches, dunes and barrier islands. *Coastal Engineering*, 56(11-12), 1133-1152. doi: 10.1016/j.coastaleng.2009.08.006
- Roelvink, J. A. (1993). Dissipation in random wave groups incident on a beach. *Coastal Engineering*, 19(1-2), 127-150. doi: 10.1016/0378-3839(93)90021-y

- Ruessink, B. G. (1998). Bound and free infragravity waves in the nearshore zone under breaking and nonbreaking conditions. *J. Geophys. Res.*, *103*(C6), 12795-12805. doi: 10.1029/98jc00893
- Ruessink, B. G., Houwman, K. T., & Hoekstra, P. (1998). The systematic contribution of transporting mechanisms to the cross-shore sediment transport in water depths of 3 to 9 m. *Marine Geology*, *152*(4), 295-324. doi: 10.1016/s0025-3227(98)00133-9
- Ruessink, B. G., Miles, J. R., Feddersen, F., Guza, R. T., & Elgar, S. (2001). Modeling the alongshore current on barred beaches. *J. Geophys. Res.*, *106*(C10), 22451-22463. doi: 10.1029/2000jc000766
- Ruessink, B. G., van den Beukel, P. G. L., & Kleinhans, M. G. (1998). Observations of swash under highly dissipative conditions. *J. Geophys. Res.*, *103*(C2), 3111-3118. doi: 10.1029/97jc02791
- Sallenger, J. A. H. (2000). Storm Impact Scale for Barrier Islands. *Journal of Coastal Research*, 890-895.
- Sallenger, J. A. H., Krabill, W. B., Swift, R. N., Brock, J., List, J., Hansen, M., . . . Stockdon, H. (2003). Evaluation of airborne topographic lidar for quantifying beach changes. *Journal of Coastal Research*, *19*(1), 125-133.
- Soulsby, R. (1997). *Dynamics of marine sands, a manual for practical applications*: Thomas Telford Publications.
- Symonds, G., Huntley, D. A., & Bowen, A. J. (1982). Two-Dimensional Surf Beat: Long Wave Generation by a Time-Varying Breakpoint. *J. Geophys. Res.*, *87*(C1), 492-498. doi: 10.1029/JC087iC01p00492
- Thornton, E. B., MacMahan, J., & Sallenger Jr, A. H. (2007). Rip currents, mega-cusps, and eroding dunes. *Marine Geology*, *240*(1-4), 151-167. doi: 10.1016/j.margeo.2007.02.018
- Tuan, T. Q., Verhagen, H. J., Visser, P., & Stive, M. J. F. (2006). Wave overwash at low-crested beach barriers. *Coastal Engineering Journal*, *48*(4), 371-393. doi: Doi 10.1142/S0578563406001453
- Van de Graaff, J., Van Gent, M. R. A., Boers, M., Diermanse, F. L. M., Walstra, D. J., & Steetzel, H. J. (2006). Technisch rapport Duinafslag.
- Van Dongeren, A., Reniers, A., Battjes, J., & Svendsen, I. (2003). Numerical modeling of infragravity wave response during DELILAH. *J. Geophys. Res.*, *108*(C9), 3288. doi: 10.1029/2002jc001332
- van Thiel de Vries, J. S. M., van Gent, M. R. A., Walstra, D. J. R., & Reniers, A. J. H. M. (2008). Analysis of dune erosion processes in large-scale flume experiments. *Coastal Engineering*, *55*(12), 1028-1040. doi: 10.1016/j.coastaleng.2008.04.004
- Walstra, D. J., & Roelvink, J. A. (2000, July 16-21, 2000). *3D calculation of wave-driven cross-shore currents*. Paper presented at the 27th International Conference on Coastal Engineering, Sydney.
- Williams, J. J., de Alegría-Arzaburu, A. R., McCall, R. T., & Van Dongeren, A. (2012). Modelling gravel barrier profile response to combined waves and tides using XBeach: Laboratory and field results. *Coastal Engineering*, *63*(0), 62-80. doi: 10.1016/j.coastaleng.2011.12.010

10 Appendix A: Results data analyses



Figure 69: DeHon shortly after the Allerheiligenstorm, with the dimensions of overwash occurrence.



Figure 70 DeHon shortly after the Allerheiligenstorm, with the dimensions of overwash occurrence.

Deltares



Figure 71: DeHon shortly after the Allerheiligenstorm, with the dimensions of overwash occurrence.

11 Appendix B: XBeach model setup

In this appendix the basic model setup of XBeach is explained. All the specific parameters values are shown in Appendix B.

11.1 Bathymetry setup

For Paal22 the grid size was chosen 3 km alongshore and 5 km cross shore. A variable grid size was used, with a maximum grid size of x (cross shore) = 50 m and minimum of x = 1 m, for the y direction also a maximum of 50 m and minimum of 1 m for.

The data analyses revealed that a coarser grid for DeHon was sufficient to represent the physical features of the area. Accordingly, a coarser grid size was selected. The maximum grid size of x (cross shore) = 50 m and minimum of x = 5 m, for the y direction also a maximum of 50 m and minimum of 5 m for.

The maximum of both grids resolution is limited to 50x50 m. This is because an even coarser grid resolution than 50x50m results in model instabilities.

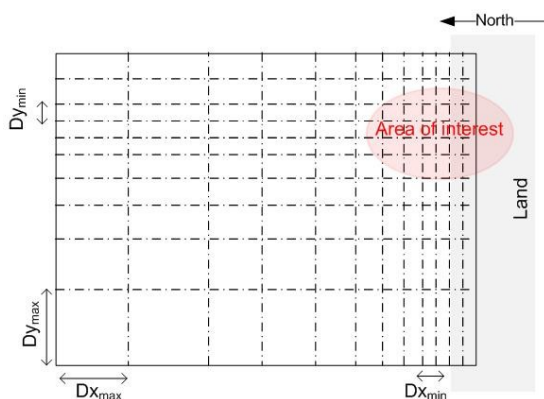


Figure 72: Representation of XBeach grid.

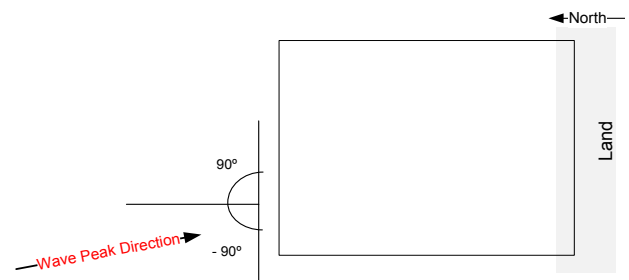


Figure 73: Representation of wave boundary condition.

11.1.1 Processing LIDAR of location Paal22

Some actions on both grids were performed for modeling purpose, because without these actions numerical instabilities will occur. The actions performed on the boundary conditions on the grid setup are:

- Lateral extend: copy the last grid cell of the lateral boundaries with 3 extra cells;
- Landward extend: extend landward border with specified elevation of 5 m;
- Seaward extend: extend seaward border to a depth of -22 m with a gradient of 1/50;
- Seaward flatten: flatten offshore boundary;
- Area of interest: x from 2470 to 2530 m and y from -4780 to -5000 m.

In Figure 74 the result of all the finalized actions are shown, resulting in the grid of location Paal22 used in XBeach.

11.1.2 Processing LIDAR of location DeHon

Some actions on grid of location DeHon was performed for modeling purpose, because without these actions numerical instabilities will occur.

- Lateral extend: copy the last grid cell of the lateral boundaries with 3 extra cells;
- Landward extend: extend landward border with specified elevation of 5 m;
- Seaward extend: extend seaward border to a depth of -22 m with a gradient of 1/50;
- Seaward flatten: flatten offshore boundary;
- Area of interest: x from 1850 to 3100 m and y from -5000 to -6000 m.

Furthermore, it is possible to model the Wadden Sea located at the west side of the island. This will result in a more accurate representation of the hydrodynamics in XBeach. The problem is that if the Wadden Sea is model, it will take extensively more compute time. Therefore, a 'landward polder' at around y -6000 m is created, what can represent the hydrodynamic influence of the Wadden Sea and take extensively less compute time. The landward polder can fill up with the sea water and can slowly flow away using the lateral boundaries.

In Figure 75 the final result of all the alterations at location DeHon is shown. This is the grid used in the XBeach simulation to represent location DeHon.

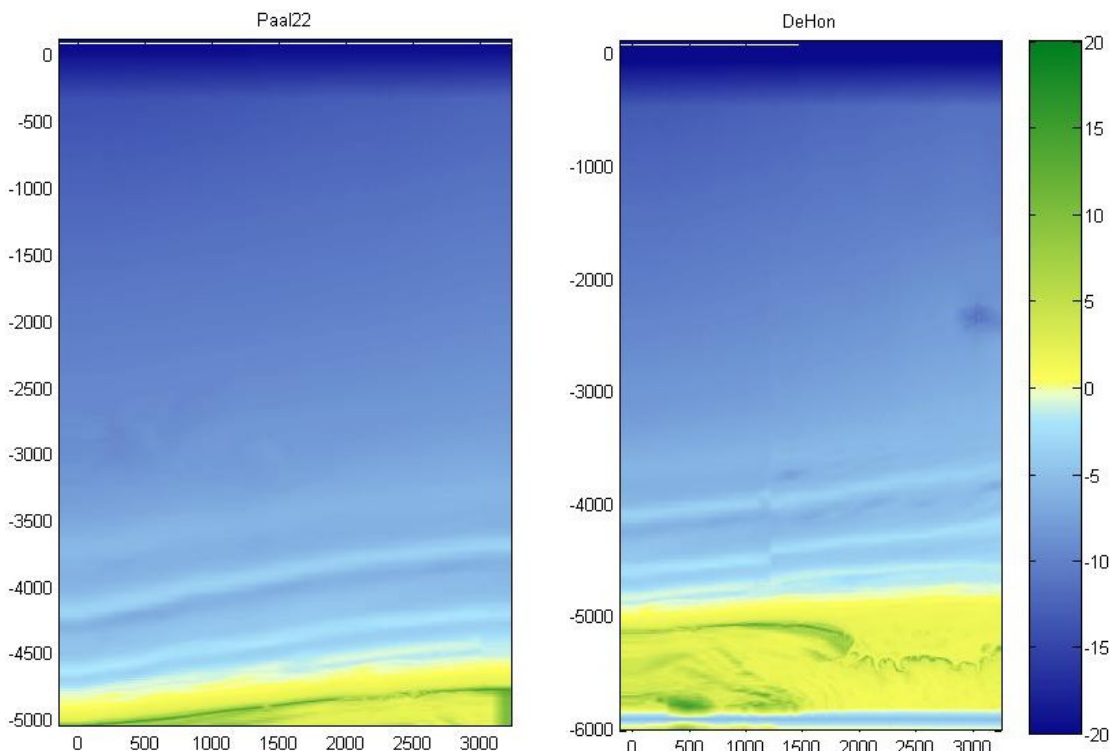


Figure 74: location Paal22.

Figure 75: location DeHon.

11.2 Wave boundary condition

With this option alongshore varying time series of the wave energy and bound long wave are generated on the basis of a specified analytical 2D SWAN spectrum. With this, second-order bound, directionally-spread seas can be created.

The analytical 2D SWAN spectrum is used in XBeach to determine the waves by the peak period, wave height, spectral peakedness, mean angle and directional spreading. More explanation can be found in the XBeach manual (Roelvink et al., 2010).

This XBeach model setup uses the SWAN 2D output files obtained from the research: "Hydro-dynamics in the Wadden Sea during storm conditions" (Alkyon Hydraulic Consultancy & Research, 2007). The used swan model output files are generated at three specific time steps: 1 November 2006, at 00:00 hr, 05:00 hr and 09:00 hr. These three time steps are used to simulate the storm in XBeach. Because of the limited input files for XBeach some assumptions are made:

The wave input conditions at 00:00 hr are used to represent the wave conditions until 03:20 hr, next the 05:00 hr wave input conditions are used until 09:00 hr and the rest of the simulation is using the 09:00 hr input wave conditions.

The conditions, used are shown in appendix D. The Significant wave peak directions vary between the -15 and -25 degree, depending on the time step. To account for refraction and diffraction, multiple bins are necessary in order to simulate these processes. It is shown that a direction wave resolution of 20 deg. sufficient to represent this process (Roelvink et al., 2010). Furthermore, an upper directional limit (north defined as 0 deg.) of 90 deg. and a lower directional limit of -90 deg. resulting in 9 bins.

12 Appendix C: Used parameters

Table 7 and Table 8 showing the parameters that differ for the default setting for location Paal22 and DeHon. The XBeach 2012 Easter MPI NetCDF release was used.

Table 7: parameters in XBeach for simulation of location Paal22.

Parameter	Name	Value
Grid	Nx	543
	Ny	250
	Alfa	-0
	Vardx	1
	Theta _{min}	-90
	Theta _{max}	90
	D _{theta}	20
	Thetanaut	1
Initial conditions	Zs0	-5
	Depthscale	1/6
Model time	Tstop	46800
Flow	C	65
Flow boundary condition	Epsi	-1
Bed composition	D ₅₀	0.00018
Sediment transport	Smax	0
Tide Boundary condition	Tideloc	1

Table 8: parameters in XBeach for simulation of location DeHon.

Parameter	Name	Value
Grid	Nx	464
	Ny	347
	Alfa	0
	Vardx	1
	Theta _{min}	-90
	Theta _{max}	90
	D _{theta}	20
	Thetanaut	1
Initial conditions	Zs0	-5
	Depthscale	1/6
Model time	Tstop	46800
Flow	C	65
Flow boundary condition	Epsi	-1
Bed composition	D ₅₀	0.00018
Sediment transport	Smax	1
Tide Boundary condition	Tideloc	2

13 Appendix D: Wave conditions

In this study the effect of wind on the hydrodynamics in the Wadden Sea were studied using water circulation models and wave models. To that the historical storms of 1 November 2006 in which the wind direction is northwest in the former and west in the latter. For the storms the water levels and currents were computed with the WAQUA model. Water level and current fields were computed based on astronomical and storm wind forcing.

The results showing large scale flows through the Wadden Sea that are crossing the shallow tidal flats south of the Wadden islands. The wind direction determines the shape of these large-scale patterns. In areas with high water levels, strong currents may occur that move parallel to the dikes.

For all of the presented conditions the wave conditions in the Wadden Sea were computed with the SWAN wave model using the measured wave conditions at the two different stations at the offshore boundary conditions and a HIRLAM wind fields as the forcing condition.

Figure 76, Figure 77 and Figure 78 the significant wave height is shown at time step 00:00 hr, 05:00 hr and 09:00 hr. In Figure 79, Figure 80 and Figure 81 the wave periods are shown at time step 00:00 hr, 05:00 hr and 09:00 hr. Figure 82, Figure 83 and Figure 84 shows at time step 00:00 hr, 05:00 hr and 09:00 hr the variance densities m^2/Hz plotted against the direction and frequency.

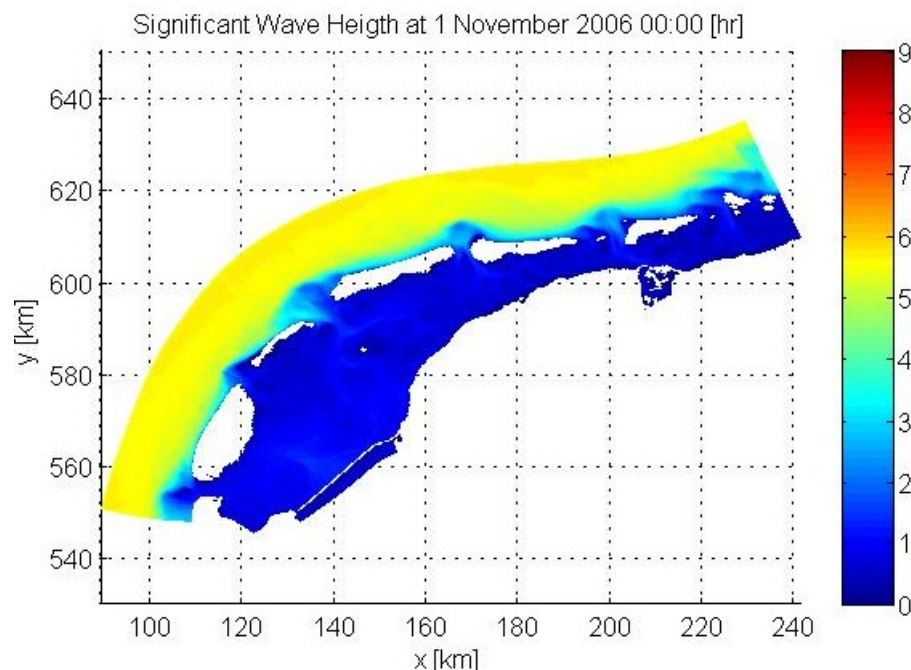


Figure 76: Significant Wave Height, simulated with SWAN at 1 November 2006 at 00:00 hr.

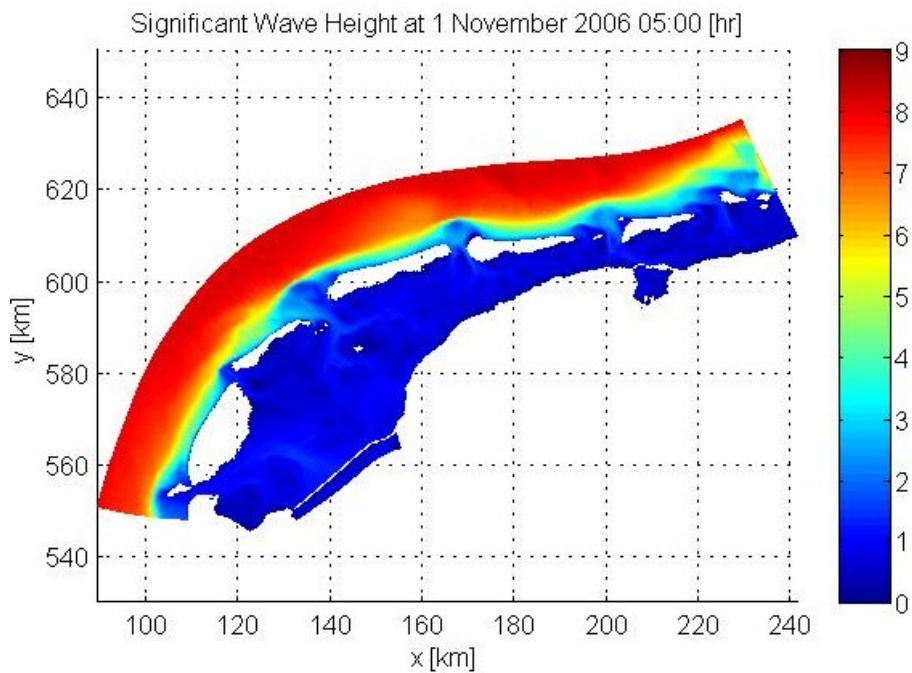


Figure 77: Significant Wave Height, simulated with SWAN at 1 November 2006 at 05:00 hr.

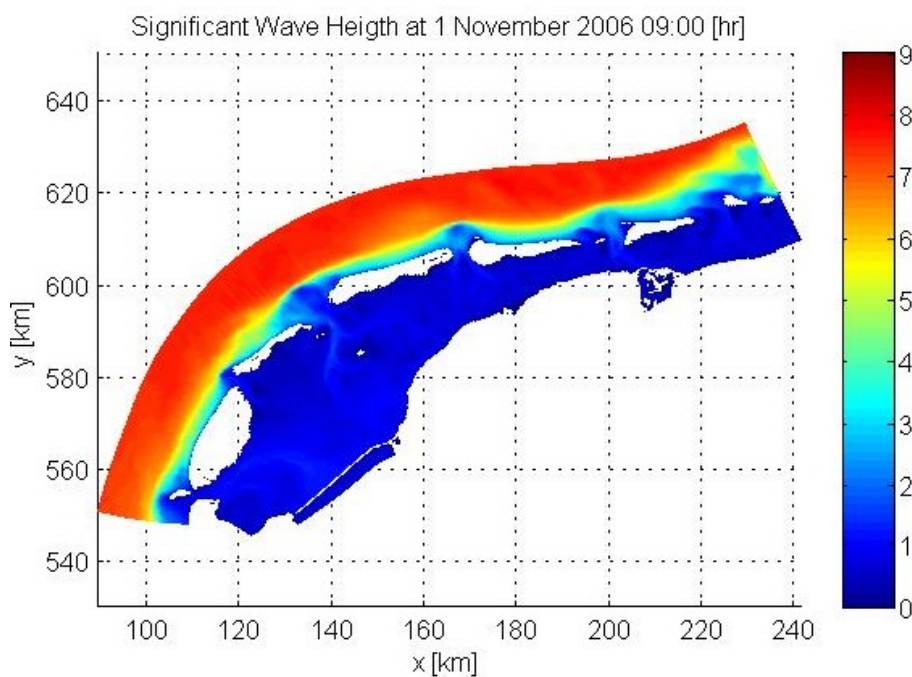


Figure 78: Significant Wave Height, simulated with SWAN at 1 November 2006 at 09:00 hr.

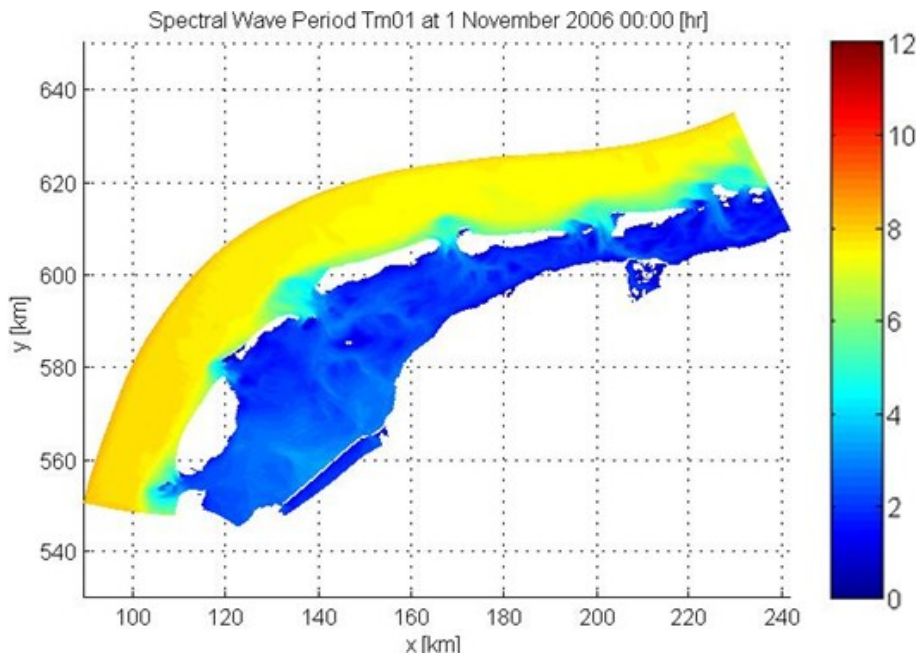


Figure 79: Spectral wave period Tm01, simulated with SWAN at 1 November 2006 at 00:00 hr.

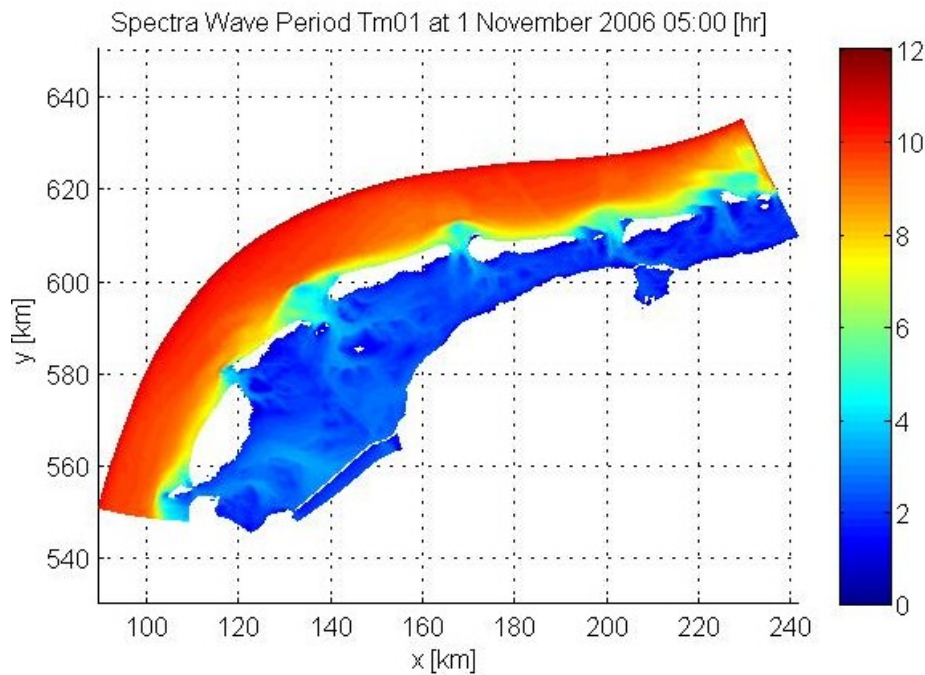


Figure 80: Spectral wave period Tm01, simulated with SWAN at 1 November 2006 at 05:00 hr.

Deltares

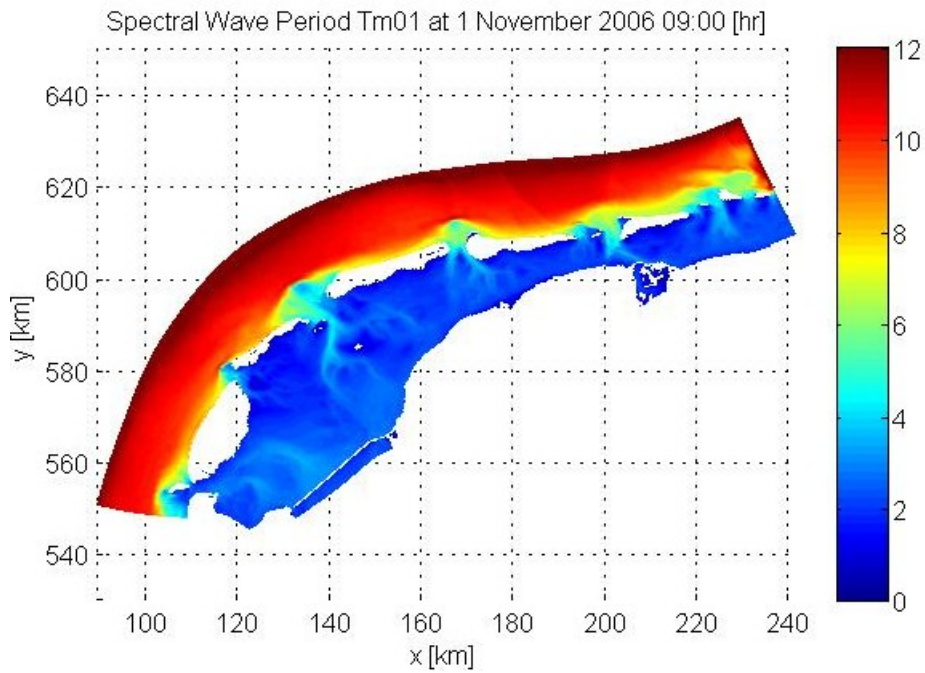


Figure 81: Spectral wave period T_{m01} , simulated with SWAN at 1 November 2006 at 12:00 hr.

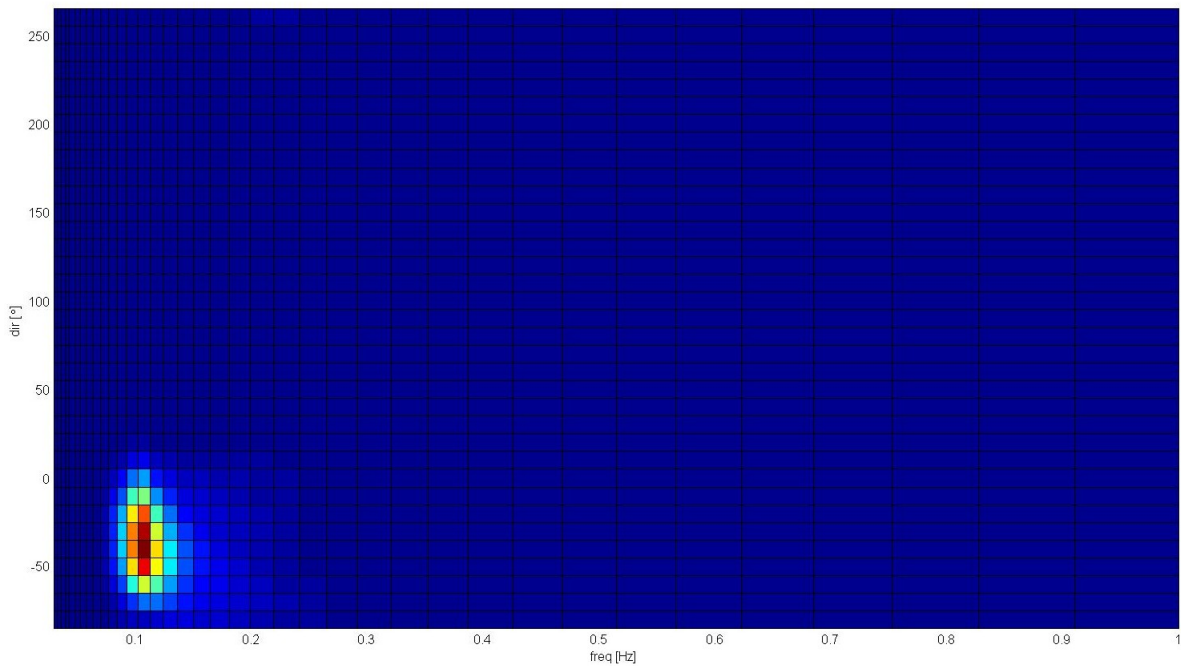


Figure 82: Simulated variance densities in m^2/Hz during 1st of November, 2006 at 01:00 by SWAN used at the off-shore model grid boundary.

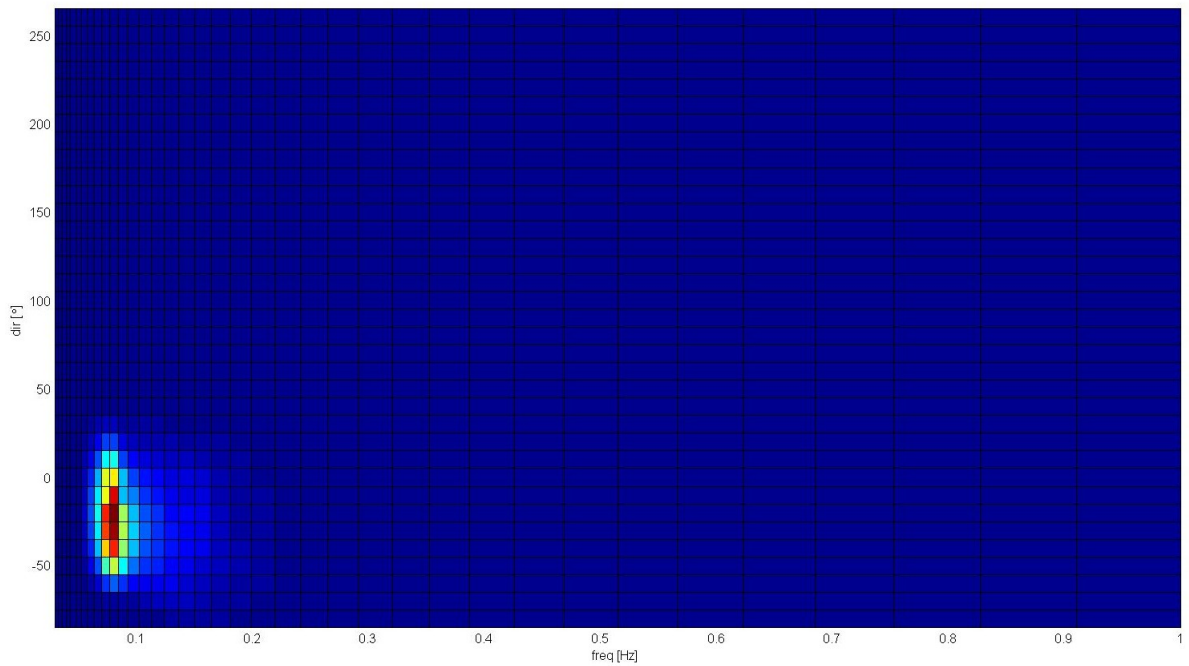


Figure 83: Simulated variance densities in m^2/Hz during 1st of November, 2006 at 05:00 by SWAN used at the off-shore model grid boundary.

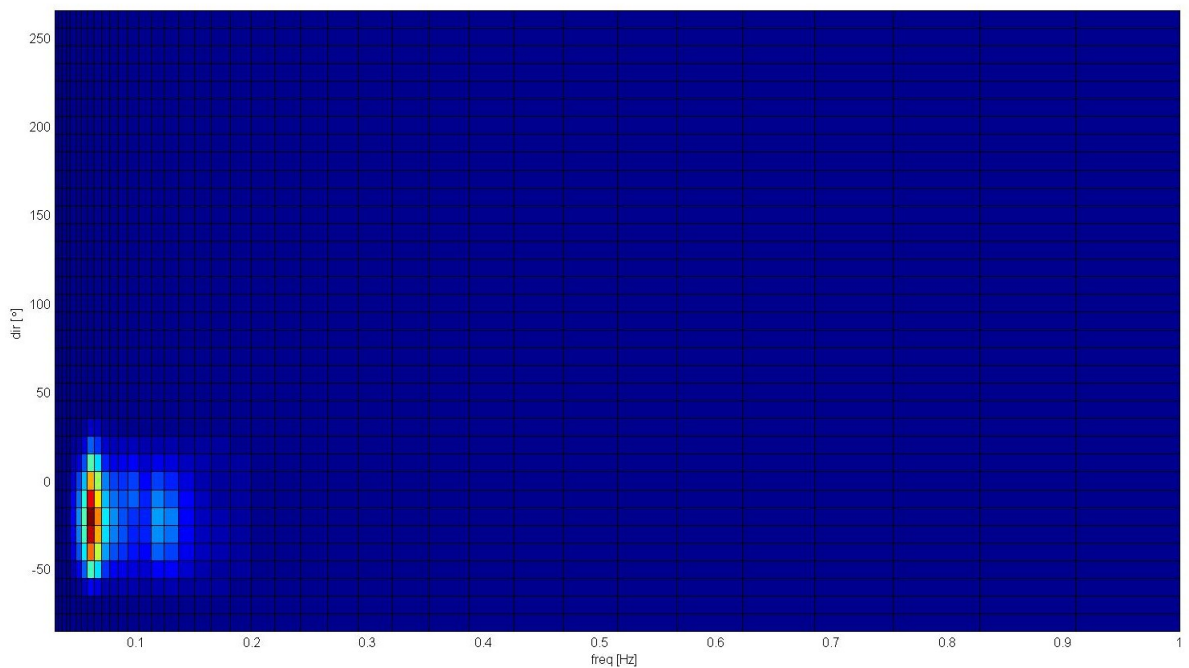


Figure 84: Simulated variance densities in m^2/Hz during 1st of November, 2006 at 01:00 by SWAN used at the off-shore model grid boundary.

14 Appendix E: Wave force error in XBeach

During analysis of the model results an unexplainable result submerged. The calculated wave forces show an unrealistic behavior.

The results of wave force simulation at time step 05:00 hr for Paal22 and DeHon. At both locations the unrealistic model behavior of extreme wave force values can be seen. Wave forces increases and decreases unrealistically. This behavior occurs relatively off-shore and at the start where the model grid size resolutions is at fines (i.e. at Paal22 at the resolution of 1x1 m and at DeHon 5x5 m)

These results also affect the other results. Model results show also this pattern in the bed level changes. At the beach and the coastal dunes the effects seems to be diminishing. Therefore, it is assumed that our model results are not significantly affected by this model error.

A quick investigation of the XBeach model error didn't reveal the source of the problem. A quick scan XBeach model code did not reveal this error. Nevertheless, this model error should be investigated more in-depth, and solved.

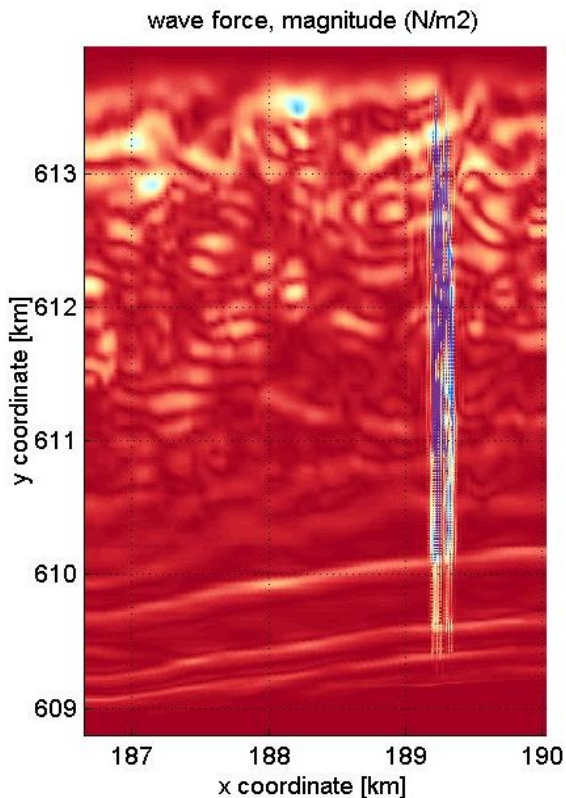


Figure 85: wave forces at Paal22.

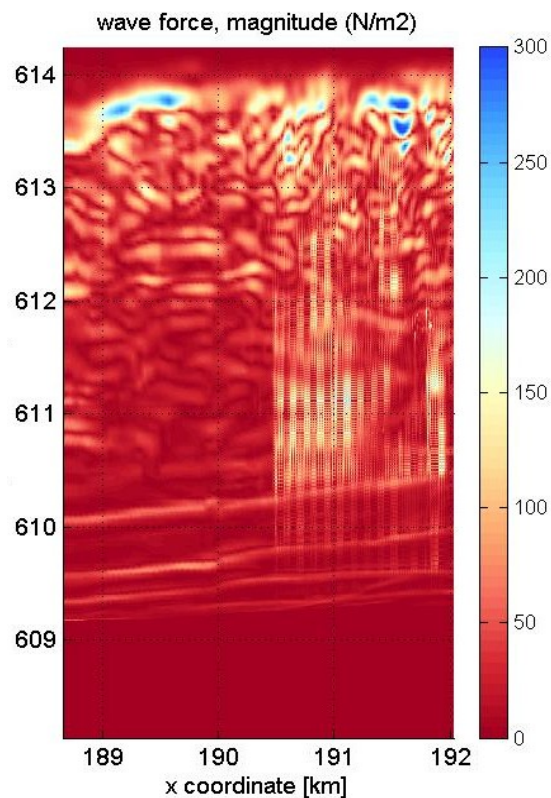


Figure 86: Wave forces at DeHon.

